Notch signaling in cell-fate specification and maintenance in the developing and adult mammalian inner ear

Byron H. Hartman

A dissertation submitted in partial fulfillment of the
requirements for the degree of

Doctor of Philosophy

University of Washington

2009

Program Authorized to Offer Degree

Biological Structure

Notch signaling in cell-fate specification and maintenance in the developing and adult mammalian inner ear

Byron H. Hartman

A dissertation submitted in partial fulfillment of the
requirements for the degree of

Doctor of Philosophy

University of Washington

2009

Program Authorized to Offer Degree: Department of Biological Structure

University of Washington

Graduate School

This is to certify that I have examined this copy of a doctoral dissertation by

Byron H. Hartman

and have found that it is complete and satisfactory in all respects,
and that any and all revisions required by the final
examining committee have been made.

Chair of the Supervisory Committee:

_____

Thomas A. Reh

Reading Committee:

_____

Thomas A. Reh

_____

Olivia Bermingham-McDonogh

_____

David W. Raible

Date:_____

In presenting this dissertation in partial fulfillment of the requirements for the doctoral degree at the University of Washington, I agree that the Library shall make its copies freely available for inspection. I further agree that extensive copying of the dissertation is allowable only for scholarly purposes, consistent with “fair use” as prescribed in the U.S. Copyright Law. Requests for copying or reproduction of this dissertation may be referred to Proquest Information and Learning, 300 North Zeeb Road, Ann Arbor, MI 48106-1346, 1-800-521-0600, to whom the author has granted “the right to reproduce and sell (a) copies of the manuscript in microform and/or (b) printed copies of the manuscript made from microform.”

Signature _____

Date _____

University of Washington

Abstract

Notch signaling in cell-fate specification and maintenance in the developing and adult mammalian inner ear

Byron H. Hartman

Chairperson of the Supervisory Committee:
Professor Thomas A. Reh
Department of Biological Structure

The inner ear contains the auditory and vestibular organs, which are sensory neuroepithelia composed of mechanosensory hair cells and glia-like supporting cells. The mammalian auditory sensory epithelium, the organ of Corti, is responsible for transduction of sound stimuli into electrical signals for hearing function. Hair cells are susceptible to damage from noise, toxins, and ageing. Mammals do not regenerate hair cells after damage, but non-mammalian vertebrates are capable of hair cell regeneration. Replacement of lost hair cells in lower vertebrates occurs through plasticity of supporting cells, which directly change fate into hair cells or proliferate to produce new cells through a recapitulation of developmental mechanisms. However, supporting cells in the mature mammalian cochlea do not exhibit the potential to change fate or proliferate in order to regenerate lost sensory cells. However, during embryonic development, hair cells and supporting cells develop from common precursors and the fate of individual cells is regulated through intercellular signaling and genetic mechanisms. The overall goal of this research is to further understand the mechanisms of specification and maintenance of sensory cell fates in the developing and adult mammalian inner ear. Understanding the way

in which cell types are developed and maintained is a crucial step in overcoming the barriers to regeneration in the mammalian inner ear. A key regulator of development in the inner ear is the Notch signaling pathway, a highly conserved cell signaling system present in most multicellular organisms. In this dissertation, after a review of relevant literature, I will describe our investigation of Notch signaling in the developing and adult mammalian inner ear. We conducted comprehensive gene expression analyses and describe novel expression patterns of two Notch ligands, Dll3 and DNER, and a key Notch effector, Hes5. We found that the Notch pathway is highly active during cochlear development but appears to be absent from the adult cochlea. We performed several transgenic gain-of-function experiments, which show that Notch signal activation during development is capable of conferring prosensory character to regions of nonsensory epithelia. However, constitutive activation of Notch in mature cochlear supporting cells was not sufficient to confer regeneration potential.

TABLE OF CONTENTS

LIST OF FIGURES

.

ACKNOWLEDGEMENTS

I am very grateful to Dr. Thomas Reh for his excellent mentorship, support, and kindness throughout my graduate studies. Tom has given me the most comprehensive and practical training I could have hoped for as a graduate student. From Dr. Reh I have learned the importance of logic, clarity, simplicity, diligence, optimism, and style. Tom has shown me how it takes machine-like persistence to Tominate™ the barriers to regeneration and push back the frontiers of science.

I am also grateful to Dr. Olivia Bermingham-McDonogh for her teaching, mentorship, encouragement and guidance as I ventured through the field of inner ear development and regeneration. I feel very fortunate to have had Olivia's support as a co-advisor and committee member. My graduate training and dissertation work would not have been complete without Olivia's generous mentorship. I also wish to extend my gratitude to Dr. David Raible and Dr. Bruce Tempel for advising me as members of my thesis committee. I have been fortunate to have such excellent scientists and supportive role models for my committee advisors.

Working with my lab-mates in the Reh and Bermingham-McDonogh labs has made my graduate training experience one of great fulfillment and friendship. I

am deeply appreciative of Dr. Branden Nelson, the genius who kindly trained me in the fine arts of molecular biology and was a comrade who shared in culinary, fermentive, and other fine delicacies and many good conversations. I was also fortunate to have a lot of help and training from Dr. Toshinori Hayashi, as well as Dr. Deepak Lamba, Dr. Mike “Moka” Karl, Dr. Joe “Jabiv” Brezenzski, Dr. Susan Hayes, Dr. Jennie Close, and Dr. Melanie Roberts. My fellow graduate students in the lab, Sean Georgi, Jule Gust, Drew McUsic, and Julia Pollak provided help and sincere suggestions that helped me with my project and presentations. Catherine Ray, Paige Etter, and Kristin Fitzpatrick have been very supportive throughout my studies.

I am very grateful to the Department of Biological Structure and chairman Dr. John Clarke for bringing me into the graduate program and providing me with community, training, and support. Tracy Cranick served as my graduate program coordinator and was very helpful, as were all of the office staff. Kate Mulligan with John Sundsten and Anita Hendrickson gave me excellent training in teaching neuroanatomy. I was also very fortunate to be supported by the interdisciplinary Developmental Biology Training Grant (DBTG), funded by NIH. Barbara Wakimoto and the other faculty and staff members working with the DBTG have been an important part of my training. I also learned a lot from the community and friendship that I shared with the other DBTG trainees. I was admitted to UW through the Department of PBIO, which was very supportive

and provided me with my first year of training, for which I am very grateful. I was also supported for one year by an NIH institutional training grant administered by Speech and Hearing Sciences, which was great training and appreciated support. I also sincerely thank Dr. Elizabeth Oesterle and Sean Campbell for consultation and help with the in vivo drug-damage protocol, and Dr. Ed Rubel and Dr. Jennifer Stone for training and helpful advice. I am also grateful to Dr. Verdon Taylor, Dr. Onur Basak, Dr. Hiroshi Takashima, Dr. Hirohito Miura, Dr. Doug Melton, and Dr. Sue McConnell for providing mice, reagents and collaboration. Dr. Susan Dowling and Linda Robinson generously helped with animal care and use.

Finally, I am deeply thankful for the support of my wonderful wife, Yukiko. Throughout my five-year tenure Yukiko has been the most significant person and source of support in my life. I could not have done this without her, and I owe her a lot of good caring and support in return. I also appreciate my parents, John S. and Libby Hartman, for being caring and supporting role models, and my grandparents Dr. John J. and Miriam Hartman, for their generous support and encouragement.

Chapter I:
Introduction and Review of Inner Ear Development

Introduction

The mammalian inner ear contains the auditory and vestibular sensory organs, which are highly specialized neuroepithelia, composed of supporting cells and mechanosensory hair cells. The cochlea contains the auditory portion of the inner ear, which in mammals is called the organ of Corti. The organ of Corti is composed of hair cells and supporting cells arranged in coiled rows that extend throughout the length of the cochlear duct (see Fig. 1.1). Hair cells in the cochlea are responsible for transduction of noise-induced mechanical stimulation into an electrical signal that is relayed to the temporal cortex through the auditory pathway. Supporting cells of the organ of Corti are a morphologically diverse population of nonsensory cells that surround hair cells and provide structural and functional support. Hair cells are susceptible to damage due to acoustic trauma, ototoxic drug exposure, and the effects of aging. A leading cause of hearing loss is hair cell damage, which is irreversible in mammals. However, birds and other nonmammalian vertebrates have been shown to be capable of hair cell regeneration, and subsequent gain of hearing function, after injury. Studies that investigate the mechanisms of cellular development, fate maintenance, and regeneration potential in the mammalian inner ear are important to further our understanding and treatment of developmental and adult inner ear disorders as well as those of other parts of the nervous system where regeneration is similarly restricted.

Earlier studies have indicated that Notch signaling plays important roles in development of the inner ear, but the precise mechanisms and effects of this pathway are yet to be elucidated. The Notch signaling pathway is a complex intercellular signaling pathway known to control many cell-fate specification events in multicellular organisms. This pathway is known as a potent regulator of progenitors, stem cells, and glia and has also shown to be required for some forms of regeneration. Evidence from previous studies have suggested that Notch is required for early specification of inner ear sensory progenitors and later in development regulates differentiation of those same progenitors into either hair cell or supporting cell fates. In mammals there are numerous and diverse homologues of Notch pathway components and, because of this complexity, the expression patterns and functions of the various members of this pathway in the inner ear are not yet completely known. Thus, it is essential to perform studies that further complete our understanding of Notch signaling in regulation of development and regeneration potential in the inner ear.

In this dissertation, I will begin with a review of normal embryological and postnatal development of the mammalian cochlea. I will include a summary of important literature related to cell fate determination, maturation, and Notch signaling in inner ear development and I will briefly describe studies of hair cell damage in mammals and regeneration in birds. In Chapter II, I will present the results of our expression and functional study of the Notch ligand Delta-like 3 (Dll3) in cochlear development. Chapter III will include presentation of the results of our investigation the downstream Notch effector Hes5 in the developing and adult inner ear and the damaged cochlea. In Chapter IV, I will describe the expression and loss of function of the putative Notch ligand Delta/Notch-like EGF-related Receptor (DNER) in the developing and adult inner

ear. Finally, Chapter V will include description of a series of transgenic gain-of-function studies to investigate the role of Notch signaling in inner ear development and regulation of regenerative potential.

Early Development of the Mammalian Inner Ear: Prosensory Specification

The inner ear develops from the otic placode, which invaginates and pinches off from the ectoderm to form the otic vesicle. The sensory organs of the inner ear are derived from a common prosensory patch in the ventromedial wall of the otic vesicle. The prosensory patch can be identified by expression of several markers, including the Notch ligand Jagged1 and the transcription factor Sox2. The mechanism of sensory patch formation, or prosensory specification, is not yet known. However, both Jag1 and Sox2 are required for this process; as mice deficient in either gene have severe defects in sensory specification (Kiernan et al., 2005b; Kiernan et al., 2006). Furthermore, the partial loss of Sox2 expression in the Jag1 conditional mutant mouse suggests that Jag1 acts upstream of Sox2 (Kiernan et al., 2006). Jag1 is thought to act through the Notch1 receptor, which is expressed throughout the early otic vesicle. Activated Notch receptor and expression of effectors of Notch signaling, HesR1 and HesR2, have been detected in the early prosensory portions of the cochlea ((Hayashi et al., 2008; Murata et al., 2006). Additionally, pharmacological inhibition of Notch in mouse cochlear explants during the prosensory phase results in a severe reduction in hair cell and supporting cell numbers (Hayashi et al., 2008). Furthermore, a gain-of-function study in the chick has shown that Notch activation outside of the normal prosensory region can result in development of ectopic sensory structures, containing hair cells and supporting cells (Daudet and Lewis, 2005). However, additional studies are needed to further

validate the Notch-dependent prosensory hypothesis and elucidate the underlying mechanisms behind prosensory specification in the mammalian auditory sensory epithelium.

The Notch pathway is a highly conserved regulator of cell fate decisions. Mammalian Notch ligands include Delta and Jagged family members, homologues of the Drosophila Delta and Serrate, (DSL ligands (Delta/Serrate/Lag2)). In response to ligand binding, the Notch receptor undergoes sequential events resulting the in the gamma-secretase dependent cleavage (S3 cleavage) of the Notch intracellular domain (NICD). In the well-studied "canonical" Notch pathway, the NICD then translocates to the nucleus and forms a trimeric complex with the DNA-binding protein CSL (CBF1, Su(H) and LAG-1) and the co-activator Mastermind (MAM). The CSL-NICD-MAM complex then binds to CSL binding sites in the promoter regions of downstream target genes, activating their expression. Targets of Notch signaling include transcriptional repressor genes of the Hes and Hes-related (HesR) families, mammalian homologues of the *hairy* and *enhancer of split* inhibitory bHLH genes (Kageyama and Ohtsuka, 1999a; Ohtsuka et al., 1999). See Fig. 1.2 for a schematic of the Notch pathway and its proposed role in prosensory specification.

Following prosensory specification, a complex series of events transforms the otic vesicle into the labyrinth containing the vestibular sensory organs and the cochlea. The organ of Corti forms from the floor of the developing cochlear duct in a process that involves multiple morphogenetic events. The primitive cochlear duct first elongates and begins to coil at around mouse embryonic day 11 (E11). Shortly afterwards, a discrete region of cells in the floor of the apex of the cochlear duct becomes mitotically quiescent. Between E12 and E14 this region of nonproliferating cells propagates in a

wave from the apex to the base (Ruben, 1967). The region of nonproliferating cells in the cochlear duct, also known as the prosensory domain, will eventually give rise to the hair cells and support cells of the organ of Corti. The cells in the prosensory domain are marked by expression of the cyclin-dependent kinase inhibitor $p27^{kip1}$ (Chen et al., 2002; Chen and Segil, 1999; Ruben, 1967). The expression of $p27^{kip1}$ is downregulated in hair cells as they begin overt differentiation, but it persists in supporting cells into adulthood (Chen and Segil, 1999). $P27^{kip1}$ negatively regulates cell proliferation in the developing organ of Corti; $p27^{kip1}$ knockout mice exhibit excess proliferation and an overproduction hair cells and supporting cells (Lowenheim et al., 1999). Still, other molecules must also regulate proliferation during this process as many supporting cells and hair cells do leave the cell cycle and differentiate in $p27^{kip1}$ knockout mice.

Cellular Differentiation

Hair cell differentiation begins in the prosensory region of the developing cochlea following terminal mitosis, or slightly overlapping with it. A key molecule for the generation of hair cells is Atoh1 (also called Math1 in mice), a homologue of the *Drosophila* proneural gene *atonal*, which encodes a basic, helix-loop-helix (bHLH) transcription factor. Proneural bHLHs, like Atoh1, activate transcription of target genes by binding to E-boxes as heterodimers with another class of bHLH transcription factors, which are similar, more ubiquitously expressed; these include homologues of the *Drosophila* Daughterless. Atoh1 expression becomes upregulated in hair cell progenitors as they begin differentiation, is maintained for several days in differentiating hair cells, then is downregulated shortly after birth. Hair cell differentiation propagates in a morphogenetic wave from the base of the cochlea to the apex and is first marked

by upregulation of Atoh1 (Chen et al., 2002; Woods et al., 2004). Atoh1-/- mice show a complete loss of hair cells and most, if not all, supporting cells in the inner ear (Bermingham et al., 1999). Similarly, overexpression of Atoh1, either in the developing organ of Corti or the adjacent greater epithelial ridge (GER), leads to induction of ectopic hair cells (Fig. 1.4, (Woods et al., 2004; Zheng and Gao, 2000)).

The model of lateral inhibition, first applied to describe the mechanism by which neuroblasts and sensory organ precursors are specified in the fly ectoderm, has strongly influenced our view of hair cell differentiation and the role of Notch signaling throughout the vertebrate nervous system. In the process of lateral inhibition, cells that become committed to a neural fate express proneural bHLHs and upregulate surface expression of Notch ligands, which activate Notch signaling in neighboring cells that results in repression of proneural genes and inhibition of neural fate in those cells (Cabrera, 1990; Chitnis, 1999; Heitzler and Simpson, 1991).

In mammals, the Notch family is composed of multiple homologues of ligands, receptors, and effectors (see Fig. 1.3). During development of the cochlea, Notch ligands, Dll1, Dll3, and Jag2 are expressed by hair cells in the mouse cochlea approximately one day after onset of Atoh1 expression (Hartman et al., 2007; Lanford et al., 1999a; Morrison et al., 1999). Dll1 and Jag2, and possibly Dll3, appear to activate Notch signaling through the Notch1 receptor, expressed throughout the developing sensory epithelium (Lanford et al., 1999a; Zhang et al., 2000). Shortly afterwards, several downstream effectors of Notch signaling (Hes1, Hes5, and HesR3) are upregulated in neighboring cells that will ultimately develop as supporting cells (Hartman et al., 2009; Hartman et al., 2007; Lanford et al., 1999a; Zheng et al., 2000; Zine et al., 2000). Hes1 and Hes5 are known repressors of proneural activity in other

systems, and Hes1 has been shown to repress Atoh1-induced hair cell production when coexpressed in the GER (Zheng et al., 2000; Zine et al., 2001).

In this system, there is a high degree of overlapping expression among Notch ligands, as well as effectors, and their apparent redundancy of function has made interpretation of knockout studies complicated. However, it is clear that a major role of Notch signaling in the developing cochlea is to restrict the number of developing hair cells to the normal one row of inner hair cells and three rows of outer hair cells. In brief, conditional deletion or knockout of Dll1, Jag2, Hes1, or Hes5 resulted in varying and mild hair cell overproduction phenotypes consisting of the formation of one or two extra rows of hair cells, usually only along a portion of the length of the cochlea (Brooker et al., 2006; Kiernan et al., 2005a; Zine et al., 2001). The disruption of Dll1 and Jag2 together, or loss of both Hes1 and Hes5, resulted in slightly more severe phenotypes than single deletions alone in both cases; which suggests functional redundancy of these ligands and effectors. We analyzed mice with a mutation in Dll3 and found that the hair cells and supporting cells developed normally; also consistent with redundancy of ligand function (Hartman et al., 2007). In contrast, conditional Notch1 mutant mice exhibit severe overproduction of hair cells, an almost three-fold increase in hair cell numbers (Kiernan et al., 2005a). Furthermore, Notch inhibition in embryonic or neonatal cochlear explants with the gamma-secretase inhibitor DAPT similarly resulted in production of multiple rows of extra hair cells (Takebayashi et al., 2007; Yamamoto et al., 2006). Many, but not all, of the above loss-of-function studies reported that reduced supporting cell numbers accompanied the hair cell overproduction phenotypes observed, consistent with a change of cell fate. While restriction of hair cell fate is clearly an important role for Notch in development of the organ of Corti, the above

experiments and the methods of analysis employed have precluded effective analysis of possible roles for Notch in supporting cell development.

Maturation of the Organ of Corti

Most mammals are born with fully developed inner ear structures. However, the mouse cochlea is immature at birth, resembling that of a human fetus of 15 weeks (Jin et al., 2003). Cellular maturation of hair cells and supporting cells in the mouse is not complete until about two weeks after birth. Onset of hearing in mice and rats occurs at about 10 days after birth, and adult levels of hearing are not reached until a few weeks later (Raphael and Altschuler, 2003).

Hair cells and supporting cells undergo a series of genetic and morphological changes to progress towards their mature phenotypes. Upon upregulation of Atoh1, nascent hair cells downregulate $p27^{kip1}$, Sox2, and Jag1. Hair cells upregulate expression of the POU domain transcription factor Brn3c about one or two days following Atoh1 expression (Erkman et al., 1996). After Brn3c, developing hair cells upregulate expression of the unconventional myosins: myosinVI, followed by myosinVIIa and myosin15 (Karolyi et al., 2003). Brn3c is required for the maturation and survival of hair cells, as Brn3c-/- mice generate hair cells that express myosinVI, myosinVIIa, and calretinin, but they fail to develop sensory hair bundles and are lost from the inner ear by P14 (Bryant et al., 2002). The unconventional myosin genes have distinct roles in development and function of the sensory hair bundle, which is an array of actin-filled stereocilia located on the hair cell's apical surface essential for the process of mechanotransduction.

Relatively little is known about the mechanisms of supporting cell maturation. From early development through adulthood supporting cells express p27kip1, Sox2, and Jag1. Prox1, a mammalian homologue of the drosophila Prospero, is expressed in developing supporting cells (Deiters' and pillar cells) from E14.5 to about P10, and appears to be briefly coexpressed with Atoh1 in nascent outer hair cells, which rapidly downregulate Prox1 expression as they differentiate (Bermingham-McDonogh et al., 2006). Prox1 downregulation in Deiters' and pillar cells coincides with the opening of the tunnel of Corti, between P7 and P10 (Bermingham-McDonogh et al., 2006). In other parts of the nervous system Prox1 is transiently expressed in subsets of progenitor cells. Thus, Prox1 expression is associated with supporting cells during development and maturation, and is downregulated in mature supporting cells. Another marker of supporting cell development is the p75 neurotrophin receptor, which is expressed in developing pillar cells from late embryogenesis to about P4 (Sano et al., 2001). However, the function of p75 in pillar cell development is unclear, as p75-/- mice develop normal functional organs of Corti (Sato et al., 2006).

Recently, several studies have indicated that supporting cells have properties similar to glial cells in other parts of the nervous system. During postnatal maturation, inner and outer phalangeal supporting cells, which surround the inner hair cells, upregulate expression of the glutamate transporter GLAST (Furness et al., 2002; Furness and Lawton, 2003; Furness and Lehre, 1997; Jin et al., 2003). GLAST is widely expressed in glial cells in the CNS and is involved in the uptake of glutamate into glial cells following its release at glutamatergic synapses. Additionally, the intermediate filament glial fibrillary acidic protein (GFAP) is expressed in supporting cells during postnatal maturation and in adult mice (Rio et al., 2002). GFAP is a classic marker for

several types of glial cells, including astrocytes and nonmyelinating Schwann cells. Rio et al. used immunofluorescence and two transgenic reporter lines to provide evidence that GFAP is expressed in supporting cells and Schwann cells in the spiral ganglion (Rio et al., 2002).

Mechanisms of hair cell regeneration

Hair cell regeneration in the avian cochlea depends on the ability of surviving supporting cells to produce new hair cells in response to injury (Bermingham-McDonogh and Rubel, 2003; Morest and Cotanche, 2004). During regeneration, new hair cells are produced through a combination of a new wave of proliferation and direct supporting cell-to-hair cell transdifferentiation (Fig. 1.6, (Duncan et al., 2006; Roberson et al., 2004)). The mature avian auditory epithelium, the basilar papilla, is normally mitotically quiescent, similar to the mammalian organ of Corti. However, the supporting cells of the avian inner ear are much less morphologically differentiated than mammalian supporting cells. In fact, avian supporting cells somewhat resemble immature mammalian supporting cells. For example, supporting cells of the chicken lack the high level of cytoskeletal specializations found in mammalian supporting cells, which are associated with supporting cell polarity, pillar cell extension, and the phalangeal processes of Deiters' cells (Raphael and Altschuler, 2003). Additionally, a subset of mature avian supporting cells retains expression of Prox1 into adulthood and expression of this gene distinguishes progenitor cells during regeneration (Stone et al., 2003; Stone et al., 2004). Similarly, embryonic and perinatal mouse supporting cells appear to retain characteristics of multipotency, such as the ability to transdifferentiate into hair cells when Notch signaling is inhibited (Takebayashi et al., 2007; Yamamoto et

al., 2006). Furthermore, mouse embryonic and neonatal supporting cells express high levels of nestin, an intermediate filament associated with progenitors and stem cells; like Prox1, nestin expression in supporting cells is severely reduced during the maturation period (Lopez et al., 2004). Thus, mammalian supporting cells progressively lose characteristics of multipotent progenitors during the postnatal maturation period. Studies are needed to define the mechanisms regulating multipotency and maturation in the mammalian cochlea and the Notch signaling pathway is a potential regulator of these processes. Furthermore, hair cell damage induces responses in the mammalian cochlea, including apoptosis and scarring, that may affect properties of multipotency in surviving cells (Fredelius, 1988; Roberto and Zito, 1988; Thorne et al., 1984). As well, studies in other systems have indicated that Notch signaling is sometimes upregulated in response to damage, affecting the damage response (Arumugam et al., 2006; Chen et al., 2005; Givogri et al., 2006; Jurynczyk et al., 2005). Therefore, studies that elucidate the role of Notch signaling in cellular differentiation and maturation as well as the effect of injury on this pathway are an important step in the process of understanding the barriers to hair cell regeneration in mammals.

Figure 1.1 The mammalian inner ear (A) houses the cochlea and vestibular organs within bony and membranous labyrinthine compartments. The auditory sensory epithelium, the organ of Corti, lies on the basilar membrane within the cochlear duct. B A schematized transverse section through the organ of Corti shows the orderly anatomical arrangement of hair cells and supporting cells. C A wholemount preparation of a neonatal mouse cochlear epithelium with hair cells and supporting cells fluorescently immunolabeled in green and red, respectively, highlights the location of the organ of Corti. D A 3D rendered confocal z-series micrograph of the organ of Corti from a neonatal Atoh1-GFP reporter mouse shows the arrangement of rows of hair cells, expressing the Atoh1-GFP transgene. E Hair cells act as mechanosensory transducers: fluid-induced displacement of stereocilia bundles results in opening of ion channels, depolarization of the cell, and release of the neurotransmitter glutamate at afferent nerve terminals, uptake of glutamate by afferent spiral ganglion neurons results in firing of action potentials which are relayed through the central auditory pathway. F A 3D rendered confocal z-series micrograph surface view of the adult organ of Corti from a transgenic mouse expressing membrane-bound tomato fluorescent protein (mTomato) allows visualization of the stereocilia bundles of the rows of inner hair cells (IHCs) and three rows of outer hair cells (OHC1-1).

The Mammalian Auditory Sensory Epithelium

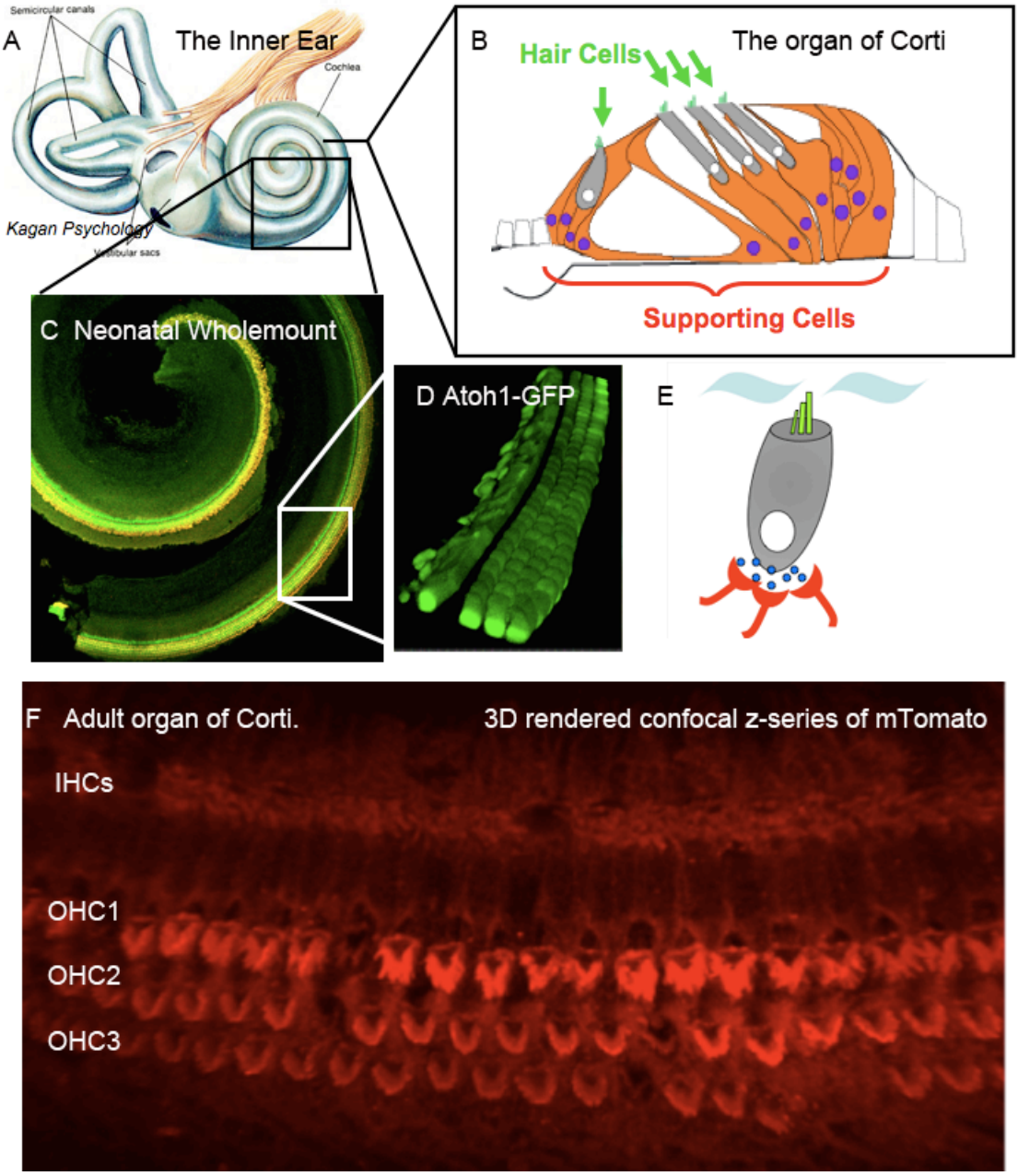

Figure 1.2 Schematic of model of Notch signaling as it regulates sensory progenitor specification and cellular differentiation in the developing cochlea. The upper panel depicts the Notch signaling mechanism, whereby Notch ligands in the Delta and Jagged families of transmembrane proteins are expressed on the surface of a "signal-sending" cell, which binds to the extracellular domain of the Notch receptor in the membrane of a neighboring "signal-receiving" cell. The activated Notch receptor undergoes a series of cleavage events, which result in the translocation of the Notch intracellular domain (NICD) to the nucleus, where it forms a transcriptional complex with cofactors Mastermind (MAM) and CBF1/*Supressor of hairless*/Lag-1 (CSL). Binding NICD converts the transcriptional complex from a repressor to an activator; it binds to CSL-binding sites in the promoter regions of downstream target genes, which primarily encode basic-helix-loop-helix transcriptional repressors of the *hairy and enhancer of spl*it (Hes) family. Hes gene products regulate transcription of other genes and, in the developing inner ear, may promote induction and maintenance of sensory progenitors and inhibit progenitor differentiation to hair cell fate. The lower panel depicts the proposed mechanisms of Notch signaling during two distinct phases of cochlear development: sensory induction (left) and cellular differentiation (right). During the sensory induction phase, which occurs early in cochlear development (about E10-E13), Jagged1 and Notch1 are coexpressed specifically in nascent sensory progenitors in the floor of the cochlear duct. Jagged1-Notch signaling occurs mutually between progenitors, which express the Notch targets, Hes-related genes *HesR1* and *HesR2*. During the later cellular differentiation phase of cochlear development (occurring between E14 and E18) another type of Notch signaling is required for accurate differentiation of hair cell and supporting cell types. Nascent hair cells upregulate expression of the Notch ligands Dll1, Dll3, and Jag2 and downregulate expression of Notch1. Neighboring nascent supporting cells continue to express Notch1 as well as well as Jag1. Differentiating hair cells (HC) activate Delta-Notch signaling in neighboring nascent supporting cells (SC), which express Hes1 and Hes5. These two Hes gene products, known to be potent inhibitors of neuronal and hair cell differentiation, inhibit nascent supporting cells from adopting a hair cell fate in a process known as lateral inhibition.

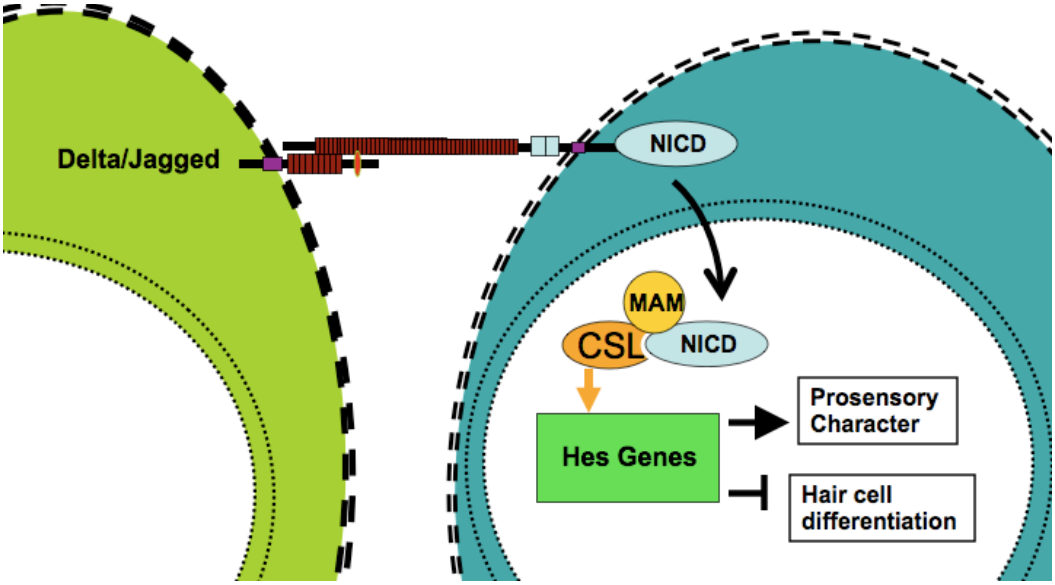
Delta/Jagged
NICD
MAM
CSL
NICD
Hes Genes
Prosensory Character
Hair cell differentiation

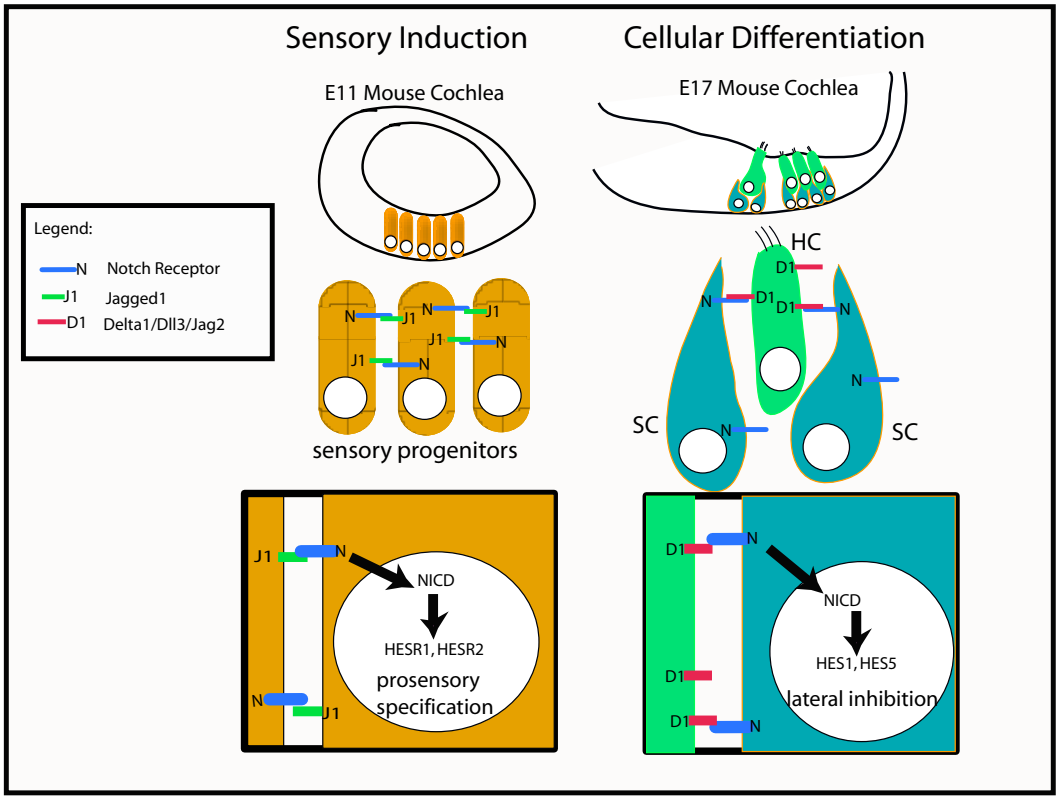
Sensory Induction
Cellular Differentiation
E11 Mouse Cochlea
E17 Mouse Cochlea
Legend:
N Notch Receptor
J1 Jagged1
D1 Delta1/Dll3/Jag2
HC
SC
SC
sensory progenitors
NICD
HESR1, HESR2
prosensory specification
NICD
HES1, HES5
lateral inhibition

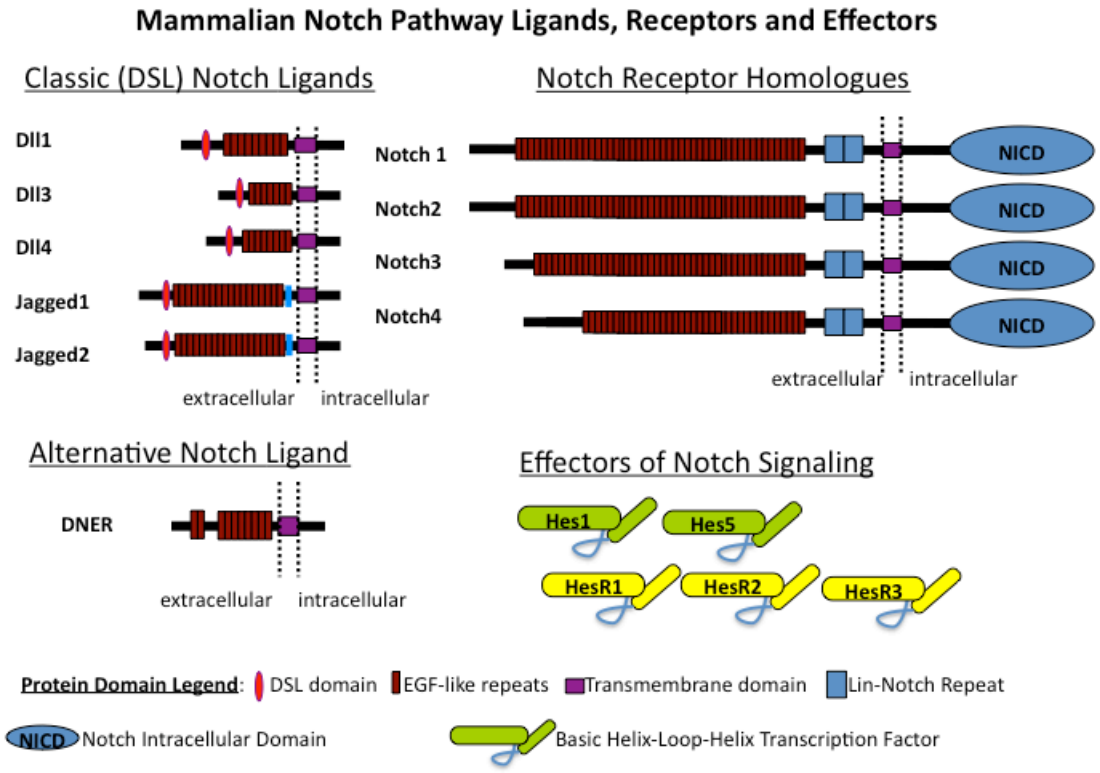

Figure 1.3 Diagram of key mammalian Notch pathway ligands, receptors, and effectors. Protein structures are schematized according to the protein domain legend at the bottom of the figure. Notch ligands and receptors have similar protein structure, both are transmembrane proteins with extracellular domains rich in EGF-like repeats. Classic Delta-Serrate-Lag2 (DSL) Notch ligands also contain a DSL domain, which is thought to bind to the Notch receptor. Mammals have three Delta-like (Dll) homologues, two Jagged homologues, and four Notch receptors. As well, Delta-Notch-like-EGF-related receptor (DNER) protein is thought to act as an alternative Notch ligand. Essential effectors of Notch signaling include hairy and enhancer of split (Hes) and Hes-related (HesR) genes, which encode basic-helix-loop-helix transcription factors that bind DNA as hetero- or homo-dimers. The mammalian Notch pathway contains abundant diversity in terms of spatial and temporal expression profiles of the Notch ligands and receptors, with many having either exclusive patterns or overlapping with their homologues depending on the context.

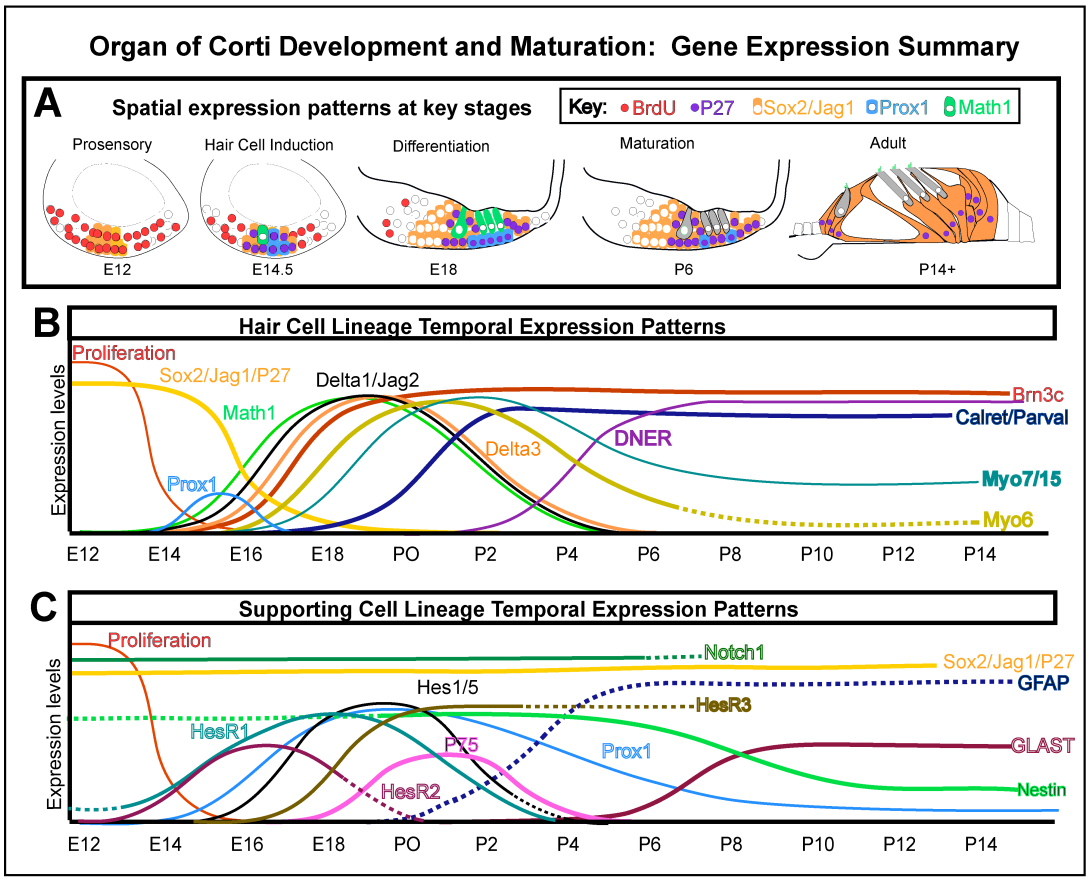

Figure 1.4 Stages of organ of Corti development with spatial and temporal summaries of gene expression patterns. A. Depiction of spatial expression patterns at five key stages of cochlear development. Stages of development and corresponding age in mice are indicated above and below the figures, respectively. They key on the right indicates the process or gene expression represented by each color. BrdU uptake and P27 expression are cell-cycle related and are indicated by red or purple nuclei, respectively. All other gene expression patterns are indicated here by cytoplasmic colors for simplicity, although all but Jag1 are transcription factors that actually localize to the nucleus. BrdU uptake in dividing cells is abundant during early development but becomes absent from nascent hair cells and supporting cells by about E14.5. Sox2 and Jag1 have nearly overlapping expression patterns within the prosensory domain and are later restricted to supporting cells. Atoh1 is strongly and specifically expressed in hair cells during embryonic development. Prox1 is initially expressed in progenitors in the outer hair cell region and becomes restricted to outer supporting cells during the cellular differentiation stage. Schematics of temporal expression patterns in cells of the hair cell lineage (B) and supporting cell lineage (C) in the developing cochlea. Expression levels over time are indicated by colored lines, and are not representative of relative expression between genes.

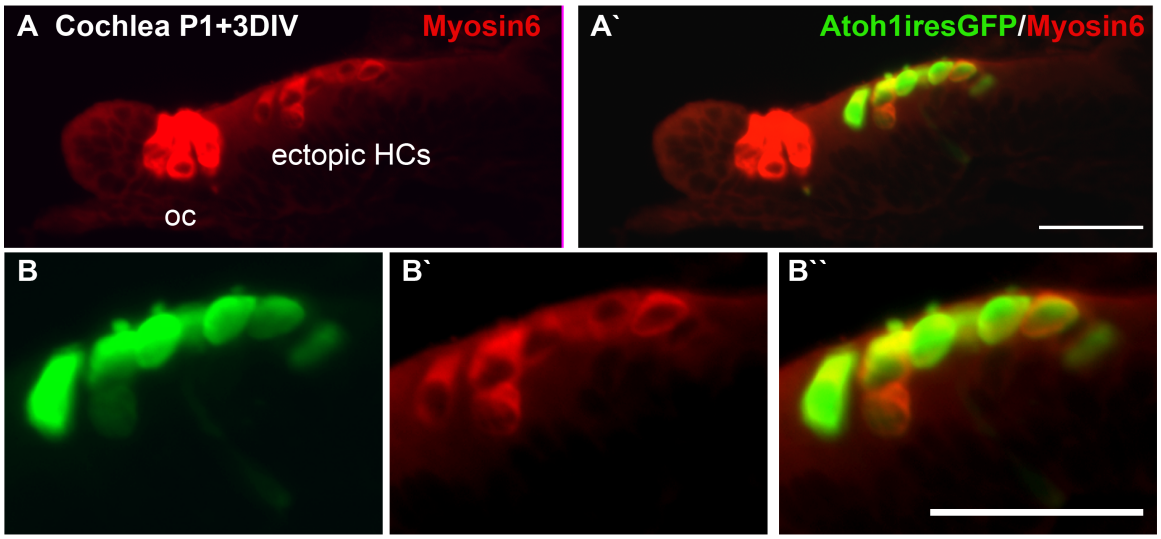

Figure 1.5 Atoh1 misexpression is sufficient to induce hair cell formation in nonsensory epithelia (GER). P1 rat cochlea explant was transfected with pMesAtoh1iresGFP and cultured for 3 days in vitro. This image shows a section stained with myosinVI, which can be seen in endogenous hair cells in the organ of Corti (OC) and ectopic hair cells induced by expression of the Atoh1 transgene. In this experiment I reproduced the results of Zheng and Gao, 2000.

Figure 1.6 Mammals do not regenerate damaged hair cells but birds and other non-mammalian vertebrates replace lost hair cells in response to damage. The upper panel in this figure illustrates the differences between mammals and birds in their response to hair cell damage as found in previous studies. Schematic transverse views of mammal and chick auditory epithelia are as indicated. Scanning EM micrographs from Lenoir and Puel (Lenoir and Puel, 1987) show surface views of the rat organ of Corti under normal conditions (left) and one month after aminoglycoside-induced hair cell damage (right). In this typical example of a severely damaged mammalian organ of Corti, inner and outer hair cells have been lost and a scarred epithelium remains. By contrast, studies such as this example in the chick from Girod et al. (Girod et al., 1989) have shown that regeneration does occur in birds and other non-mammalian vertebrates in response to hair cell damage. Scanning EMs here show a normal chick cochlea (BP, left), a lesioned BP 6 hours after acoustic trauma (center), and a regenerated BP 30 days after completion of noise exposure and subsequent functional recovery of hearing loss (right). The lower panel in this figure summarizes mechanisms of hair cell regeneration elucidated by earlier and more recent studies of the avian BP. A. A schematic of the normal chick BP illustrating hair cells and supporting cells. In the absence of damage the mature chick BP is mitotically quiescent. B. In response to noise- or drug-induced hair cell damage, hair cells are extruded from the epithelium and lost. C. Shortly after hair cell damage, the first mechanism of hair cell regeneration to occur is direct transdifferentiation of supporting cells to hair cells. D. The second mechanism by which regeneration occurs is proliferation of supporting cells, which results in *de novo* production of new hair cells as well as supporting cells. E. Through combination of transdifferentiation and proliferative regeneration mechanisms the mosaic of hair cells and supporting cells is nearly perfectly restored within several weeks of hair cell loss.

Mammals Do Not Regenerate Hair Cells

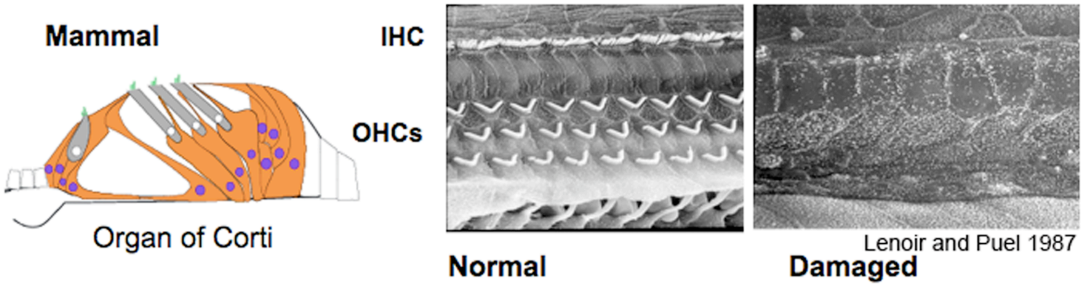

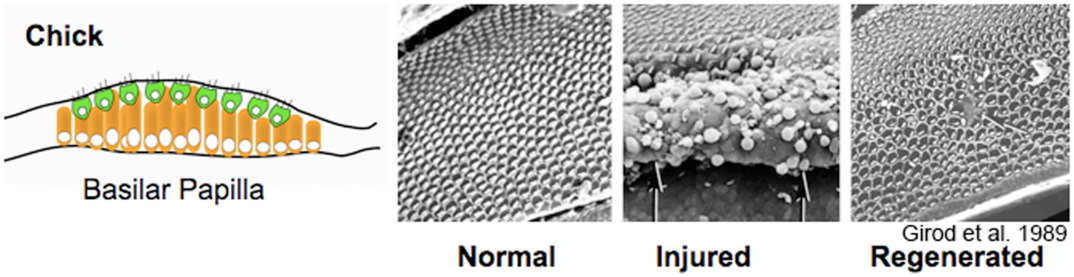

Mechanisms of Auditory Regeneration from Studies in the Avian Basilar Papilla

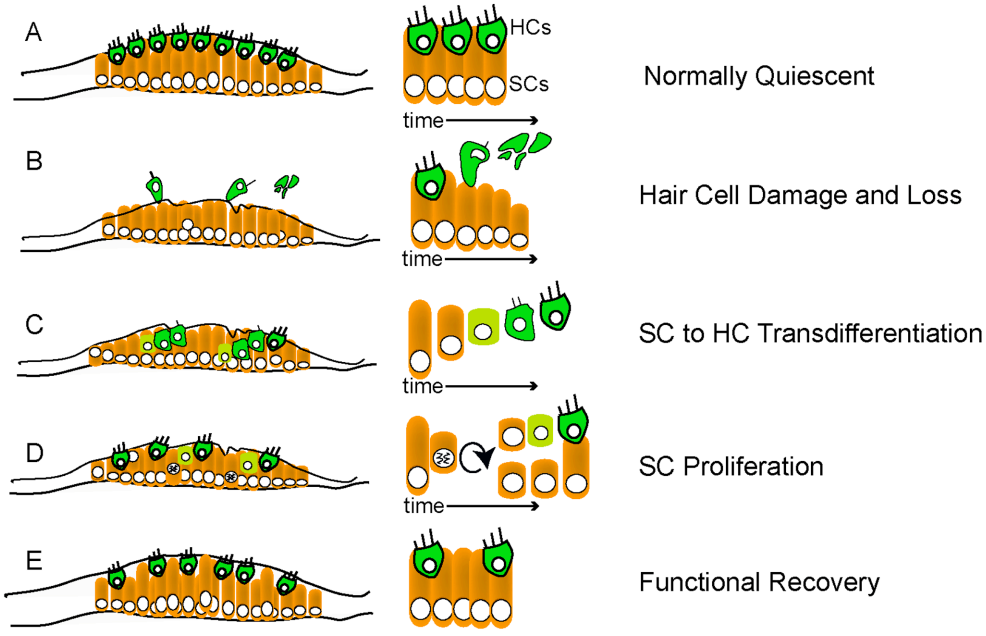

Chapter II:
Dll3 is expressed in developing hair cells in the mammalian cochlea[1]

SUMMARY

The Notch signaling pathway mediates the process of lateral inhibition that controls the production of sensory hair cells in the vertebrate inner ear. Nascent hair cells are known to express Notch ligands Dll1 and Jag2, which are thought to signal through the Notch1 receptor in adjacent supporting cells. However, recent genetic and pharmacological studies have suggested that the level of Notch-mediated lateral inhibition is greater than can be accounted for by Dll1 and Jag2. Here, we report that another Notch ligand, Dll3, is expressed in developing hair cells, following expression of Atoh1, and in a pattern that overlaps that of Dll1 and Jag2. We analyzed the cochleae of Dll3^{pu} mutant mice but did not detect any abnormalities. However, earlier studies have demonstrated that there is functional redundancy among Notch ligands in cochlear development and loss of one ligand can be at least partially compensated for by another. The expression pattern of Dll3 suggests a functional role in lateral inhibition complementing that of Dll1 and Jag2.

INTRODUCTION

The mammalian cochlea contains a specialized sensory epithelium called the organ of Corti, which mediates auditory function. The organ of Corti is composed of a highly ordered mosaic of mechanosensory hair cells and nonsensory supporting cells arranged in coiled rows. The orderly cellular arrangement and spatial and temporal

[1] Previously published in Developmental Dynamics, August 2007

gradients of differentiation in the organ of Corti offer advantages as a model system for sensory development and signaling. Interestingly, development of the organ of Corti has been found to rely on several highly conserved mechanisms and much of our understanding of this model system has drawn on advances in the field of *Drosophila* neural development.

One of the key signaling pathways that regulate the development of the organ of Corti is the Notch pathway. In many model systems, from the *Drosophila* neuroblast to vertebrate sensory organs, Notch is best known for its role in lateral inhibition. In the process of lateral inhibition, cells that become committed to a particular cell fate express Notch ligands and activate the Notch receptor in neighboring cells, preventing them from adopting the same fate (Cabrera, 1990; Heitzler and Simpson, 1991). In the mammal, there are four Notch receptors and several ligands including Delta-like (Dll) 1, 3 and 4; and Jagged (Jag) 1 and 2, referenced in (Sparrow et al., 2002).

There is a good deal of evidence to show that lateral inhibition mediated by Notch signaling controls final cell fate determination in the cochlea, regulating formation of the orderly mosaic of hair cells and support cells. In the mouse, Notch1 is expressed in the developing cochlea and there is evidence that Dll1 and Jag2 act through Notch1 to regulate lateral inhibition in the ear (Kiernan et al., 2005a; Lanford et al., 1999b; Zhang et al., 2000). Dll1 and Jag2 are expressed in nascent hair cells and loss of either gene in the developing cochlea has been shown to result in extra rows of hair cells (Brooker et al., 2006; Kiernan et al., 2005a; Lanford et al., 1999b; Morrison et al., 1999). When mutations in Dll1 and Jag2 were combined in Dll1hyp/- Jag2-/- mutant mice, cochleae displayed a greater increase in hair cell numbers, indicating that Dll1 and Jag2 act synergistically in hair cell development (Kiernan et al., 2005a).

In addition to Jag2 and Dll1, recent evidence suggests that there is an additional ligand for Notch in the developing organ of Corti. First, conditional Notch1 mutations in the otic epithelium of FoxG1-Cre Notch$^{flox/-}$ mice resulted in a far more dramatic increase in hair cell numbers than that observed in the Dll1$^{hyp/-}$ Jag2$^{-/-}$ cochlea (Kiernan et al., 2005a). Second, severe hair cell overproduction phenotypes were observed in cochlear explants treated with Notch1 antisense oligonucleotides or pharmacological inhibitors of Notch signaling (Takebayashi et al., 2007; Yamamoto et al., 2006; Zine et al., 2000). Here we report for the first time that Dll3 is expressed in developing hair cells in a pattern that closely overlaps with Dll1 and Jag2 throughout cochlear development. The pattern of Dll3 expression is consistent with a contributing role for Dll3 in lateral inhibition.

RESULTS

Dll3 is coexpressed with Dll1 and Jag2 in developing presumptive auditory inner hair cells at E15.5.

We used in situ hybridization to determine whether Dll3 is expressed in the developing cochlea. We were first able to detect this gene in the developing cochlea at E15.5 in a patch of one or two cells in the upper layers of the prosensory domain. In order to compare the temporal and spatial expression profiles of Dll3 with the other Notch ligands, Dll1 and Jag2, we probed similar E15.5 cochlear sections for these genes. Dll3, Dll1, and Jag2 are expressed in overlapping domains in the E15.5 mouse cochlea (Fig.1 A-L), in the presumptive inner hair cell domain, but not in the presumptive outer hair cell domain at this time.

We further confirmed that Dll3 is localized to the presumptive inner hair cell domain, by post-in situ immunolabeling for $p27^{Kip1}$ and Neurofilament-M (NF-M). The cell cycle regulator, $p27^{Kip1}$ labels the zone of nonproliferating cells and marks the location of the sensory precursor domain (Chen and Segil, 1999). Immunolabeling of probed tissues confirms that Dll3, Dll1, and Jag2 are expressed along the medial edge of the $p27^{Kip1}$ domain, in the two most basal turns of the cochlea at E15.5 (Fig.1M-O, and data not shown). Immunolabeling with antibody to NF-M reveals that the domain of Dll3 expression is within the region of extension of the peripheral processes of spiral ganglion neurons (Fig.1M-O).

We found that Dll3 expression follows slightly behind expression of Dll1 during cochlear development. It was previously reported that Dll1 and Jag2 are expressed in developing cochlear hair cells beginning at approximately E14.5 (Lanford et al., 1999b; Morrison et al., 1999). Similarly, we were able to detect strong expression of Dll1 in the basal turns of most E14.5 cochlea (Fig.2B,D); however, Dll3 was not detectable at this age (Fig. 2.2A,C). Even at E15.5, Dll1 and Jag2 expression appeared stronger than Dll3 expression in similar sections (Fig.1A-L), particularly in the mid-basal turn (Fig.1 B, E, H), which is less differentiated than the base. As well, while early Dll1 and Jag2 expression was observed in columns extending through the thickness of the epithelium (Fig1. E, H), Dll3 was restricted to cells near the lumen, which are presumably more differentiated. Thus, it appears that Dll3 is expressed slightly after Dll1 during the process of hair cell differentiation.

To further define the timing of Dll3 expression, we probed similar E15.5 sections for myosinVIIa and found that this marker of hair cells is not yet expressed in the

cochlea (data not shown). Therefore Dll3 expression occurs after Atoh1 and Dll1 but before expression of myosinVIIa in developing hair cells.

To investigate the temporal relationship between Dll3 expression and cell division, we labeled dividing cells at E14.5 with a two hour pulse of BrdU in-utero. We then probed tissue for expression of Dll3 and Dll1 with in situ hybridization and used immunofluorescence to identify cells that had incorporated BrdU. Expression of Dll1 in the cochlea was usually one or two cell diameters away from the BrdU positive region. However, we occasionally observed BrdU-positive cells within the region of Dll1 expression in the most basal portions of the E14.5 cochlea (Fig. 2.2F arrow). We never observed Dll3 expression to overlap with BrdU labeling.

Dll3 is expressed in developing inner and outer hair cells in the E17 mouse cochlea.

Dll3 continues to be expressed at later stages of cochlear development. In situ hybridization of cochleae at E17 revealed that Dll3 follows the wave of hair cell differentiation (Chen and Segil, 1999; Lim and Anniko, 1985) and is highly overlapping with expression of Dll1, Atoh1, and myosinVIIa (Fig. 2.3A-D and G-J). In the E17 cochlea, Dll3 is expressed in developing hair cells in a base to apex gradient that extends to the middle turn (Fig. 2.3A). Jag1 is expressed in supporting cells throughout most of the developing organ of Corti at this stage (Fig. 2.3E). Jag2 expression is also very similar to that of Dll3 at E17. Jag2 is expressed in developing hair cells, strongly in the basal turns and at a low level in the middle turn at E16.5 (Fig. 2.3M).

A close examination of the basal turn of E17 cochlear duct reveals that, in this region, Dll3 is expressed at a low level in inner hair cells and more strongly in outer hair

cells (Fig. 2.3G). Dll1, Atoh1, and myosinVIIa are also expressed at low levels in inner hair cells and higher levels in outer hair cells in the basal turn at this stage (Fig. 2.3H-J). This pattern is consistent with an inner hair cell to outer hair cell sweep of gene expression, where downregulation has begun in inner hair cells in the most basal region at this stage. In similar basal portions of the E17 cochlear duct, Jag1 is expressed at low levels in support cells and at higher levels in a subset of cells in the greater epithelial ridge medial to the region of developing inner hair cells (Fig. 2.3K). In the basal turn, Jag2 is expressed at a moderate level in inner hair cells and strongly in outer hair cells at this stage (Fig. 2.3N).

We used a combination of immunohistochemistry and in situ hybridization to examine the expression profile of Hes1 protein and Hes5 mRNA, two downstream targets of Notch signaling. In the E18 cochlea Hes1 is expressed in supporting cells and a population of cells in the greater epithelial ridge, medial to the inner hair cell region (Fig. 2.3O). Hes1 is also expressed in presumptive glial cells associated with the processes of spiral ganglion neurons. At E17, Hes5 expression is detected in developing Dieters' cells in the basal and middle turns of the cochlea (Fig. 2.3F, L).

Dll3 is downregulated in auditory hair cells in postnatal animals.

We also analyzed the expression of Dll3 in postnatal mouse cochlea. We probed sections of postnatal mouse cochlea (P0, P3, and P5) for expression of Dll3 and Dll1 to examine the time course of expression of these genes. All postnatal sections contained other head tissues known to express Dll3 and Dll1, such as brain and retina, and these served as positive controls (not shown). Low power views of similar P0 cochlea sections show that both Dll3 and Dll1 are expressed in hair cells at this stage

(Fig. 2.4A and B). Dll3 and Dll1 expression levels are strongest in the most apical hair cells and expression is low or undetectable in hair cells in the more basal regions. Furthermore, expression of Dll3 and Dll1 is stronger in outer hair cells than inner hair cells at this stage. Additionally, at P0, expression signal of Dll3 appears stronger than Dll1 and is still present in the middle turn while Dll1 is extremely low (Fig. 2.4C and D). By P3, we find that Dll3 and Dll1 are only expressed in hair cells in the most apical extremity of the organ of Corti, and expression is absent from all hair cells in the middle and basal regions (data not shown). Dll3 and Dll1 are not expressed in the cochlea of P5 animals, although high levels of expression were observed in retina at this stage. Thus Dll3 is downregulated after Dll1 in maturing hair cells.

Dll3 is not required for the normal development of the cochlea.

To test whether the expression of Dll3 is required for normal cochlear development, we examined the postnatal cochlea of Dll3 Pudgy (Dll3^{pu}) mutant mice (Kusumi et al., 1998). The Dll3^{pu} mutation is a 4-bp deletion in the third exon of Dll3, which leads to a frame shift and early truncation of the predicted protein product, prior to the DSL (Delta/Serrate/Lag2) domain (Gruneburg, 1961; Kusumi et al., 1998). Dll3^{pu} homozygous mutant mice are viable, but they exhibit a number of defects, including severe skeletal dysplasia and body truncation due to abnormal somite development (Kusumi et al., 1998). We crossed Dll3^{pu} homozygous mutant males with C57BL/6J females to create heterozygous progeny, which we then intercrossed to produce litters of mixed genotype. Dll3^{pu} homozygous mutant mice were identified by phenotype and all mice were genotyped for the 4-pb *pu* mutation with PCR.

We examined the inner ears from Dll3^{pu} homozygous mutants and wild-type control littermates at P3. The gross morphology of the inner ears from mutant mice was normal (data not shown). We processed cochlea for whole-mount fluorescent immunostaining with antibodies to myosinVIIa, to label hair cells, and Prox1, to label developing Dieters' and pillar cells (Bermingham-McDonogh et al., 2006). We examined the cochleae from seven Dll3^{pu} mutants and five control animals, obtained from three different P3 litters. The morphology and arrangement of hair cells and support cells was normal in Dll3^{pu} mutants, as compared to wild-type controls (Fig. 2.5). The normal appearance of one inner and three outer hair cells (Fig. 2.5A,B,E,F) and three Dieters' and two pillar cells (Fig. 2.5C,D,E,F) was observed throughout the length of the cochlea in all animals, with only minor exceptions. There was an average of 2-3 double inner hair cells per cochlea and regions of mild support cell disorganization in both mutant and control animals, which is likely attributed to the strain background (JAX® GEMM® Strain – Mutant Stock descended from an x-rayed (101/RI x C3H/RI) F1 male). Thus, our analysis indicates that Dll3 is dispensable for normal development of the cochlea.

DISCUSSION

Here we have reported that Dll3 is coexpressed with Dll1 and Jag2 in developing auditory hair cells beginning at E15.5. Previous studies have shown that hair cell differentiation in the cochlea propagates from the base to apex and from the inner hair cell domain to the outer hair cell domain and is marked by the concentrated expression of the proneural bHLH transcription factor Atoh1 (Bermingham et al., 1999; Chen et al., 2002; Hayashi et al., 2007; Lanford et al., 2000; Woods et al., 2004). We find that expression of hair cell-specific Notch ligands follows closely behind Atoh1

expression in the developing cochlea. While the onset of Dll1 expression in developing inner hair cells at E14.5 closely coincides and occasionally overlaps with cell cycle exit (Fig. 2.2.F), Dll3 expression occurs in the same population of cells approximately one day later. Lateral inhibition is thought to occur in cells surrounding Atoh1 expression, and possibly within the Atoh1 expressing population, beginning at E14.5. Therefore, although Dll3 is expressed slightly later than Dll1 in the developing hair cell domain, Dll3 is still expressed at the right time and place to play a role in lateral inhibition during cochlear development.

Dll3 continues to be coexpressed with Dll1 and Jag2 in developing inner and outer hair cells until birth and is downregulated during the first postnatal week. Expression of Dll3 in the cochlea follows the wave of hair cell differentiation as it sweeps from base to apex and inner hair cell to outer hair cell from E15.5 to P0. The period of Dll3 upregulation is followed by a wave of downregulation that occurs between E17 and about P3. Interestingly, this indicates that the duration of expression of Dll3, as well as Dll1 and Jag2, in individual hair cell precursors is only about three or four days, although duration of expression in cochlear hair cells as a whole lasts about eight days. Throughout this period of Dll3 expression, Dll1 and Jag2 are also expressed in hair cells, and undergo a similar down-regulation in the early postnatal period. The similarity in expression patterns among these three Notch ligands is consistent with an ongoing role for Dll3 in lateral inhibition.

The expression patterns of Hes1 and Hes5 indicate that they are potential downstream targets of Dll3/Notch signaling, and earlier studies have implicated Hes1 and Hes5 in lateral inhibition in the cochlea (Zine et al., 2001; Zine and de Ribaupierre, 2002). However, it is also likely that both Hes1 and Hes 5 also mediate the Notch signal

activated by Dll1 and Jag2. Another DSL ligand, Jag1 is expressed in the cochlea, but the expression pattern and results of knockout studies indicate that it does not function in lateral inhibition, but may have a role in prosensory specification that is still poorly understood (Fig. 2.3E,K) (Kiernan et al., 2001; Kiernan et al., 2006).

Dll3 is likely redundant for lateral inhibition with Dll1 and Jag2, since mice mutant in Dll3 (Pudgy Dll3^{pu}) do not have a defect in hair cell patterning. This result is not surprising given the redundancy of expression of DSL ligands in developing hair cells. Earlier studies have shown that loss of Jag2 or Dll1 alone results in relatively modest increases in hair cell numbers (Brooker et al., 2006; Kiernan et al., 2005a). More significant hair cell overproduction phenotypes in cochlea that carried mutations in both Jag2 and Dll1 indicate that there is synergistic function between ligands, and loss of one Notch ligand in hair cells can be compensated by others (Kiernan et al., 2005a). Therefore, Dll3 compensation could account for the mild phenotypes observed in Dll1 and Jag2 loss-of-function studies as compared to Notch1 mutation or Notch inhibition experiments (Lanford et al., 1999b; Takebayashi et al., 2007; Yamamoto et al., 2006).

Dll3 is the most divergent DSL ligand. Understanding of Dll3 function has been complicated by conflicting reports (Dunwoodie et al., 1997; Ladi et al., 2005). DSL ligands are thought to function in two ways, first in the well-characterized activation of Notch signaling through cell-cell interactions, and secondly as cell autonomous inhibitors of Notch signaling (Henrique et al., 1997; Jacobsen et al., 1998; Sakamoto et al., 2002). It has recently been reported that Dll3 does not activate Notch signaling like other DSL ligands, but that Dll3 does act as a cell autonomous inhibitor of Notch signaling (Ladi et al., 2005). Since we were unable to detect a phenotype in the Dll3 deficient mice, we are unable to determine whether Dll3 differs functionally from other

DSL ligands. Further studies, such as the generation of Dll3/Dll1/Jag2 double or triple mutants, may provide insight into this issue and the role of Dll3 in cochlear development.

METHODS

Animals

Mice were housed in the Department of Comparative Medicine and all procedures were performed in accordance with the guidelines of the Institutional Animal Care and Use Committee at the University of Washington. Embryonic and postnatal tissues from Swiss Webster mice were used for in situ hybridization and immunostaining. Dll3^{pu} mutant mice were obtained from Jackson Labs (stock # 00306). We crossed Dll3^{pu} homozygous mutant males with C57BL/6J females to create heterozygous progeny, which we then intercrossed to generate homozygous Dll3^{pu} and wild-type littermates for phenotypic analysis. Dll3^{pu} mice were genotyped for the 4-bp pudgy deletion in Dll3 exon 3 as described previously (Kusumi et al., 1998), with minor changes. Briefly, tail DNA was collected from postnatal mice and subjected to PCR using the following primers (5'-ACGAGCGTCCCGGTCTATAC-3' and 5'-AGGTGGAGGTTGGACTCACC-3'). The Dll3pu product (114bp) and wild type product (118bp) were resolved using 4% MetaPhor Agarose gel (Cambrex).

Paraffin In Situ Hybridization and Immunostaining

Embryos were collected from timed pregnant Swiss Webster or C57BL/6J mice and staged according to (Kauffman, 1992). For postnatal mice, P0 was defined as the day of birth. For BrdU incorporation study, timed pregnant E14.5 females received an

intraperitoneal injection of BrdU (50mg/kg) two hours prior to sacrifice. In situ hybridization was performed as previously described (Hayashi et al., 2007; Nelson et al., 2004). Briefly, embryonic whole heads or postnatal half-heads were fixed overnight at 4°C in a modified Carnoy's solution (60% EtOH/30% formaldehyde/10% acetic acid), dehydrated though an EtOH series, prepared for paraffin embedding, and sectioned at 8 µm. Digoxigenin-labeled probes were in vitro transcribed from linearized cDNA clones corresponding to: Dll3 (BC052002, IMAGE:6404029), Dll1 (BC057400, IMAGE:6402691), Jag2 (BC009082, IMAGE:3598850), Jag1 (BC058675, IMAGE:6834418), Atoh1 (BC051256, IMAGE:6530849), Hes5 (BC103539, IMAGE:40039948), and myosinVIIa (PCR clone corresponding to bp 1-1090 of NM_008663.1 cloned into pCRII-TOPO plasmid, O.BMcD.). Overnight hybridization and subsequent washes were carried out at 68^{o}C. Hybridized probe was detected using anti-Digoxygenin alkaline phosphatase conjugated antibody (1:2000 dilution, Roche Biochemicals, Indianapolis, IN) and visualized with NBT/BCIP for a blue precipitate. After in situ hybridization, sections were post-fixed in 4% paraformaldehyde and rinsed in PBS.

For immunostaining performed on paraffin sections following in situ hybridization, slides were blocked for 1 hr in 10% goat serum PBS with 0.1% TritonX-100 at room temperature. Primary antibodies were diluted in block and incubated overnight at 4^{o}C: mouse anti-p27 (1:500 dilution, BD Transduction Laboratories), rabbit anti-neurofilament-M (145 kDa; 1:1,000 dilution, Chemicon), rabbit anti-calretinin (1:2000 dilution, Swant). For BrdU labeling, rat anti-BrdU (1:100 dilution; Accurate Chemical) was diluted in blocking solution supplemented with100 Kunitz units/ml DNAse1. Slides were washed and incubated with corresponding goat secondary

antibodies at 1:500 for 1 hr at room temp. Secondary antibodies were species-specific AlexaFluor 488 or 568 nm (1:500, Invitrogen).

For Hes1 immunostaining of paraffin sections, antigen retrieval was performed by incubation in Revealit-Ag (Immunosolution; Jesmond, Australia) overnight at 37^{o}C. Slides were washed in PBS then blocked for 1 hr at room temperature. Primary antibody, rabbit anti-Hes1 (H140; 1:250 dilution, SantaCruz Biotechnology), was diluted in block and incubated overnight at 4^{o}C. Slides were washed and incubated with goat anti-rabbit alkaline phosphatase conjugated secondary antibody (A9919; 1:200 dilution, Sigma) for 2 hrs at room temperature. Slides were washed in PBS, equilibrated to alkaline pH in NTMT (100 mM NaCl, 100 mM Tris pH 9.5, 50 mM MgCl2, 0.1% Tween 20) and incubated with BCIP/NBT liquid substrate (Sigma) to form a blue precipitate.

After immunostaining, slides were coverslipped in Fluoromount G (Southern Biotechnology, Birmingham, AL). Images of stained sections were acquired on a Zeiss Axioplan 2 microscope equipped with DIC optics and a Spot camera. Images were compiled with Adobe Photoshop 7.0.

Whole Mount Immunostaining

Inner ear tissues were harvested from P3 mice and fixed in 4% paraformaldehyde for 3 hr at 4^{o}C then washed in PBS and the cochlear ducts were dissected from surrounding tissues. To expose the organ of Corti, the anlage of the stria vascularis was removed using fine forceps. Tissue was permeabilized in PBS/0.1% TritonX-100 for 1hr at room temperature and blocked for 2 hr in 10% goat serum PBS with 0.1% TritonX-100 at room temperature. Primary antibodies were diluted in block and tissues were incubated overnight at 4^{o}C: rabbit anti-Prox1 (AB5475;

1:1000, Chemicon) and guinea pig anti-myosinVIIa (1:2000 dilution, gift from Stefan Heller, Stanford University). Tissues were washed in block and incubated overnight at 4^{o}C in secondary antibodies: chicken anti-rabbit AlexaFluor 488 nm and goat anti-guinea pig AlexaFluor 568 nm (both at 1: 500, Molecular Probes). Tissues were washed in PBS and coverslipped in PBS/Glycerol. Confocal images of whole mounts were captured on a Zeiss LSM Pascal confocal microscope. Images were processed using Improvision Volocity (3.0.2) and Adobe Photoshop (7.0).

Figure 2.1 Dll3 is coexpressed with Dll1 and Jag2 in developing presumptive inner hair cells at E15.5. Similar sections of E15.5 cochlea were probed for expression of Dll3 (A-C), Dll1 (D-F), Jag2 (G-I), and Atoh1 (J-L) with in situ hybridization. On the right are high magnification views of mid-basal (B, E, H, K) and basal (C, F, I, L) turns boxed in (A, D, G, J), respectively. (A-C) Expression of Dll3 is observed in the presumptive inner hair cell domain strongly in the basal turn (C) and at a low level in the mid-basal turn (B). Expression patterns of Dll1 and Jag2 are similar to Dll3, but both are expressed more highly than Dll3 in the mid-basal turn (compare B to E, H). (J-L) Strong expression of Atoh1 (Math1) marks the column of presumptive inner hair cell precursors (arrowheads) and weaker, more lateral expression of Atoh1 marks the region of presumptive outer hair cell precursors (brackets). (M-O) Post *in situ* hybridization immunolabeling with p27 (green) and NF-M (red) confirms that expression of Dll3 is localized to the presumptive inner hair cell domain. Scale bar in A is 100μm and applies to A, D, G, J. Scale bar in B is 50μm and applies to B,C, E, F, H, I, K, L.

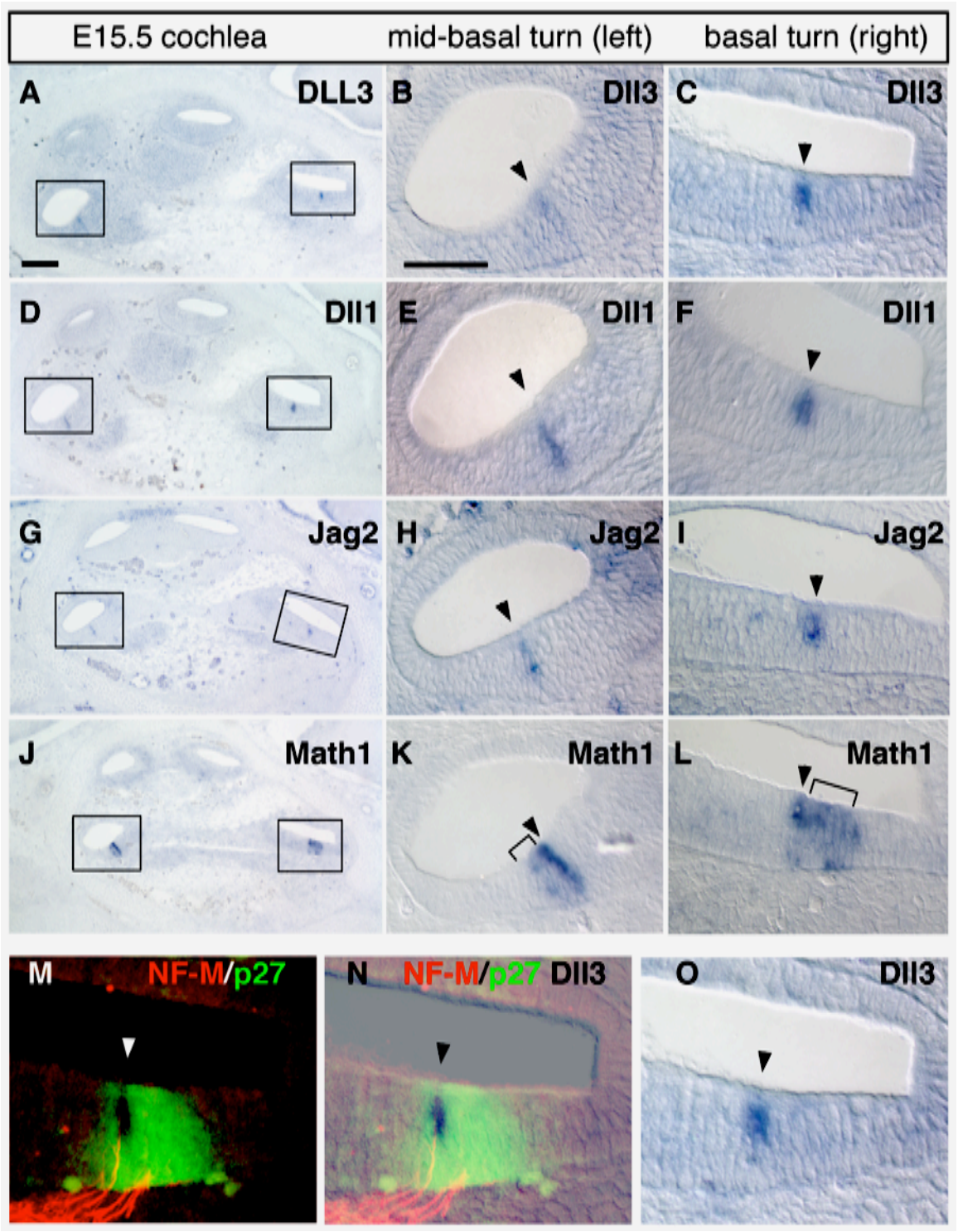
E15.5 cochlea
mid-basal turn (left)
basal turn (right)
A
DLL3
B
Dll3
C
Dll3
D
Dll1
E
Dll1
F
Dll1
G
Jag2
H
Jag2
I
Jag2
J
Math1
K
Math1
L
Math1
M
NF-M/p27
N
NF-M/p27 Dll3
O
Dll3

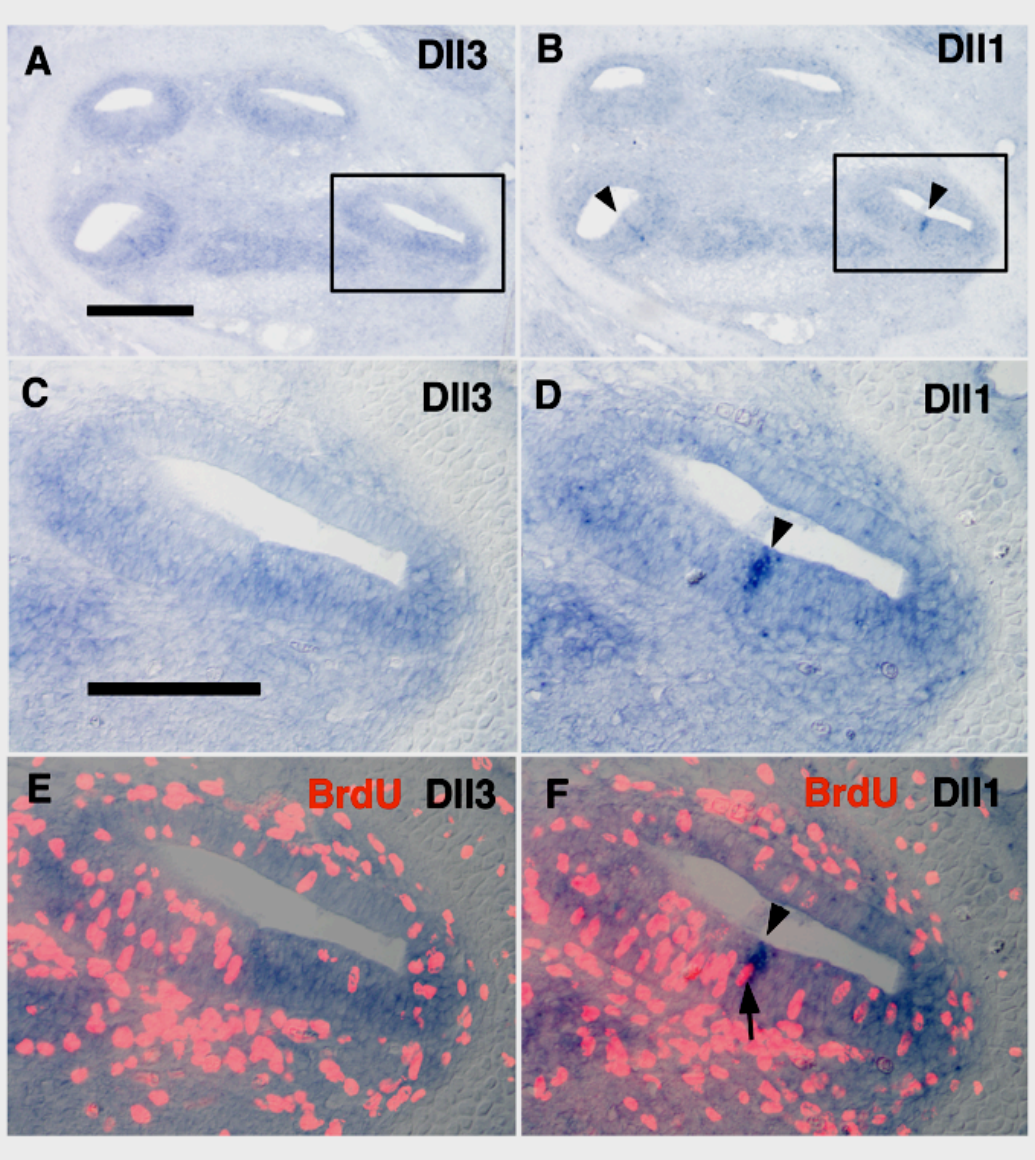

Figure 2.2 Onset of Dll3 expression occurs after expression of Dll1. Adjacent sections of E14.5 mouse cochlea were probed for expression of Dll3 (A,C,and E) or Dll1 (B,D,F) with in situ hybridization. Dll3 is not expressed at this stage, while Dll1 is expressed in the two basal turns. Embryos were given a 2 hour pulse of BrdU in-utero and sections were stained with antibody to BrdU after processing for *in situ* hybridization. The region of Dll1 expression was typically one or two cell diameters away from the nearest BrdU positive cells. Occasionally BrdU-positive cells were observed to overlap Dll1 expression (D,F arrow). Scale bar in A is 200μm and applies to A,B. Scale bar in C is 100μm and
applies to C-F.

Figure 2.3 (A-D) *In situ* hybridization of similar E17 sections shows that the pattern of Dll3 expression in developing inner and outer hair cells is highly overlapping with expression of Dll1, Atoh1, and myosinVIIa, while Jag1 and Hes5 have distinct patterns of expression in support cells (asterisks indicate regions of expression). (G-L) High power DIC images of the boxed regions in A-F. (Inner hair cells and outer hair cells are indicated with arrows and arrowheads, respectively.) (G-J) Expression of Dll3, Dll1, Atoh1, and myosinVIIa is observed in a low level in inner hair cells and a stronger level in outer hair cells. (K) Jag1 is expressed in support cells as well as a population of cells in the greater epithelial ridge. (L) Hes5 expression is detected in the region of presumptive Deiters' cells. (M) Jag2 expression at E16.5 is found in inner and outer hair cells (N) High power view of boxed region in M. (O) Hes1 antibody staining (blue) in E18 cochlea is found in supporting cells and a population of cells in the greater epithelial ridge. Scale bar in A is 200μm and applies to A-F,M. Scale bar in G is 100μm and applies to G-L,N,O.

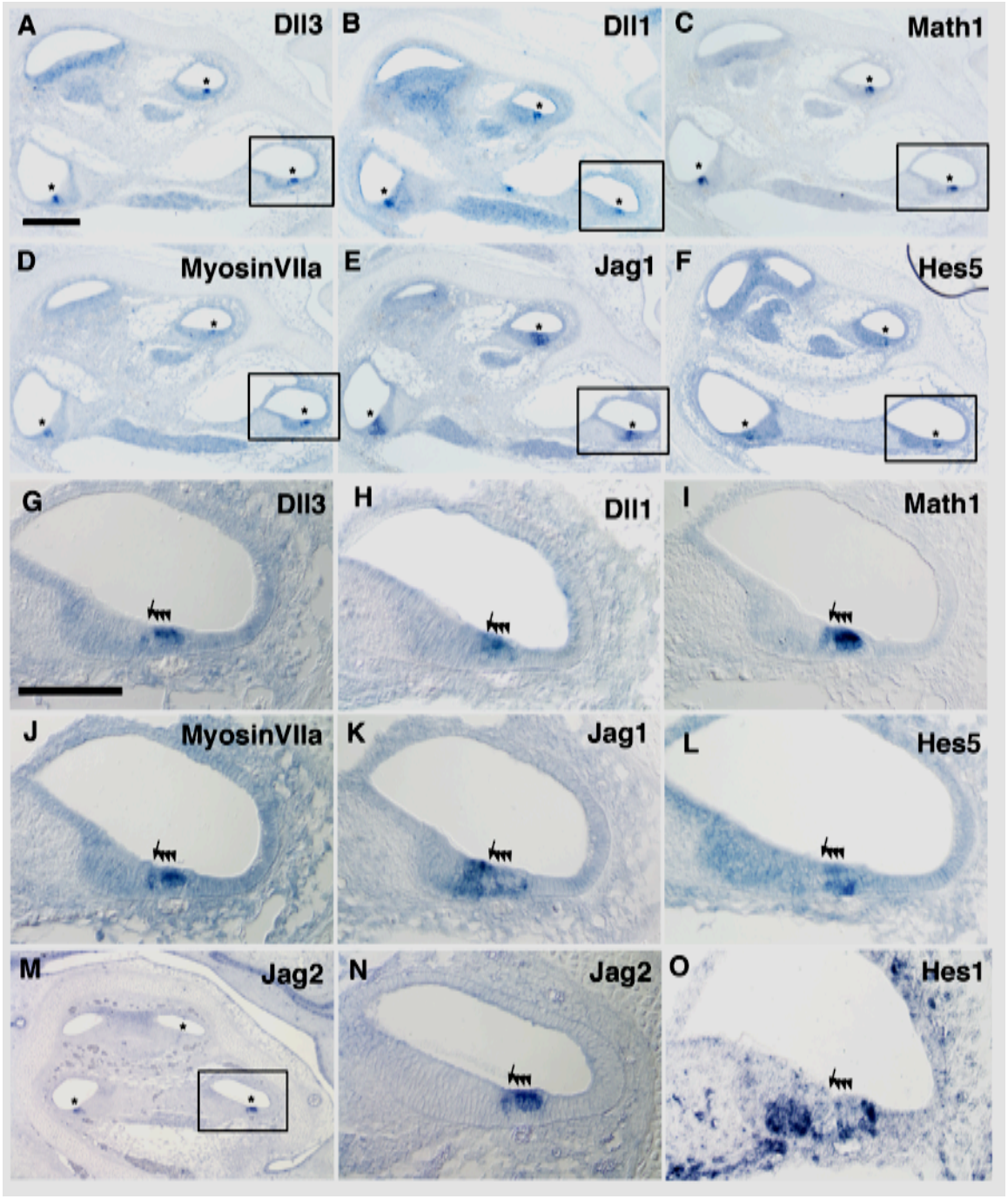
A
Dll3
B
Dll1
C
Math1
D
MyosinVIIa
E
Jag1
F
Hes5
G
Dll3
H
Dll1
I
Math1
J
MyosinVIIa
K
Jag1
L
Hes5
M
Jag2
N
Jag2
O
Hes1

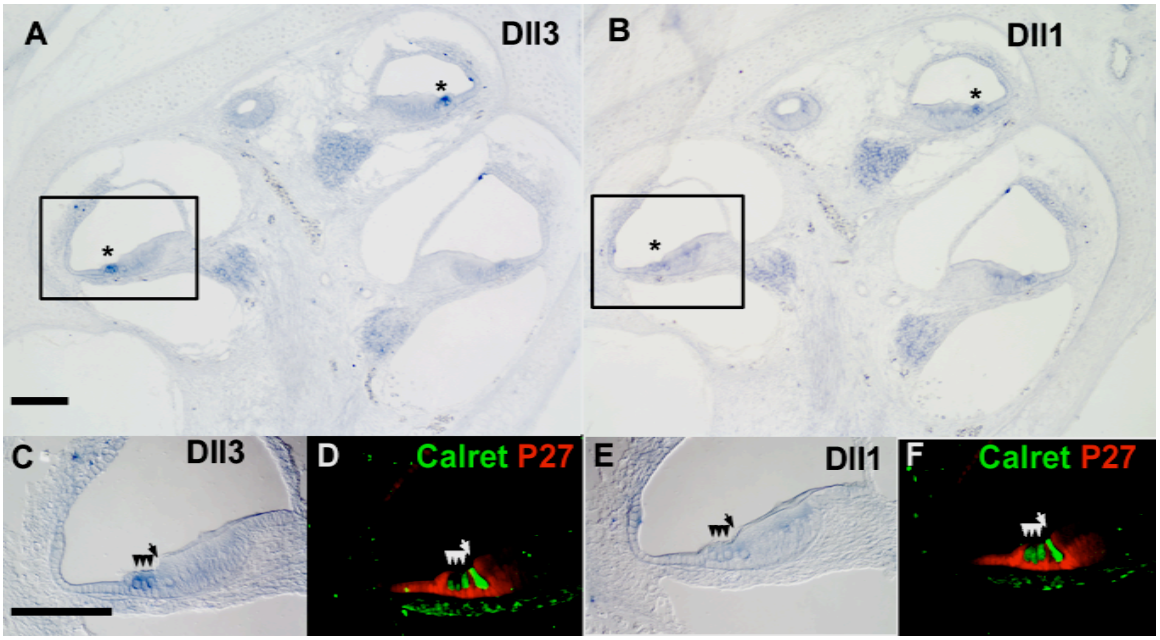

Figure 2.4 Dll3 is downregulated in auditory hair cells in the postnatal cochlea. (A,B) Low power images of similar P0 cochlea sections containing two middle turns and one apical turn probed for Dll3 and Dll1 show that both genes are expressed in hair cells at this stage. Expression of Dll3 and Dll1 is strongest in the hair cells in the two most apical turns and is low or absent in hair cells of the lower middle turn (regions of expression marked by asterisks). (C-F) High power images of the upper middle turn region show expression of Dll3 (C) and Dll1 (E) in hair cells. D and F are the same fields as C and E, respectively. Post *in situ* hybridization immunolabeling with calretinin (hair cells, green) and p27 (support cells, red) confirms that expression of Dll3 and Dll1 is restricted to hair cells (D,F). Scale bars: 100μm.

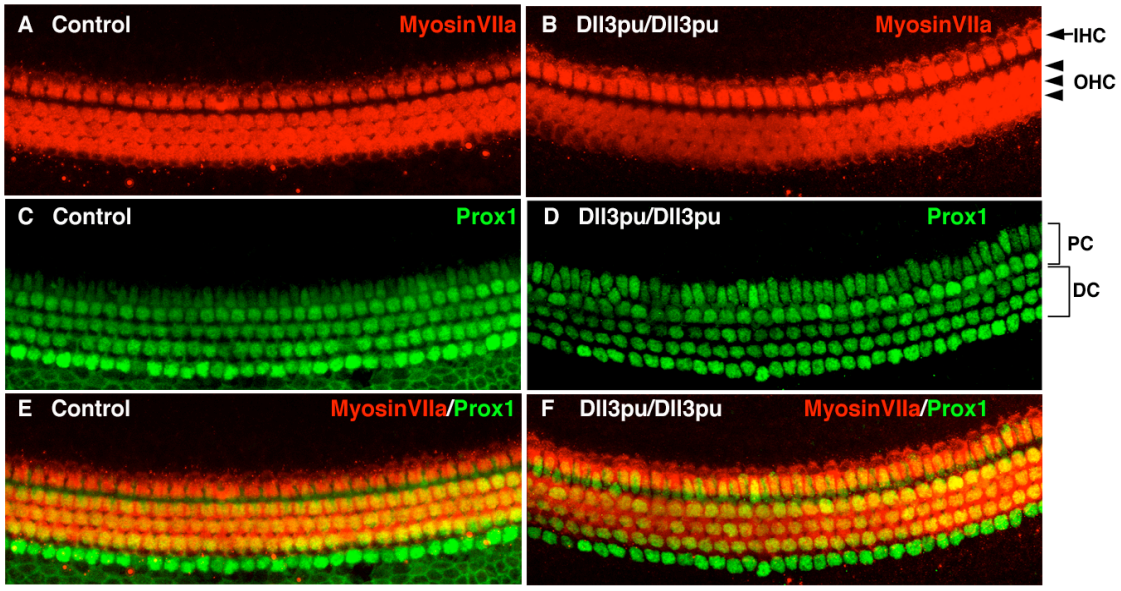

Figure 2.5 Dll3 is not required for normal development of hair cells and support cells. (A,B) myosinVIIa immunolabeling (red) of basal turn hair cells of wild-type control and Dll3pu homozygous mutant cochlea collected at P3. Control and mutant cochlea both have the normal arrangement of one inner hair cell (IHC, arrow) and three outer hair cells (OHC, arrowheads). (C,D) Prox1 immunolabeling (green) of the same basal turn cochlear regions as in A and B indicates that Dll3pu mutants exhibit normal pillar cell (PC, small bracket) and Deiters' cell (DC, large bracket) development. (E,F) Merged views of A and C and B and D, respectively.

Chapter III:
Hes5 expression in the postnatal and adult mouse inner ear and the drug-damaged cochlea[2].

SUMMARY

The Notch signaling pathway is known to have multiple roles during development of the inner ear. Notch signaling activates transcription of *Hes5*, a homologue of *Drosophila hairy and enhancer of split*, which encodes a basic helix-loop-helix (bHLH) transcriptional repressor. Previous studies have shown that *Hes5* is expressed in the cochlea during embryonic development, and loss of *Hes5* leads to overproduction of auditory and vestibular hair cells. However, due to technical limitations and inconsistency between previous reports, the precise spatial and temporal pattern of *Hes5* expression in the postnatal and adult inner ear has remained unclear. Here, we use Hes5-GFP transgenic mice and in situ hybridization to report the expression pattern of *Hes5* in the inner ear. We find that *Hes5* is expressed in the developing auditory epithelium of the cochlea beginning at embryonic day 14.5 (E14.5), becomes restricted to a particular subset of cochlear supporting cells, is downregulated in the postnatal cochlea and is not present in adults. In the vestibular system, we detect *Hes5* in developing supporting cells as early as E12.5 and find that *Hes5* expression is maintained in some adult vestibular supporting cells. In order to determine the effect of hair cell damage on Notch signaling in the cochlea, we damaged cochlear hair cells of adult Hes5-GFP mice *in vivo*, using injection of kanamycin and furosemide. Although outer hair cells were killed in treated animals and supporting cells

[2] Previously published in the Journal of the Association for Research in Otolaryngology, 2009

were still present after damage, supporting cells did not upregulate Hes5-GFP in the damaged cochlea. Therefore, absence of Notch-Hes5 signaling in the normal and damaged adult cochlea is correlated with lack of regeneration potential, while its presence in the neonatal cochlea and adult vestibular epithelia is associated with greater capacity for plasticity or regeneration in these tissues; which suggests that this pathway may be involved in regulating regenerative potential.

INTRODUCTION

The mammalian inner ear sensory epithelia are composed of mechanosensory hair cells and nonsensory supporting cells. Auditory hair cells, in the cochlea, detect sound, while hair cells in the five vestibular organs detect signals associated with angular and linear movements of the head. Supporting cells share a common progenitor with hair cells (Fekete et al., 1998) and are a morphologically diverse population of epithelial cells that surround hair cells and provide structural and functional support.

Auditory hair cells are susceptible to damage due to a variety of environmental factors and hair cell death is irreversible in mammals. However, birds and other nonmammalian vertebrates have been shown to be capable of hair cell regeneration, and subsequent gain of hearing, after injury (for reviews, see (Bermingham-McDonogh and Rubel, 2003; Oesterle and Stone, 2008; Stone and Cotanche, 2007). In mammals, when damaged hair cells are extruded from the organ of Corti, supporting cells close the lesions and are reorganized but they do not proliferate or transdifferentiate into new hair cells (Forge, 1985; McDowell et al., 1989; Oesterle et al., 2008; Raphael and Altschuler, 1991; Taylor et al., 2008; Wu et al., 2001). Little is known, however, about

the changes in gene expression that do occur in mammalian supporting cells after hair cell damage, and whether or not developmental mechanisms are reinitiated.

The Notch signaling pathway is a potent regulator of progenitors and stem cells and known to play several key roles during inner ear development: initially Notch activity is essential to establish prosensory domains (Brooker et al., 2006; Daudet et al., 2007; Daudet and Lewis, 2005; Hayashi et al., 2008; Kiernan et al., 2006); subsequently it is involved in establishing hair cell and supporting cell fates and patterning via “lateral inhibition” (Brooker et al., 2006; Chitnis, 1995; Daudet and Lewis, 2005; Kiernan et al., 2005a; Lanford et al., 1999b; Pickles and van Heumen, 2000). Notch signaling activates transcription of *Hes5*, a mammalian homologue of *Drosophila hairy and enhancer of split*, which encodes a basic helix-loop-helix (bHLH) transcriptional repressor (Kageyama and Ohtsuka, 1999b; Ohtsuka et al., 1999). Previous studies have shown that *Hes5* is expressed in subsets of cochlear and vestibular supporting cells during embryonic development (Lanford et al., 2000; Li et al., 2008b; Shailam et al., 1999; Tang et al., 2006; Zheng et al., 2000; Zine et al., 2001); however, due to technical limitations and inconsistency between previous reports, the precise spatial and temporal pattern of *Hes5* expression in the developing and adult inner ear has remained unclear. Here, we use Hes5-GFP transgenic mice (Basak and Taylor, 2007) and in situ hybridization to report the expression pattern of *Hes5* in the inner ear through embryonic and postnatal development and in adults. We find that Hes5-GFP mimics the expression of *Hes5* and provides superior sensitivity and cellular resolution. In the cochlea, we describe the onset of Hes5-GFP expression at E14.5, its subsequent restriction during development to a subset of supporting cells where it persists through the first postnatal week, after which it becomes downregulated and is

no longer expressed in the adult. In the vestibular system, we report that Hes5-GFP is expressed in supporting cells of all five vestibular organs during development and continues to be expressed in a subset of supporting cells in the adult.

In order to further understand the responsiveness of mammalian cochlear supporting cells to hair cell death, we induced hair cell damage in adult Hes5-GFP mice via injections of kanamycin and furosemide and analyzed cochlear tissues to see if Hes5-GFP is upregulated in the damaged cochlea. Although outer hair cells were rapidly lost in treated Hes5-GFP animals and supporting cells remained largely intact, there was no upregulation of Hes5-GFP. Thus, Notch-Hes5 signaling is not active in the mature cochlea under normal or damaged conditions. Taken together with earlier studies, our findings indicate that absence of Notch-Hes5 signaling in the adult cochlea is correlated with lack of regeneration potential, while its presence in the neonatal cochlea and adult vestibular epithelia is associated with greater capacity for plasticity or regeneration in these tissues; which suggests that this pathway may be involved in regulating regenerative potential.

RESULTS

Hes5-GFP expression in the developing cochlea mimics the pattern of *Hes5* transcription.

Hes5 has been reported to be expressed in the embryonic cochlea; however there is some debate over the specific spatial and temporal pattern of its expression (Lanford et al., 2000; Tang et al., 2006; Zheng et al., 2000; Zine et al., 2001). Moreover, the expression pattern of *Hes5* in the postnatal and adult mammalian cochlea has not been investigated. We used Hes5-GFP transgenic mice and in situ hybridization to

determine the expression pattern of *Hes5* in the embryonic and postnatal cochlea. In order to determine the spatial and temporal pattern of *Hes5* expression during embryonic and neonatal development, we performed in situ hybridization for *Hes5* in paraffin sections of mouse cochlear tissues from E12.5 – P0. We compared the pattern of *Hes5* in situ hybridization signal with the pattern of Hes5-GFP expression in similar cochlear sections from age-matched Hes5-GFP mice (Fig. 3.1). At all ages, we found that the pattern of Hes5-GFP mimics the pattern of *Hes5* mRNA labeling via in situ hybridization with remarkable precision. Using both methods, we first detected *Hes5* in the developing auditory epithelium of the cochlea at E14.5, where it appears as a restricted band of cells in the medial floor of cochlear duct (Fig. 3.1A-A' and B-B'). Hes5-GFP immunolabeling was detectable at this age in the base and apex of the cochlear duct as well as in the spiral ganglia (Fig. 3.1A-A'). In the auditory sensory epithelium at this age, the intensity of Hes5-GFP expression was stronger in the basal turns than in the most apical turn, where it appeared faint and dispersed (Fig. 3.1A). In situ hybridization signal for *Hes5* in the cochlea at this early time-point was weak but clearly restricted to a similar narrow band of cells in the central floor of the cochlear duct in the basal turns and presumptive glial cells in the spiral ganglia (Fig. 3.1B-B'). In the apex of the cochlea, at this age, we were not able to discriminate signal from background using in situ hybridization for *Hes5,* presumably due to lower sensitivity of in situ hybridization compared to detection of Hes5-GFP (Fig. 3.1B-B'). We did not detect *Hes5* expression in the nascent cochlear duct or spiral ganglia at E12.5 or E13.5 using in situ hybridization or Hes5-GFP, although we did find Hes5-GFP expression in the developing vestibular patches at both of these ages, consistent with earlier findings (data not shown, (Shailam et al., 1999). At E17.5, developing inner and outer hair cells

(arrows and arrowheads, respectively, in Fig. 3.1C and D) and supporting cells have become specified and can be identified, based on their location and morphology, in transverse sections through the auditory epithelium. With in situ hybridization, we found that *Hes5* expression at this stage is restricted to a particular subset of cochlear supporting cells. Specifically, *Hes5* expression appears to be strong in the region of Dieters' and outer pillar cells, which lie underneath the outer hair cells, and less intense in the more medial supporting cells, which surround the inner hair cells, and a population of cells in the greater epithelial ridge (GER) (Fig. 3.1D). Similarly, Hes5-GFP expression at E17.5 (Fig. 3.1C) is strong in Dieters' and outer pillar cells. Lower intensity expression is seen in the supporting cells surrounding the inner hair cells, including the inner pillar cells, inner phalangeal cells, border cells, and a portion of the cells in the GER. At birth the pattern of *Hes5* expression in the Hes5-GFP mouse and tissue probed with *Hes5* (Fig. 3.1E and F, respectively) is similar to that seen at E17.5, strong in the four supporting cells that underlie the outer hair cells and less intense in the more medial supporting cells. The organ of Corti is more differentiated at this stage and individual cells can more easily be identified in these transverse sections, but the overall pattern of *Hes5* expression at birth is very similar to that at E17.5. The Hes5-GFP signal in the spiral ganglia appeared strongest at E14.5, where it could be seen in glia surrounding the spiral ganglion neuron cell bodies and, weakly, in glia tracking along the nerve fibers to the developing organ of Corti (Fig. 3.1A and A'). By E17.5 the Hes5-GFP expression was notably reduced in the spiral ganglia compared to the organ of Corti, only faintly visible surrounding the spiral ganglion neuron cell bodies and undetectable in the fiber tracks (data not shown, and Fig. 3.1C.) Hes5-GFP could still

be very faintly detected in glia surrounding the spiral ganglion neurons as late as P3 (data not shown), but was not seen at later ages.

Hes5-GFP is expressed in the developing organ of Corti at E14.5.

We used Sox2 and Jag1 immunolabeling to further characterize the spatial pattern of Hes5-GFP in the E14.5 cochlea. At this time point in cochlear development, the prosensory region has been specified and hair cell differentiation, marked by expression of *Atoh1*, is just beginning (Chen et al., 2002; Woods et al., 2004). *Jagged1* (*Jag1*) encodes a Notch ligand known to be expressed in, and required for establishment of, the early prosensory domains of the inner ear during development and later becomes restricted to auditory and vestibular supporting cells (Brooker et al., 2006; Kiernan et al., 2001; Lewis et al., 1998; Morrison et al., 1999; Oesterle et al., 2008; Tsai et al., 2001; Zine et al., 2000). We labeled E14.5 Hes5-GFP cochlea cryosections with antibodies to Jag1 and GFP (Fig. 3.2A and B-B''). We found that the region of Hes5-GFP expression, in the central floor of the cochlear duct, is adjacent to and partially overlapping with the Jag1 domain on the medial side (Fig. 3.2B-B''). The region of Jag1 labeling appears most intense at its lateral edge, where it merges with the Hes5-GFP region. Similarly, the strongest Hes5-GFP labeling can be seen at the medial side of the Hes5-GFP domain, adjacent to the Jag1 region.

Sox2 is a HMG-box transcription factor required for development of the inner ear sensory epithelia (Kiernan et al., 2005b). Expression of Sox2 marks the early prosensory domain of the cochlea, and is restricted to supporting cells during development and in the mature cochlea (Dabdoub et al., 2008; Hume et al., 2007; Kiernan et al., 2005b; Oesterle et al., 2008). At E14.5, Sox2 is expressed at high levels

in the medial floor of the cochlear duct and a lower level in the region of the GER (Fig. 3.2C'-C''). The region of high Sox2 expression is overlapping with Hes5-GFP (Fig. 3.2C''). Thus, *Hes5* expression first occurs in the central floor of the cochlear duct at E14.5 within the prosensory domain from which the organ of Corti arises.

Hes5-GFP is restricted to a specific subset of cochlear supporting cells during development.

Our initial analysis of *Hes5* expression with in situ hybridization and Hes5-GFP indicated that expression of this gene is restricted to a subset of supporting cells during late embryonic development (Fig. 3.1C-F). We found that this pattern of *Hes5* expression in the organ of Corti is maintained in the neonatal cochlea. To further characterize the pattern of *Hes5* expression and understand the arrangement and cellular structure of the *Hes5*-positive supporting cell population we performed immunolabeling and imaging analysis of Hes5-GFP cochlea at P3 (Fig. 3.3). Prox1 specifically marks the nuclei of the two rows of pillar cells and three rows of Dieters' cells in the developing and postnatal cochlea (Fig. 3.3B-B', (Bermingham-McDonogh et al., 2006; Kirjavainen et al., 2008). We used Prox1 immunolabeling in whole-mount preparations of P3 Hes5-GFP cochlea to confirm the expression of Hes5-GFP in the Prox1-positive supporting cell population (Fig. 3.3A–C and A'-C'). In surface (XY plane, Fig. 3.1A'-C') and transverse (ZY plane, Fig. 3.3A-C) views of P3 cochlea taken from confocal z-sectioned micrographs, all Prox1-positive supporting cells are labeled with Hes5-GFP. The Hes5-GFP fills the supporting cells, revealing the long extensions of the pillar cells and Dieters' cells that intercalate between the hair cells and span the depth of the epithelium (Fig. 3.3A).

We used similar preparations and imaging methods of whole-mount P3 cochlea labeled with anti-calretinin to examine the spiral ganglion nerve endings and their spatial relationship with the Hes5-GFP-positive supporting cells (Fig. 3.3D-F'). Calretinin is a calcium binding protein expressed in type I spiral ganglion cells and inner and outer hair cells in the neonatal cochlea ((Dechesne et al., 1994; Sage et al., 2000) Fig. 3.3E-E'). At P3, type I spiral ganglion neurons are in a stage of refinement and plasticity, where they innervate both inner and outer types of hair cells (Echteler, 1992; Huang et al., 2007; Pujol, 1985; Simmons, 1994). Consistent with these earlier studies, we found that anti-calretinin-labeled spiral ganglion neurites in the P3 cochlea projected to the inner spiral plexus (isp, bracket Fig.3 E') region beneath the row of inner hair cells and extended beyond this, as neurites projected to the OHC region and formed three rows of outer spiral bundles (osb, arrowheads, Fig.3 E') beneath the OHCs (Fig. 3.3 E-E'). Earlier studies have shown that some neurite fibers in the organ of Corti are in close contact with supporting cells (Burgess et al., 1997; Huang et al., 2007; Jagger and Housley, 2003; Okamura et al., 2002). Consistent with this, we found that the neurite projections in the P3 cochlea are closely associated with the supporting cells labeled by Hes5-GFP (Fig. 3.3 D-D', E-E', and F-F'). The cochlear nerve fibers projecting into the organ of Corti, through the osseous spiral lamina (osl) to the IHC region, run between clusters of Hes5-GFP-labeled GER and border cells. Similarly, the nerve endings within the inner spiral plexus (isp, bracket, Fig. 3.3 E'), forming calyceal innervation to the IHCs, overlay the Hes5-GFP-positive inner phalangeal cells. Most strikingly, the three rows of outer spiral bundles, which run longitudinally beneath the outer hair cells, were found to track precisely between the four rows of more lateral supporting cells, the outer pillar and Dieter's cells (Fig. 3.3 D-D', E-E', and F-F'). Thus,

calretinin labeling here highlights the tracts made by spiral ganglion neurite projections in the neonatal organ of Corti which are closely associated with the Hes5-GFP-positive population of supporting cells.

We also labeled P3 Hes5-GFP cochlea cryosections with Jag1, to examine the relationship between these two Notch pathway components in the late stages of cochlear development (Fig3. G-G''). At this stage, Jag1 labels the membranes of the cochlear supporting cells and a portion of the GER (Fig. 3.3 G). We found a remarkable degree of overlap in the Hes5-GFP and Jag1 labeled supporting cell populations. Like Hes5-GFP, Jag1 labels the supporting cells that lie directly underneath the hair cells, including the Dieters', pillar, border, and inner phalangeal cells. At this age, neither Jag1 nor *Hes5* is expressed in the nonsensory epithelial cells lateral to the Dieters' cells, specifically the Hensen's and Claudius cells. The Jag1 labeling in the GER extends slightly more medially than the Hes5-GFP, but otherwise the two populations appear to overlap at this age.

We used an antibody specific to the activated form of Notch1 to examine the spatial pattern of Notch1 signal activation at P3 (Fig. 3.3. H-H''). In paraffin sections of P3 cochleae, actNotch1 immunolabeling was visualized with alk-phos NBT/BCIP (blue stain), hair cells and nerve fibers were labeled with anti-calretinin and nuclei were stained with DAPI (Fig. 3.3H-H''). The pattern of activated Notch1 expression is also similar to that of Hes5-GFP at this age, appearing strong in more lateral supporting cells and slightly less intense in the GER (compare Fig. 3.3G to H). An earlier study used this antibody to report the pattern of activated Notch1 in cochlear development and described a rapid downregulation during the first postnatal week, with only very weak expression at P3 (Murata et al., 2006). We found that the actNotch1 expression pattern

was similar to the previous report, but in our hands was still detectable in supporting cells at P3. The differences between our observations could be due to slight differences in mouse strain background (we use the C57BL6, which is the background of the Hes5-GFP, while Murata et al. worked with CBA/N mice) or differences in our tissue preparation and staining methods. Thus, we find that the expression of activated Notch1 correlates with the pattern of Hes5-GFP and *Hes5* in situ hybridization signal in the early postnatal period of cochlear development.

In order to resolve and identify the individual cells that make up the Hes5-GFP population in the developing cochlea we imaged whole-mount preparations of P3 cochlea with high resolution 2-photon excitation microscopy. While similar imaging may have been accomplished with confocal microscopy, 2-photon excitation microscopy allowed collection of large numbers (~80) of thin optical sections (0.5 μm) with little photo-bleaching of the GFP. We generated and analyzed z-series images and 3D projections (Fig. 3.3I-I') of 2-photon excitation micrographs and were able to readily discern the individual Hes5-GFP labeled cells and identify them based on their positional arrangement and cellular morphology. An oblique view of a 3D projection of the P3 Hes5-GFP cochlea shows the orderly arrangement and cellular shape of the supporting cells, their lumenal projections ensheathing hair cells, which appear as empty spaces in the epithelium (Fig. 3.3I). Close examination of the transverse optical section that appears on the front edge of the projection shows the profiles of individual supporting cells, arranged in their respective rows (Fig. 3.3I''). The Hes5-GFP labeled supporting cells include a cluster of cells in the GER, the border cells and inner phalangeal cells (which underlie and surround the inner hair cell), the inner and outer pillar cells and three rows of Dieters' cells (labeled GER, b, ph2, ip, op, d1, d2, and d3,

respectively in Fig. 3.3I'). In general, we found that the level of Hes5GFP expression in the P3 cochlea appears more intense in the Dieters' cells and outer pillar cells than in the supporting cells on the medial side of the organ of Corti (see Fig. 3.3A,A',D,D',and G). However, the relative GFP intensity levels of the individual cells are not apparent in the 3D-projection (Fig. 3.3 I-I') because of the contrast and density settings required for rendering. This pattern is present throughout late embryonic and neonatal development and suggests that the more lateral supporting cells have comparatively higher levels of Notch1-Hes5 signaling than the supporting cells on the medial side of the organ of Corti and in the GER. In contrast to earlier in situ hybridization studies (Zheng et al., 2000; Zine et al., 2001), we did not detect *Hes5* expression in the more lateral supporting cells of the lesser epithelial ridge, i.e. the Hensen's and Claudius cells, at any time during cochlear development.

***Hes5* expression persists in the cochlea through the first postnatal week, after which it is rapidly downregulated.**

In order to determine the pattern of *Hes5* expression in the inner ear during postnatal development, we again turned to a combination of in situ hybridization and Hes5-GFP. We performed in situ hybridization for *Hes5* on inner ear tissues from mice collected at P3, P5, P7, P14 and adult ages. We found that, in the early postnatal period of P3, *Hes5* mRNA expression was still detectable in a similar pattern to that of P0 throughout the organ of Corti but was only faintly expressed in the basal turn (data not shown). At P5, *Hes5* mRNA was still detectable in the apex in a similar pattern to earlier ages (Fig. 3.4A) but in the basal region was nearly imperceptible (Fig. 3.4C). We found that *Hes5* mRNA is not expressed in the auditory epithelium at P7 (data not shown) or P14 (Fig.

3.4F). Thus, our *Hes5* mRNA expression analysis of the postnatal cochlea indicates that expression of this gene is downregulated rapidly in a base to apex sweep that begins shortly after birth and is concluded around P7.

We next analyzed the pattern of Hes5-GFP expression in the postnatal cochlea, to see how it correlated with our in situ hybridization study. In the P7 cochlea Hes5-GFP is expressed in the apex in a similar pattern to that observed at earlier ages, appearing in the Dieters' and outer pillar cells and, at a lower level, in the more medial supporting cells and the GER (Fig. 3.4B). In the base of the P7 cochlea, we found that Hes5-GFP is quite faint, detectable only dimly in the supporting cells (Fig. 3.4D). We were still able to visualize endogenous Hes5-GFP in the apex of whole mount cochlea preparations as late as P8, and used confocal z-series microscopy to generate 3D projections of the pattern in the apex at this age (Fig. 3.4E). Undetectable in the base at P8, Hes5-GFP was restricted to the extreme apex at this age and was notably dim compared to similar whole-mount preparations at P3 (see Fig. 3.3), requiring higher laser power and detector gain for visualization with confocal microscopy. Due to the low levels of Hes5-GFP in the supporting cells at this age, compared to P3, the cellular resolution in images is reduced and cells appear less dense (compare Fig. 3.3A,D,and I with 4E). Hes5-GFP was completely undetectable in the auditory sensory epithelium of tissues examined at P12 (not shown), P16 (Fig. 3.4G), and adult ages (Fig. 3.6A - A'). Thus, we found that Hes5-GFP expression in the cochlea is downregulated in a base to apex gradient beginning with reduced expression in the base around P7 and loss of expression in the apex between P8 and P12. This result is consistent with the findings of our *Hes5* in situ hybridization analysis, where we saw a similar basal to apical

downregulation of *Hes5* mRNA during the first postnatal week, though the loss of GFP is delayed relative to the in situ expression.

Hes5 is expressed in vestibular supporting cells throughout development and in adults.

We found that *Hes5* mRNA and Hes5-GFP are expressed in developing vestibular patches as early as E12.5 (data not shown), and in vestibular supporting cells at E17.5 (Fig. 3.4J and J'). The Hes5-GFP pattern in the developing utricle and cristae includes expression in nearly all of the supporting cells of these organs, which can be seen surrounding nearly every hair cell of the utricle and horizontal crista in sections at E17.5 (Fig. 3.4J and J'). We also found Hes5-GFP expression in the developing saccule, where it was typically restricted to the peripheral edges and appeared less intense than the utricle or cristae (Fig. 3.4J and J', asterisk).

To determine the expression pattern of *Hes5* during postnatal development and in adults, we collected cristae and utricles from Hes5-GFP animals at P14 and adult ages and processed them for *Hes5* in situ hybridization. We found that *Hes5* mRNA was detectable in vestibular organs at P14 and adult ages (Fig. 3.4H, K, and L). In oblique sections through the P14 utricle, *Hes5* expression was visible in supporting cells in a honeycomb pattern surrounding Hes5-negative hair cells (Fig. 3.4H). Similarly, Hes5-GFP was expressed in supporting cells throughout the P16 utricle, which are seen to span the depth of the epithelium in transverse sections (Fig. 3.4I). We also detected *Hes5* expression in adult cristae, visible in the peripheral supporting cells in transverse and oblique sections (Fig. 3.4K and L, respectively, brackets). We were able to visualize *Hes5* mRNA and Hes5-GFP in the same sections by

immunostaining for GFP after in situ hybridization (Fig. 3.4K-K' and L-L'). We confirmed the colocalization of the Hes5-GFP with *Hes5* expression in the adult cristae, where, in transverse sections, it was highest in supporting cells in the peripheral margins and low or absent from the apices (Fig. 3.4K-K'). Similarly, in oblique sections of the adult posterior crista, Hes5-GFP colocalized with *Hes5* expression in peripheral supporting cells and was low or absent in the apices, marked by anti-calbindin labeling (Fig. 3.4L-L').

We further examined the Hes5-GFP expression pattern in whole-mount preparations of adult vestibular organs (Fig. 3.5). In surface views of adult utricles, Hes5-GFP is expressed in supporting cells in a mosaic pattern throughout the epithelium (Fig. 3.5A-B). We consistently observed highest levels of Hes5-GFP in the medial posterior region of the adult utricle, where most supporting cells are labeled with the transgene. Within the striolar region of the utricle, labeled by calbindin, Hes5-GFP expression was markedly reduced (Fig. 3.5B-B'' and enlarged in C-C'). In a 3D projection of the region at the posterior tip of the striola (upper box in Fig. 3.5B''), the Hes5-GFP labeled supporting cells can be seen adjacent to the anti-calbindin-labeled striolar calyces (Fig. 3.5D). The Hes5-GFP supporting cells in the adult utricle have a radial morphology, which spans the depth of the sensory epithelium (Fig. 3.5D). We never saw coexpression of Hes5-GFP in anti-myosinVI or anti-calbindin labeled hair cells. Although we also found that Hes5-GFP is expressed in the adult saccule, Hes5-GFP expression in this organ was primarily restricted to a few scattered cells in the peripheral edges of the epithelium and appeared quite faint compared to the robust levels observed in the cristae and utricle.

In adult whole-mount preparations of the cristae of the semicircular canals, Hes5-GFP is expressed in supporting cells surrounding the peripheral margins of the epithelia (Fig. 3.5E-F). Hes5-GFP expression is strong in discrete bands of supporting cells along the lateral edges but is absent from the central apices of the three cristae (Fig. 3.5E-E''). In reptiles, birds, and some mammals the anterior and posterior (vertical) cristae, but not the horizontal crista, are divided by a nonsensory structure, whose function is unknown, called the eminentia cruciatum (for review, see (Lysakowski and Goldberg, 2004)). Interestingly, the regions of Hes5-GFP expression in the anterior and posterior cristae extend over the apices of the epithelia adjacent to either side of the eminentia, essentially forming a border around the periphery of each half of the crista (Fig. 3.5F-F''). This suggests that the eminentia does not merely bisect a single concentric structure, but that it divides each vertical crista into two hemicristae, similar to those in birds and reptiles. The expression of *Hes5* specifically in the peripheral supporting cells of the cristae suggests that these supporting cells may be intrinsically different from supporting cells in the apices.

***Hes5* is not expressed in the adult cochlea after hair cell damage.**

Our findings that *Hes5* is not expressed in the adult cochlea under normal conditions are consistent with the terminally differentiated status of adult cochlear supporting cells. Auditory hair cell regeneration from supporting cells in lower vertebrates appears to require their up-regulation of Notch signaling (Ma et al., 2008; Stone and Rubel, 1999). In order to determine whether the supporting cells of the mammalian cochlea respond to hair cell damage by a similar up-regulation in Notch signaling, we analyzed the Hes5-GFP mice after hair cell damage. We induced hair cell damage by a single high-dosage

injection of kanamycin followed by a single injection of the loop diuretic furosemide (Oesterle et al., 2008). We sacrificed injected animals and uninjected littermate controls at two days (n=3) and four days (n=5) after treatment. OHCs were lost throughout most of the cochlea of injected animals, but inner hair cells were largely intact (Fig. 3.6). Hes5-GFP was not expressed in any of the normal adult cochlea (Fig. 3.6A-A' and merged with anti-myosinVI in Fig. 3.6A''-A'''), nor we did not find any expression in the cochlea after ototoxic drug injections (Fig. 3.6B-B'''). To ensure detection of low levels of Hes5-GFP we performed immunolabeling for GFP on adult tissues. We processed and analyzed damaged and control cochlear tissues together and included vestibular organs from the same animals as positive control tissues for Hes5-GFP immunolabeling. A comparison of Hes5-GFP expression in the positive control utricle tissue, processed and imaged alongside the cochlear tissues in Fig. 3.6A-A''' and B'-B''', is shown in Fig. 3.6C-C'''. In frozen transverse sections of control and damaged Hes5-GFP cochlea (Fig. 3.6D and E, respectively) Hes5-GFP expression is also absent, while strong expression can be seen in a P3 frozen section stained and imaged alongside the adult specimens (Fig. 3.6F). Sox2 antibody labels the supporting cell nuclei in the same control and damaged adult sections (Fig. 3.6D' and E') and, as reported by Oesterle et al., is unchanged in the damaged cochlea (Fig. 3.6E'). Thus, although supporting cells are still present in the damaged cochlea and express Sox2, they do not upregulate Hes5-GFP in response to hair cell death.

DISCUSSION

Hes5-GFP reports Notch signal activity in the inner ear

The reporter construct used to generate the Hes5-GFP mice used in this study contains a 3kb portion of the *Hes5* gene, including 1.6kb of the 5-prime flanking region, with eGFP cloned into the endogenous translational start site (Basak and Taylor, 2007). The expression pattern of GFP in this transgenic line has been well characterized in the developing central nervous system, where it is expressed in neural progenitors and correlates strongly with self-renewal capacity and multipotency (Basak and Taylor, 2007). Hes5-GFP was found to be inducible by Notch1 and expression was nearly completely absent from Notch1-deficient embryos (Basak and Taylor, 2007). Among the four Notch receptors, only Notch1 has been conclusively shown to be expressed in the developing mammalian cochlea (Lewis et al., 1998; Murata et al., 2006; Shailam et al., 1999; Zine et al., 2000), although Notch3 was reported to be expressed in the early rat otocyst, prior to cochlear differentiation (Lindsell et al., 1996). Hes5-GFP expression strongly correlates with expression of activated Notch1 in the developing inner ear; such that they appear to be nearly identical spatial and temporal patterns (Fig. 3.3 and (Murata et al., 2006)). Thus, Hes5-GFP appears to be a reliable readout of Notch signal activity in the inner ear.

***Hes5* in embryonic development of the organ of Corti**

In this study we have used a combination of approaches to define the pattern of expression of *Hes5* in the developing and mature inner ear. In the organ of Corti, we show that *Hes5* is expressed at a low level in the E14.5 cochlea, approximately 12-24 hours earlier than previously reported. *Hes5* expression at E14.5 appears in a discrete region in the central floor of the cochlear duct, which is largely overlapping with Jag1 and Sox2. Earlier studies from our lab and others have reported that nascent hair cells

express the Notch ligand-encoding genes *Dll1* and *Jag2* beginning at E14.5; and *Dll3* is expressed in hair cells about 24 hours later (Hartman et al., 2007; Kiernan et al., 2005a; Lanford et al., 1999b; Morrison et al., 1999; Zhang et al., 2000). Expression of these hair cell-specific Notch ligands has been shown to be restricted to the developing hair cells, which appear at this stage as a single row of presumptive inner hair cells on the medial edge of the prosensory domain. Thus, the pattern of *Hes5* expression at E14.5 is slightly broader than that which might be expected to result from Notch signaling initiated by hair cell-specific ligands alone. Since Jag1 protein is expressed throughout most of the Hes5-positive region, and the most intense region of Jag1 labeling is adjacent to the brightest Hes5-GFP cells, it is possible that Jag1-Notch signaling contributes to the expression of *Hes5* at E14.5. Further studies, such as examination of Hes5-GFP expression in *Jag2*/*Dll1* mutants, would be necessary to determine how specific ligands contribute to Hes5 signaling.

Notch signaling has been shown by several recent studies be active during, and essential for, specification of the prosensory domains, which is thought to occur in the mouse inner ear around E12.5 (Brooker et al., 2006; Daudet et al., 2007; Daudet and Lewis, 2005; Hayashi et al., 2008; Kiernan et al., 2006; Murata et al., 2006). Since we confirmed that *Hes5* is not expressed at this early stage and earlier studies showed that *Hes5* ablation does not inhibit sensory patch formation (Zine et al., 2001), it is unlikely that *Hes5* participates in the process of sensory specification. Other Hes-family transcription factors, *HesR1* and *HesR2* are expressed during the prosensory specification phase of early cochlear development and are more likely to be involved in this process (Hayashi et al., 2008). Thus, the expression of *Hes5* in the prosensory region at E14.5 may represent a baseline of low-level Notch-Hes5 signaling that is set

up with contributions from Jag1 just prior to initiation of lateral inhibition by hair cell-specific Notch ligands.

The expression of Hes5-GFP in the glia of the spiral ganglia during early embryonic development (Fig. 3.1A-A' and B-B') suggests that the developing neurons express a Notch ligand which activates Notch signaling in the developing glia. This is consistent with known roles for Notch signaling in glial development and differentiation throughout the nervous system (Gaiano et al., 2000; Ge et al., 2002; Hojo et al., 2000; Morrison et al., 2000; Tanigaki et al., 2001; Taylor et al., 2007).

The expression pattern of *Hes5* during the middle and late stages of cochlear development, from E17.5 through the neonatal period, is consistent with a role for this gene in lateral inhibition. In this model, Notch signaling is activated in nascent supporting cells by ligands presented on the surface of hair cells. Consistent with this, *Hes5* expression levels during cellular differentiation of the cochlea appear to be highest in the supporting cells in direct contact with hair cells. This is particularly evident by the high levels of *Hes5* present in the more lateral supporting cells, the Dieters' and outer pillar cells, which are each in contact with multiple outer hair cells (Fig. 3.3). Similarly, *Hes5* null mice produce extra cochlear hair cells that appear in three specific patterns: a row of additional outer hair cells along the lateral edge, occasional extra inner hair cells, and some ectopic hair cells in the GER (Zine et al., 2001). These extra hair cells likely arise from the same population of supporting cells that are labeled with Hes5-GFP during embryonic development. Additionally, *Hes5* appears to function in parallel with *Hes1* and *HesR2* (*Hey2*), which are expressed in partially overlapping regions with *Hes5,* and combination of mutations in either of these

genes with loss of *Hes5* increases the overproduction of hair cells (Li et al., 2008b; Zine et al., 2001).

Our description here substantially improves on earlier in situ hybridization studies that reported *Hes5* expression in the embryonic cochlea (Lanford et al., 2000; Li et al., 2008b; Shailam et al., 1999; Tang et al., 2006; Zheng et al., 2000; Zine et al., 2001). While several of these studies accurately showed *Hes5* expression in the region of the Dieter's cells, most did not pick up the expression in other supporting cells or the GER and none provided single cell resolution of the *Hes5*-positive population. Some of the earlier studies also reported *Hes5* expression in the more lateral supporting cells of the lesser epithelial ridge, i.e. the Hensen's and Claudius cells, (Zheng et al., 2000; Zine et al., 2001), where we did not detect *Hes5* expression at any time during cochlear development.

Hes5 in the neonatal cochlea correlates with supporting cell plasticity

Hes5 downregulation in the cochlea during the first postnatal week (Fig. 3.4) correlates with a similar loss of expression of Notch ligands in hair cells. Earlier we reported that *Dll1* and *Dll3* are downregulated from base-to-apex in neonatal hair cells between P0 and P3, and expression of these two Notch ligands is lost from hair cells by P5 (Hartman et al., 2007). Thus, the spatial and temporal pattern of loss of *Hes5* expression in supporting cells closely follows the downregulation of Notch ligands in hair cells. The expression pattern of Notch ligands thus offers further support that *Hes5* expression is a result of Notch signaling initiated by ligands presented on the surface of hair cells. However, it is also possible that Jag1, expressed on supporting cell membranes, contributes to Hes5 signaling during embryonic and postnatal

development, particularly in the GER, where *Hes5* is expressed in cells that do not appear to contact hair cells.

Another possible source of Notch ligands that could contribute to the *Hes5* signal in the organ of Corti are the spiral ganglion neurons. The expression of Hes5-GFP in the glia of the spiral ganglia during embryonic and neonatal development suggests that spiral ganglion neurons express Notch ligands. Additionally, we found that the spiral ganglion nerve endings are in close contact with Hes5-GFP-positive supporting cells in the neonatal cochlea (Fig. 3.3 D-F'). Although expression of Notch ligands in auditory nerve fibers has not been reported, Delta has been shown to be trafficked to neurites of other neurons, such as *Drosophila* ventral nerve cord neurons (Cornbrooks et al., 2007). Notch signaling has also been shown to be involved in regulating contact-dependent neurite growth in mammalian neuronal cultures (Franklin et al., 1999; Sestan et al., 1999), suggesting that Delta-Notch signaling occurs in some neurites. Additionally, spiral ganglion neurons undergo a period of neurite retraction and pruning between P3 and P6 (Huang et al., 2007), which we found correlates spatially and temporally with loss of *Hes5* in the organ of Corti. Although intriguing, these findings are only correlative; further studies would be needed to directly address the hypothesis that Notch ligands presented on spiral ganglion neurites contribute to Notch-Hes5 signaling in the organ of Corti.

Recent studies have demonstrated that, under certain conditions, neonatal mouse cochlear supporting cells are capable of proliferation and/or differentiation into new hair cells (Chardin and Romand, 1997; Doetzlhofer et al., 2009; Takebayashi et al., 2007; White et al., 2006; Yamamoto et al., 2006). Inhibition of Notch signaling in cochlear explant cultures with DAPT was shown to lead to transdifferentiation of

supporting cells into hair cells as late as P3 (Hayashi et al., 2008; Takebayashi et al., 2007; Yamamoto et al., 2006). Two other recent studies found that cells isolated from neonatal cochleae can be maintained *in vitro* and can give rise to cells with hair cell characteristics; however, the expression of progenitor markers and the capacity for proliferation of isolated supporting cells decreases dramatically during postnatal development (Oshima et al., 2007; White et al., 2006). These findings indicate that supporting cells retain some degree of plasticity even into the neonatal period and that Notch signaling may have a role in preventing spontaneous cell-fate changes. Since loss of Notch-Hes5 signaling in postnatal supporting cells correlates with diminishment of stem cell features, this pathway is a potential candidate for regulation of supporting cell plasticity.

Hes5 in development of vestibular epithelia

The pattern of *Hes5* expression in vestibular supporting cells is similar to that of the cochlea and suggests a similar role for this gene in vestibular development, regulating progenitor maintenance and differentiation. *Hes5* null mice, analyzed at birth, were found to have slight increases in hair cell numbers in the utricle and saccule (Zine et al., 2001). The increase in the number of hair cells in the utricle of *Hes5* mutants was relatively greater than the increase observed in the saccule (Zine et al., 2001), which is consistent with our observation that *Hes5* is more broadly expressed in the utricle than the saccule (Fig. 3.4J and J'). Hes1 appears to have distinct and overlapping roles with *Hes5* in vestibular development, since loss of either gene alone or together in double heterozygotes, leads to production of extra vestibular hair cells (Zine et al., 2001). Although the cristae of *Hes5* mutant mice have not been analyzed, it is reasonable to

expect a hair cell overproduction phenotype in the cristae of mice lacking Hes5; given that *Hes5* is strongly expressed in the developing cristae.

***Hes5* in adult vestibular supporting cells is correlated with regeneration potential**

We found that *Hes5* expression is maintained in some adult vestibular supporting cells, particularly in the cristae and the utricle (Fig. 3.5). Previous studies indicate that mammalian vestibular sensory epithelia retain some potential for proliferation and regeneration. Early studies performed *in vitro* showed that supporting cells in mammalian utricular sensory epithelia proliferate after hair cell loss caused by treatment with the aminoglycosides and new immature hair cells appear after several weeks (Forge et al., 1993; Warchol et al., 1993). It was also found that treatment of cultured adult mouse utricles with mitogenic growth factors stimulates proliferation of supporting cells (Yamashita and Oesterle, 1995). More recent *in vivo* studies in rats and mice show that hair cells spontaneously regenerate in aminoglycoside-damaged utricular sensory epithelia (Kawamoto et al., 2008; Oesterle et al., 2003). Additionally, cells isolated from adult vestibular organs are capable of forming spheres and can give rise to a variety of cell types, including cells with hair cell characteristics (Li et al., 2003; Oshima et al., 2007). In addition, significant hair cell regeneration has been show to occur in the chinchilla crista ampullaris following hair cell damage (Lopez et al., 1997; Tanyeri et al., 1995). Interestingly, Lopez et al. reported that hair cells appeared to regenerate first in the peripheral areas of the crista and that type II hair cells, but not type I hair cells, were regenerated. Since we find that Hes5-GFP is highly enriched in the peripheral areas of the cristae, where most type II hair cells are found, this result provides further correlation between *Hes5* expression and regenerative capacity. Thus,

in sharp contrast to the cochlea, adult mammalian vestibular epithelia exhibit regenerative capacity, which appears to rely on supporting cells with stem cell features. The presence of active Notch-Hes5 signaling in adult vestibular epithelia correlates with maintenance of regenerative capacity in these tissues. This correlation needs further evaluation; but it suggests the hypothesis that *Hes5*-positive supporting cells are endowed with greater regenerative potential than other vestibular supporting cells. Future studies should address this hypothesis directly and investigate the potency of individual supporting cell populations, one of which can now be identified by expression of Hes5-GFP.

Absence of Notch-Hes5 signaling in the damaged mammalian cochlea and implications for regeneration

Although the adult vestibular epithelium has clear *Hes5* expression, the adult mammalian cochlea lacks Notch-Hes5 signaling. Moreover, Hes5-GFP is not expressed in the adult cochlea even in response to hair cell damage. The apparent lack of Notch signal activity in the adult cochlea could be due to absence of Notch ligand expression in hair cells, which downregulate *Delta-like 1* (*Dll1*) and *Dll3* postnatally (Hartman et al., 2007). However, Jag1 is still expressed in the adult cochlea (Oesterle et al., 2008), and Notch1 expression persists through at least P7 (Murata et al., 2006), indicating that key elements of this pathway may be present in the adult cochlea. Future studies will be necessary to resolve this issue.

The absence of Notch signaling in the mature, damaged mammalian organ of Corti may be related to the lack of regeneration in this tissue. Hair cell regeneration in birds and fish has been shown to depend on proliferation and/or direct

transdifferentiation of supporting cells (Roberson et al., 2004; Stone et al., 1999), and Notch signaling is active in regenerating sensory epithelia and appears to play a role in regulating the regeneration process. Delta-Notch signaling was shown to be active in the normal chick utricle and becomes upregulated in the basilar papilla during hair cell regeneration (Stone and Rubel, 1999). Additionally, Notch signaling was shown to regulate the extent of hair cell regeneration in the zebrafish lateral line (Ma et al., 2008). Similarly, in the regenerating posthatch chick retina Notch activity is necessary for the de-differentiation/proliferation of Muller glia (Hayes et al., 2007), while in the central nervous system, Notch has been shown to be required for maintaining progenitors and neural stem cells in development and adults (Alexson et al., 2006; Givogri et al., 2006).

In summary, we showed conclusively that *Hes5* is expressed in discrete populations of supporting cells in the developing mouse inner ear. We found that *Hes5* is downregulated in the cochlea during the first postnatal week, during the period of cochlear maturation and diminishment of stem cell features. In contrast, *Hes5* expression is maintained in adult vestibular sensory epithelia, which are known to retain capacity for proliferation/regeneration. Importantly, *Hes5* is absent in the normal and drug-damaged adult mammalian cochlea, indicating a failure in Notch signaling, consistent with the lack of regenerative capacity. Since loss of Notch-Hes5 signaling in postnatal supporting cells correlates with diminishment of stem cell features, reactivating this pathway in mature cochlear support cells may provide a means of restoring regenerative capacity.

METHODS

Animals

Mice were housed in the Department of Comparative Medicine and the Institutional Animal Care and Use Committee approved experimental methods and animal care procedures. Hes5-GFP transgenic mice, on the C57/BL6 background, were generated as previously described (Basak and Taylor, 2007) using a 3kb portion of the *Hes5* gene, including 1.6 kb of the 5-prime flanking region, with eGFP cloned into the translational start site. Mice were euthanized according to approved procedures: neonatal mice were sacrificed by decapitation after 5 min of hypothermia, juvenile and adult mice were killed by anesthesia with CO_2 followed by cardiac perfusion with 4% PFA.

Drug-damage paradigm

Outer hair cells were experimentally lesioned in adult mice (2-5 months old) as previously described (Oesterle et al., 2008). Briefly, mice were given single subcutaneous injections of kanamycin (1000mg/kg USP grade Sigma-Aldrich Cat. No. K1637, in sterile PBS) followed 30-45 min later by single intraperitoneal injections of furosemide (400mg/kg, Hospira Inc. Lake Forest, IL, Cat. No. RL-1206). Animals were killed 2 or 4 days after the injections. Uninjected littermates were used as controls.

Paraffin *In Situ* Hybridization

Digoxigenin-labeled probe was *in vitro* transcribed from a linearized cDNA clone corresponding to *Hes5* (BC103539, IMAGE: 40039948). Embryos were collected from timed pregnant Hes5-GFP or wild type C57/BL6 mice and staged according to (Kauffman, 1992). For postnatal mice, postnatal day 0 (P0) was defined as the day of birth. In situ hybridization was performed as previously described (Hayashi et al., 2007; Nelson et al., 2004). Briefly, embryonic whole heads, P0-P7 half-heads (with brains

removed), or P14-Adult isolated vestibular and cochlear tissues were fixed overnight at 4°C in modified Carnoy's solution (60% ethanol, 11.1% formaldehyde (30% of 37% stock), 10% glacial acetic acid), dehydrated though an EtOH series, prepared for paraffin embedding, and sectioned at 6-8 µm. Slides were baked overnight at 68°C, dewaxed in Xylene, rinsed in 100% EtOH, and air-dried at room temperature. Overnight hybridization and subsequent washes were carried out at 68°C. Hybridized probe was detected using anti-Digoxygenin alkaline phosphatase conjugated antibody (1:2000 dilution, Roche Biochemical, Indianapolis, IN) and visualized with NBT/BCIP for a blue precipitate. After *in situ* hybridization, sections were post-fixed in 4% PFA, rinsed in PBS, and processed for fluorescent immunohistochemistry as described below.

Antibodies

For section and whole-mount immunohistochemistry, performed as described below, we used the following primary antibodies: chicken anti-GFP (1:500 dilution, Abcam, USA, Cat. No. AB13970); goat anti-Jag1 (1:300, Santa Cruz Biotechnology, Jag1 C-20 Cat. No. SC-6011); goat anti-Sox2 (1:500, Santa Cruz Biotechnology, USA, Sox2 Y-17 Cat. No. SC-17320); rabbit anti-Prox1 (1:500, Chemicon, USA, Cat. No. AB5475); rabbit anti-calretinin (1:2000, Swant, Switzerland); rabbit anti-actNotch1 (1:500, Cell Signaling Tech, cleaved Notch 1 Val1744); rabbit anti-myosinVI (1:1000 Proteus Biosciences, USA, Cat. No. 25-6790); rabbit anti-calbindin (1:500, Millipore, USA, calbindin D-28k Cat. No. AB1778).

Activated Notch1 Immunohistochemistry

Immunolabeling for activated Notch1 was performed as described (Nelson et al., 2007). Briefly, P3 half-heads, with brains removed, were fixed overnight at 4°C in modified Carnoy's solution, dehydrated though an EtOH series, prepared for paraffin embedding, and sectioned at 6-8 µm. Slides were baked overnight at 68°C, dewaxed in Xylene, rinsed in 100% EtOH, and air dried at room temperature. Antigen retrieval was accomplished by autoclave treatment (5 min, 105 °C) in TE buffer (10 mM TrisCl, 1 mM EDTA, pH 9.0). Sections were washed with PBS, blocked in 10% goat serum in PBT for 1 h, incubated with rabbit anti-actNotch1antibody overnight, washed 4 X with PBS, incubated with goat-anti rabbit alkaline phosphatase (1:500, Sigma) for 1 h, washed 4 X with PBT, equilibrated with NTMT, pH 9.0, and incubated in NBT/BCIP substrate (Sigma). Sections were washed in PBS and subjected to sequential immunolabeling and fluorescent detection with primary and secondary antibodies as described below, followed by DAPI counterstaining and mounting.

Fluorescent Immunohistochemistry of Frozen and Paraffin Sections

Embryos were collected from timed pregnant Hes5-GFP mice and staged according to Kauffman (Kauffman, 1992). For postnatal mice, P0 was defined as the day of birth. Embryonic whole heads or P0-P5 half-heads, were fixed overnight in 4% PFA in PBS at 4°C. Adult cochlea were isolated from temporal bones, the stapes was removed from the oval window, a small opening was made in the apex, and cold 4% PFA in PBS was perfused through the cochlea with a syringe. Perfused cochlea were then fixed overnight in 4% PFA in PBS at 4°C, washed 3 X 30 minutes in PBS, and decalcified in 0.27M EDTA in PBS for 48hr at 4°C. After fixation and decalcification (for adult cochlea) whole cochlea or heads were cryoprotected through graded sucrose in PBS

(10% sucrose, 15% sucrose, 15% sucrose with 50% OCT) then embedded in OCT (Tissue Tek), frozen in a bath of ethanol and dry ice, sectioned at 10 µm, and mounted on Superfrost+ slides (Fisher Scientific). Slides with cryosections (or paraffin sections already processed for act-Notch1 immunolabeling or in situ hybridization) were then washed briefly in PBS and blocked for 1 hr in 10% FBS in PBS with 0.1% TritonX-100 at room temperature. Primary antibodies were diluted in block and incubated overnight at 4^{o}C. Slides were then washed in PBS 3 X 10 min, and incubated in species-specific fluorescent-labeled secondary antibodies AlexaFluor 488, 568, or 594 nm (1:500, Invitrogen). After immunostaining, slides were coverslipped in Fluoromount G (Southern Biotechnology, Birmingham, AL). Images of most stained sections were acquired on a Zeiss Axioplan 2 microscope equipped with DIC optics and a Spot camera. Images of adult cochlear sections were also captured on a Zeiss LSM Pascal confocal microscope and processed using Improvision Volocity (3.0.2). Images were compiled with Adobe Photoshop 7.0. Within each figure, comparable imaging settings were used to capture all images of Hes5-GFP immunolabeling from sectioned tissues so that expression levels could be compared between ages and tissues.

Whole-Mount Immunohistochemistry

Adult inner ears were isolated from temporal bones, the stapes was removed from the oval window, a small opening was made in the apex, and cold 4% PFA in PBS was perfused through the cochlea with a syringe. Perfused cochlea were then fixed overnight in 4% PFA in PBS at 4^{o}C, washed 3 X 30 min in PBS, decalcified in 0.27M EDTA in PBS for 48hr at 4^{o}C and washed in PBS 3 X 30 min. P3 cochlea were dissected from temporal bones and fixed in 4% PFA in PBS for 3 hr at 4^{o}C then washed

in PBS 2 X 30 min. P3 and decalcified adult inner ears were then dissected to isolate the cochlea and vestibular organs from the bony capsule. To expose the organ of Corti, the anlage of the vascularis and the tectorial membrane were removed using fine forceps. The vestibular organs were dissected to expose the epithelia and otoconia were removed from the utricle and saccule by directing a stream of PBS across the surface from a syringe with a 30G needle. Tissue was permeabilized in PBS/0.1% TritonX-100 for 1hr and blocked for 2 hr in 10% FBS in PBS with 0.1% TritonX-100 at room temperature. Primary antibodies were diluted in block and cochlear and vestibular tissues were incubated together overnight at 4^{o}C. Tissues were washed in block and incubated overnight at 4^{o}C in species-specific fluorescent-labeled secondary antibodies: AlexaFluor 488 or 568 nm (1:500, Invitrogen). Tissues were washed in PBS and coverslipped in PBS/Glycerol. Confocal images of whole-mounts were captured on a Zeiss LSM Pascal confocal microscope. Images were processed using Improvision Volocity (3.0.2) and Adobe Photoshop (7.0). We were able to visualize the endogenous Hes5-GFP (without immunostaining) in live or fixed whole mount cochlear tissue from P0-P8 mice and vestibular tissue from P0-adult mice using standard fluorescent microscopy. However, in cochlear tissue from embryonic mice or mice older than P8 we found the endogenous GFP to be too weak to image clearly and it was sensitive to photo bleaching. Therefore, we used immunofluorescent labeling with antibodies against GFP to visualize and image the pattern of Hes5-GFP in the cochlea prior to P0 and after P8. In the adult vestibular sensory epithelia, the endogenous GFP was bright enough to image without immunostaining. However, to improve photostability and intensity for whole mount confocal z-sectioning we typically used immunolabeling against GFP in these tissues.

Figure 3.1 Hes5-GFP mimics expression of *Hes5* in supporting cells of the developing cochlea. Hes5-GFP expression in embryonic cochlear sections (**A**, **A'**, **C**, and **E**) compared to similar sections probed for expression of *Hes5* with in situ hybridization (**B**, **B'**, **D**, and **F**). **A** Low magnification view of an E14.5 cochlea section shows that Hes5-GFP is expressed in three turns of the cochlea (asterisks) and in the spiral ganglion (sg). **B** Low magnification view of an E14.5 cochlea section probed for expression of *Hes5* (blue) shows low level of signal in the two basal turns of the cochlea (asterisks) and the spiral ganglion (sg). **A'** High magnification view of the boxed region in (**A**), mid-basal turn of the E14.5 cochlea, where Hes5-GFP labeling (bracket) is visible in a narrow band of cells in the floor of the cochlear duct. **B'** High magnification view of the boxed region in (**B**), mid-basal turn of the E14.5 cochlea. *Hes5* in situ hybridization labeling (bracket) is low but visible in a narrow band of cells in the floor of the cochlear duct, similar to Hes5-GFP (compare **A'** to **B'**). **C** Section of E17.5 Hes5-GFP cochlea middle turn; expression is seen in supporting cells that surround inner hair cells (arrow) and outer hair cells (arrowheads), and in a small part of the GER. **D** E17.5 cochlear middle turn section probed for expression of Hes5; signal is localized to supporting cells in a similar pattern to Hes5-GFP at this age (compare **C** to **D**). **E** P0 middle cochlear turn shows Hes5-GFP expression is strong in supporting cells that underlie and surround the outer hair cells and slightly weaker in more medial supporting cells and the GER. **F** P0 cochlea section probed for expression of *Hes5* has a similar pattern to Hes5-GFP (E). Dotted lines in left panels outline the lumena of the cochlear duct. *sg*: spiral ganglia. Scale bars in **A** and **E**=100 μm. Scale bar in **A** applies to panels (**A**-**B**); scale bar in **E** applies to (**A'**-**B'** and **C**-**F**).

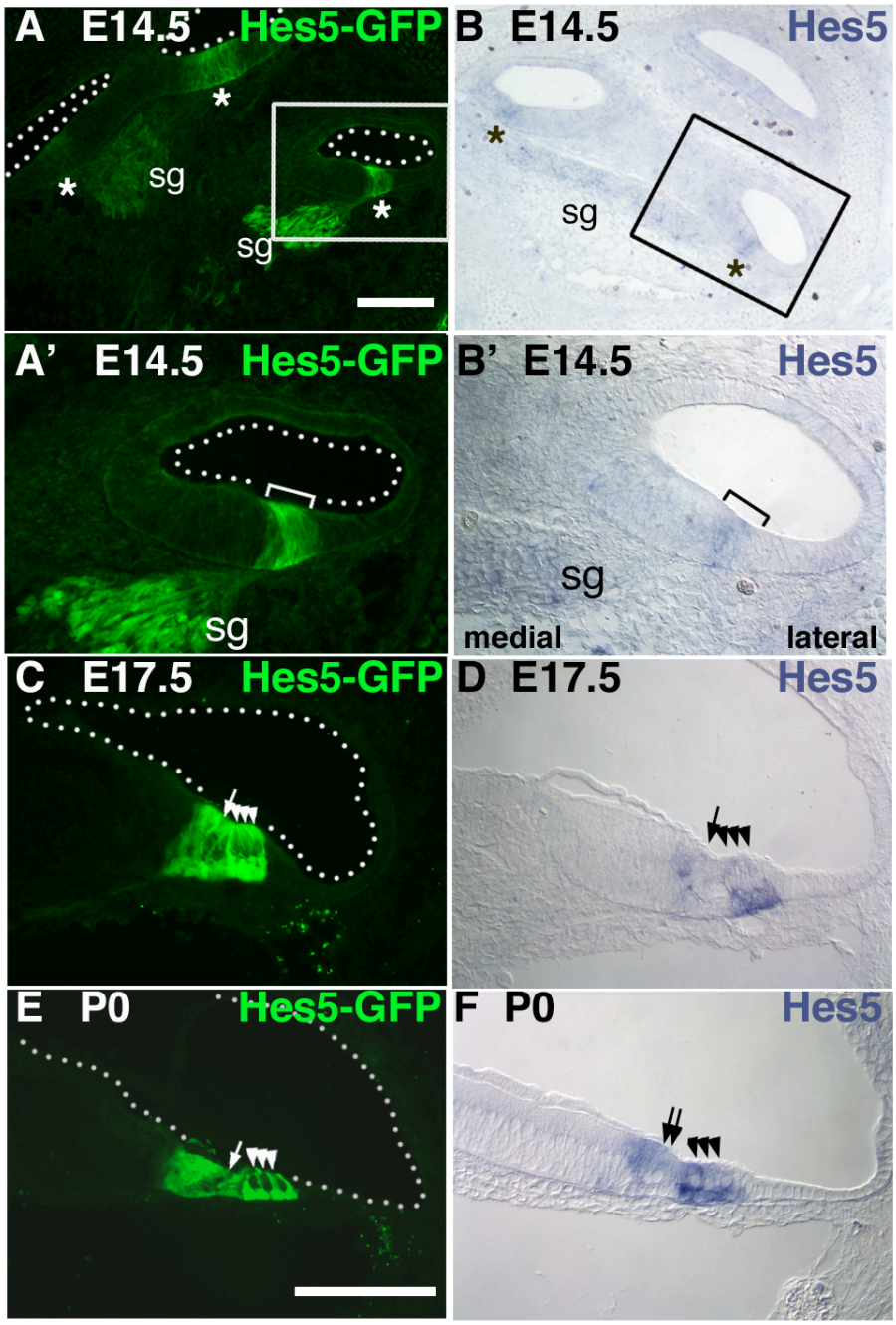
A E14.5 Hes5-GFP
B E14.5 Hes5
sg
sg
sg
A' E14.5 Hes5-GFP
B' E14.5 Hes5
sg
sg
medial
lateral
C E17.5 Hes5-GFP
D E17.5 Hes5
E P0 Hes5-GFP
F P0 Hes5

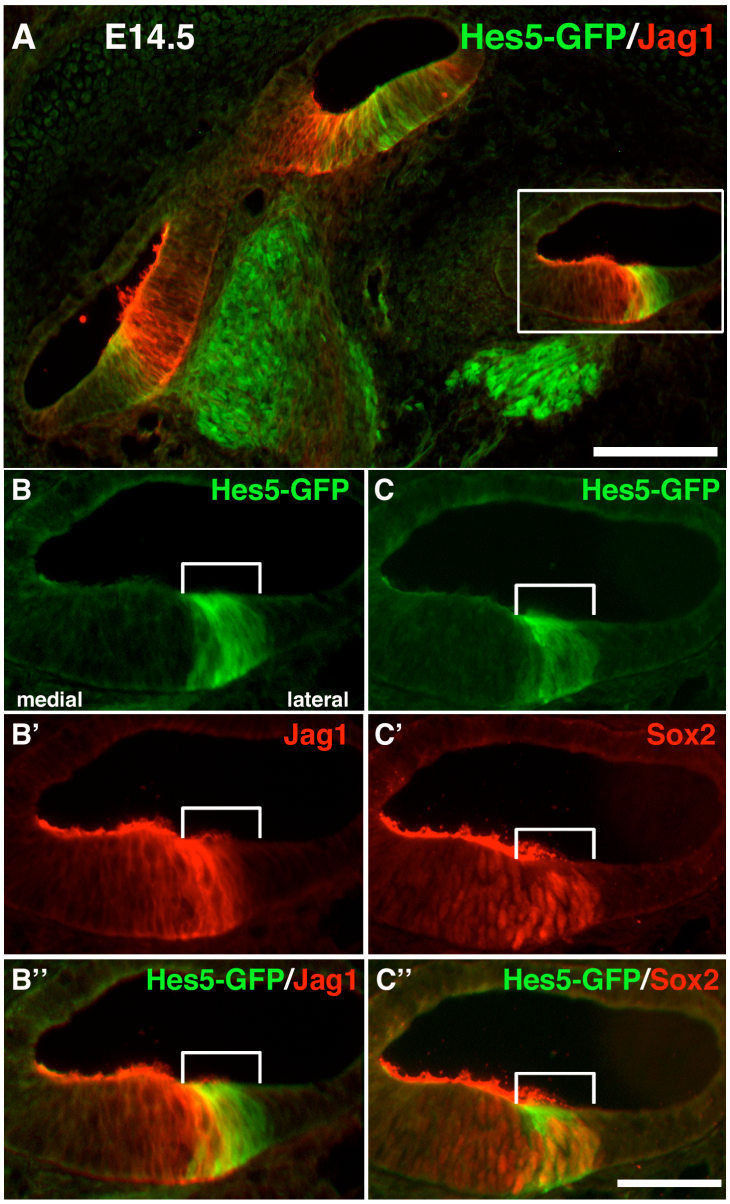

Figure 3.2 Hes5-GFP overlaps partially with Jag1 expression and lies within the Sox2-labeled prosensory domain of the developing cochlea at E14.5. Sections of E14.5 Hes5-GFP cochlea were labeled with antibodies to GFP and Jag1 (**A**, **B**-**B''**) or Sox2 (**C**-**C''**). **A** Low magnification view of three Hes5-GFP cochlear turns stained for Jag1 and GFP. **B**-**B''** High magnification views of boxed region in (**A**), mid-basal turn showing Hes5-GFP (brackets, **B**), Jag1 (**B'**) and merged (**B''**). **C**-**C''** Similar mid-basal turn labeled with Hes5-GFP (**C**), Sox2 (**C'**), and merged (**C''**). Note that there is nonspecific labeling of the tectorial membrane in B'-B" and C'-C". Scale bar in **A**=100 μm. Scale bar in **C''**=50 μm and applies to (**B**-**B''** and **C**-**C''**).

Figure 3.3 Hes5-GFP is expressed in a specific population of cochlear supporting cells in a pattern similar to activated Notch1. P3 cochlear tissues from Hes5-GFP mice were processed for immunohistochemistry with antibodies against Prox1 (**A**-**C**, **A'**-**C'**), calretinin (**D**-**F**, **D'**-**F'**), Jag1 and GFP (**G**-**G''**), or activated-Notch1 and calretinin (**H**-**H''**), and patterns were compared to Hes5-GFP. **A**-**C** and **A'**-**C'** ZY plane section and XY projection views, respectively, of a confocal image through the epithelium of a P3 Hes5-GFP organ of Corti labeled with anti-Prox1. The XY projection (**A'**-**C'**) is of a subset of the total Z series that spans the basal supporting cell nuclei, marked by the bracket in (**A**). **D**-**F** and **D'**-**F'** ZY plane section and XY projection views, respectively, of a confocal image through the epithelium of a P3 Hes5-GFP organ of Corti labeled with anti-calretinin. The XY projection (**D'**-**F'**) is of a thin subset of the total Z series in the region of neurite projections underlying the hair cells, marked by the bracket in (**D**). Bundled cochlear nerve fibers (arrow points to one example), traverse through the osseous spiral lamina (osl), in close contact with Hes5-GFP-labeled GER cells. Calyceal nerve endings forming the inner spiral plexus (isp), overlay the Hes5-GFP-positive inner phalangeal cells; the three rows of outer spiral bundles (osb), which run longitudinally beneath the outer hair cells, track precisely between the four rows of outer pillar and Dieter's cells. **G**-**G''** Transverse cryosection through a P3 Hes5-GFP cochlea immunolabeled for Jag1 and GFP. The dotted line outlines the lumenal surface; above is nonspecific staining of the tectorial membrane. **H**-**H''** Transverse paraffin section through a P3 cochlea labeled with antibodies to activated Notch1 and calretinin. Arrow and arrowheads denote inner hair cell and outer hair cells, respectively. **I**-**I'** 3D projection of a P3 Hes5-GFP cochlea rendered from a two photon excitation z-series micrograph. *osl*: osseous spiral lamina, *isp*: inner spiral plexus, *osb*: outer spiral bundles, *GER*: greater epithelial ridge, *b:* border cell, *iph*: inner phalangeal cell, *ip:* inner pillar cell, *op:* outer pillar cell, *d1-d3:* Dieters' cells. Scale bar in **F'**=100 μm and applies to **A**-**F** and **A'**-**F'**. Scale bar in **H''**=100 μm and applies to (**G**-**G''** and **H**-**H''**). Scale bars in **I** and **I'**= 50 μm.

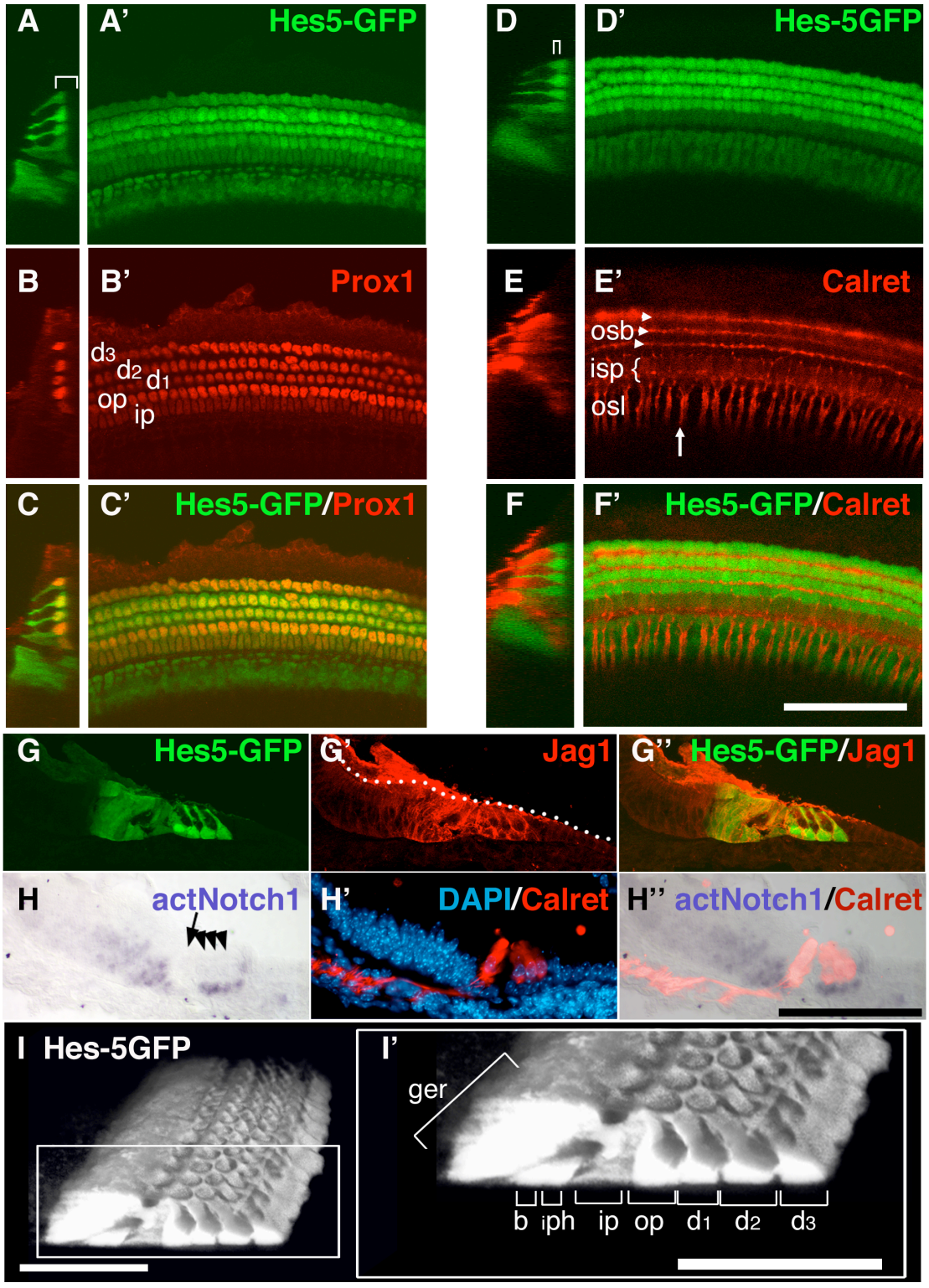
A
A'
Hes5-GFP
D
D'
Hes-5GFP
B
B'
Prox1
d3
d2
d1
op
ip
E
E'
Calret
osb
isp {
osl
C
C'
Hes5-GFP/Prox1
F
F'
Hes5-GFP/Calret
G
Hes5-GFP
G'
Jag1
G''
Hes5-GFP/Jag1
H
actNotch1
H'
DAPI/Calret
H''
actNotch1/Calret
I
Hes-5GFP
I'
ger
b
iph
ip
op
d1
d2
d3

Figure 3.4 *Hes5* is downregulated in the neonatal cochlea but is expressed in mature vestibular supporting cells. Postnatal and juvenile cochlear sections were probed for *Hes5* (**A**, **C**, **F**) and compared to similar sections of Hes5-GFP cochlea immunolabeled for GFP and the hair cell marker myosinVI (**B**, **D**, **G**). *Hes5* is expressed in cochlear supporting cells in the apex at P5 (**A**), but is nearly undetectable in the base at this age (**C**), and is not detectable at P7 (not shown) or P14 (**F**). **B,D,G** Hes5-GFP is similarly downregulated in cochlear supporting cells, such that it is present in the apex at P7 (**B**), but only weakly expressed in the base at P7 (**D**), and is not detectable at P16 (**G**). Hes5-GFP could still be detected in the apex as late a P8, and was bright enough to be visualized with confocal z-series microscopy to generate a 3D projection, immunolabeled with anti-myosinVI (**E**). Although *Hes5* was not detectable in the juvenile cochlea, it was clearly expressed in supporting cells of the P14 utricle, shown here in an oblique section (**H**). Similarly, Hes5-GFP was expressed in supporting cells of the P16 utricle (**I**). **J-J'** Cryosection through an E17.5 Hes5-GFP inner ear immunolabeled with antibodies to GFP (**J**) and myosinVI (merged, **J'**). Hes5-GFP is expressed in supporting cells throughout the utricle and horizontal crista, and in a subset of supporting cells in the periphery of the saccule (asterisk, **J'**). Adult Hes5-GFP vestibular tissues were probed for *Hes5* and then immunolabeled for GFP (**K**-**K'** and **L**-**L'**), to confirm that the transgene expression mimics expression of *Hes5.* **K**-**K'** Transverse section of an adult posterior crista shows *Hes5* in situ hybridization signal (**K**) and Hes5-GFP (**K'**) are colocalized in the peripheral supporting cells (brackets). **L**-**L'** Oblique section through an adult posterior crista shows similar overlap between *Hes5* in situ signal and Hes5-GFP (brackets, **L** and **L'**, respectively), but neither are overlapping with the central zone (type I) hair cell calyx marker calbindin (asterisk, **L'**). Scale bar in **G**=100 µm and applies to **A**-**D** and **F**-**G**. Scale bar in **E**=100 µm. Scale bar in **I**= 100 µm and applies to **H** and **I**. Scale bar in J'=100 µm and applies to J and J'. Scale bar in **K'**= 50 µm and scale bar in L= 100 µm.

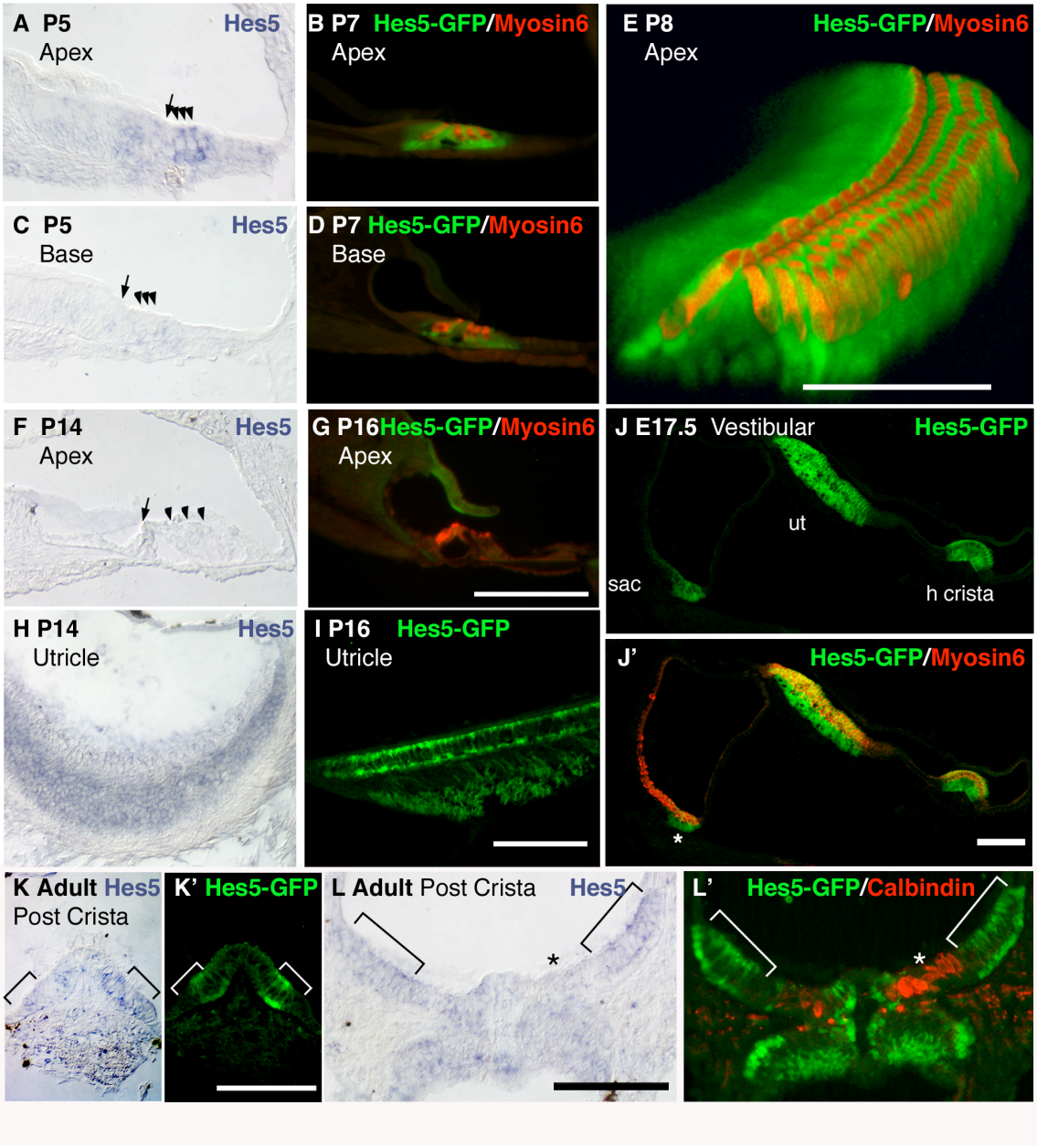
A P5 Hes5
Apex
B P7 Hes5-GFP/Myosin6
Apex
E P8 Hes5-GFP/Myosin6
Apex
C P5 Hes5
Base
D P7 Hes5-GFP/Myosin6
Base
F P14 Hes5
Apex
G P16Hes5-GFP/Myosin6
Apex
J E17.5 Vestibular Hes5-GFP
ut
sac
h crista
H P14 Hes5
Utricle
I P16 Hes5-GFP
Utricle
J' Hes5-GFP/Myosin6
*
K Adult Hes5
Post Crista
K' Hes5-GFP
L Adult Post Crista Hes5
*
L' Hes5-GFP/Calbindin
*

Figure 3.5 Hes5-GFP is expressed in a subset of adult vestibular supporting cells. Adult Hes5-GFP vestibular organs were immunolabeled for GFP and the hair cell marker myosinVI (**A**-**A''** and **E**-**E''**), or the striolar (type I) hair cell calyx marker calbindin (**B**-**B''**, **C**-**C'**, and **D**), or calretinin (**F**-**F''**) which labels both hair cells and type I hair cell calyxes. Images are brightest point projections (**A**-**A''**, **B**-**B''**, **C**-**C'**, and **E**-**E''**) or 3D projections (**D** and **F**-**F''**) of confocal z-series micrographs. Hes5-GFP is expressed in a mosaic pattern in the adult utricle; there is an area of high expression in the medio-posterior region of the macula and scattered cells throughout the epithelium (**A** and **B**). Only a few Hes5-GFP labeled cells are found within the striolar region, labeled with anti-calbindin (B-B''). The large boxed regions in **B** and **B''** are shown at higher magnification in **C** and **C'**, respectively. The smaller boxed region in **B''** is shown as an oblique 3D projection in **D**, rotated slightly counterclockwise; the radial profiles of Hes5-GFP labeled supporting cells can be seen at the margins of the striolar region, marked by the calbindin labeled striolar calyxes (asterisk). **E**-**E''** A horizontal crista shows Hes5-GFP labeling in supporting cells of the peripheral margins. **F**-**F''** The anterior crista has Hes5-GFP labeling surrounding the periphery of each half of the organ in a concentric pattern. Scale bar in **F''**=100 μm and applies to **A**-**D** and **F**-**G**. Scale bar in **B''**=100 μm and applies to **A**-**A''** and **B**-**B''**. Scale bars in **C'**, **E''** and **F''**= 100 μm. Scale bar in **D**=50 μm.

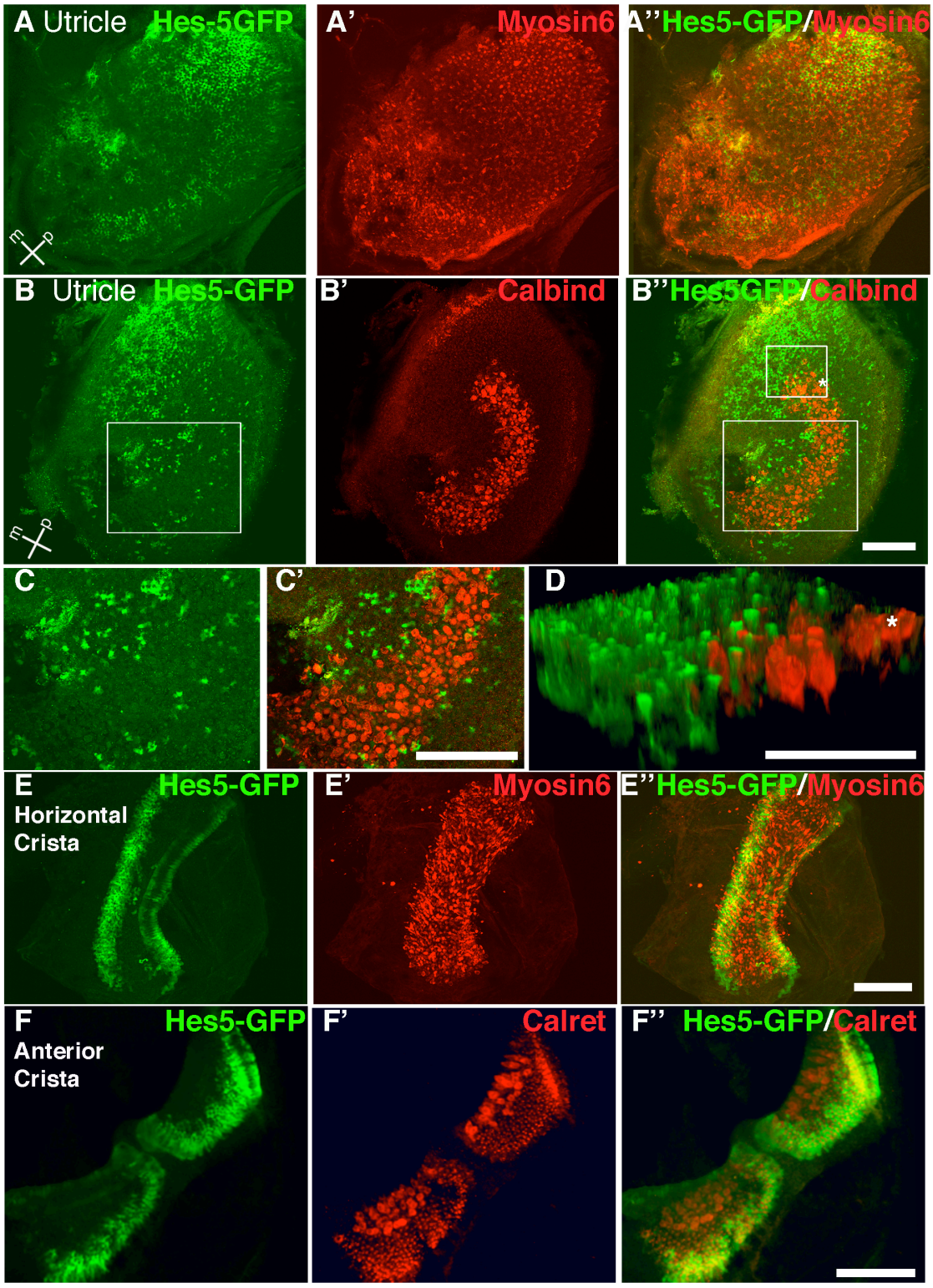
A Utricle Hes-5GFP
A' Myosin6
A'' Hes5-GFP/Myosin6
B Utricle Hes5-GFP
B' Calbind
B'' Hes5GFP/Calbind
C
C'
D
E Hes5-GFP
Horizontal Crista
E' Myosin6
E'' Hes5-GFP/Myosin6
F Hes5-GFP
Anterior Crista
F' Calret
F'' Hes5-GFP/Calret

Figure 3.6 Hes5-GFP is not upregulated in the adult cochlea after damage. Adult Hes5-GFP mice were given ototoxic injections and sacrificed two days or four days later. Tissues were collected from injected mice and uninjected littermate controls and processed for either whole mount (**A**-**A'''**, **B**-**B'''**) or cryosection (**D**-**D'**, **E-E'**) immunohistochemistry alongside positive control tissues: whole mount adult utricles (**C**-**C'''**) or cryosectioned P3 cochlea (**F**-**F'**). **A**-**A'''** Normal adult Hes5-GFP cochlea processed for whole mount immunohistochemistry with antibodies to GFP and myosinVI shows no expression of Hes5-GFP. ZY plane (**A'** and **A'''**) and brightest point XY projection views (**A'** and **A''**) are shown. The normal arrangement of inner and outer hair cells are seen in the merged views (**A'** and **A'''**). **B**-**B'''** Hes5-GFP is also not expressed in a drug-damaged cochlea four days after ototoxic injection, which caused complete outer hair cell loss. **C**-**C'''** Hes5-GFP immunolabeling is clearly present in utricle tissue from uninjected animal processed and imaged alongside cochlear tissues in A-A''' and B-B'''. **D**-**D'** A normal adult Hes5-GFP cochlea cryosection was immunolabeled with antibodies to GFP and Sox2. No Hes5-GFP was detected. Anti-Sox2 labeled supporting cell nuclei. **E**-**E'** In a drug-damaged adult Hes5-GFP cochlea cryosection, four days after injection, GFP was also not detected. However, supporting cells were still present and labeled with anti-Sox2. **F**-**F'** A P3 Hes5-GFP cochlear cryosection was processed alongside adult tissues shown in **C** and **D**, and shows strong labeling of Hes5-GFP and Sox2. Scale bar in **A'''**=100 μm and applies to **A**-**A'''**, **B**-**B'''**, and **C**-**C'''**. Scale bar in **F'=** 100 μm and applies to **D**-**D', E'**-**E',** and **F**-**F'**.

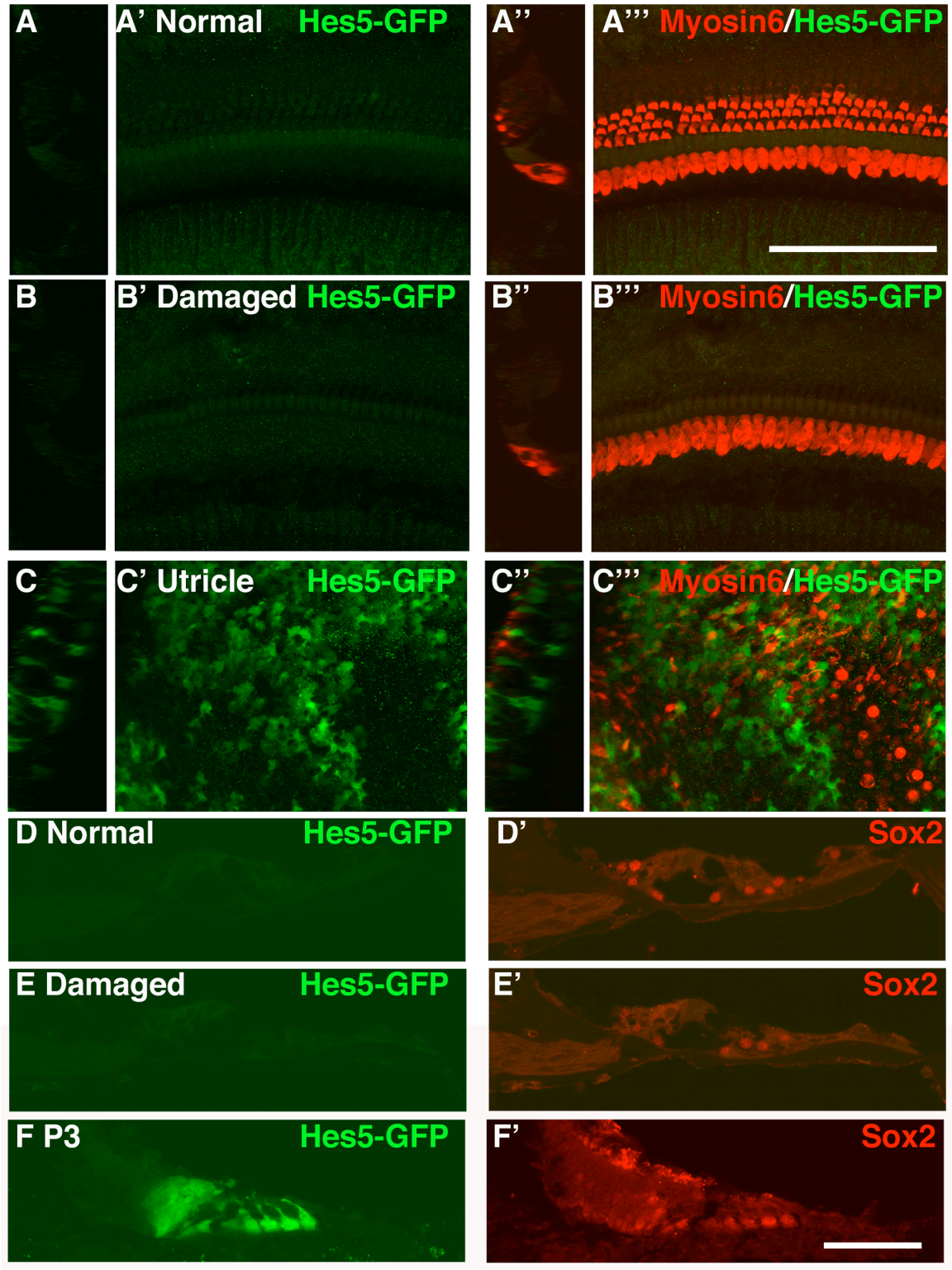
A
A' Normal Hes5-GFP
A''
A''' Myosin6/Hes5-GFP
B
B' Damaged Hes5-GFP
B''
B''' Myosin6/Hes5-GFP
C
C' Utricle Hes5-GFP
C''
C''' Myosin6/Hes5-GFP
D Normal Hes5-GFP
D'
Sox2
E Damaged Hes5-GFP
E'
Sox2
F P3 Hes5-GFP
F'
Sox2

Chapter IV:
Delta/Notch-Like EGF-related Receptor (DNER) is expressed in hair cells and neurons in the developing and adult mouse inner ear.

SUMMARY

The Notch signaling pathway is known to play key roles in cochlear development. Previous studies have shown that the Notch1 receptor and Notch ligands in the Delta and Jagged families are important for cellular differentiation and patterning of the organ of Corti. DNER (Delta/notch-like epidermal growth factor (EGF)-related receptor) is a novel Notch ligand expressed in developing and adult CNS neurons (Eiraku et al., 2002). DNER has been shown to actively promote morphological and functional maturation of glia through activation of Notch signaling in the cerebellum (Eiraku et al., 2005; Saito and Takeshima, 2006). In this study we have used in situ hybridization and an antibody against DNER to carry out expression studies of the mouse cochlea and vestibule. We find that DNER is expressed in spiral ganglion neuron cell bodies and peripheral processes during embryonic development of the cochlea and expression in these cells is maintained in adults. DNER becomes expressed in auditory hair cells during postnatal maturation in the mouse cochlea and immunoreactivity for this protein is strong in hair cells and afferent and efferent peripheral nerve endings in the adult organ of Corti. In the vestibular system, we find that DNER is expressed in hair cells and vestibular ganglion cells and processes during embryonic development and in adults. In order to investigate whether DNER plays a functional role in the inner ear, perhaps similar to its described role in glial maturation, we examined cochleae of DNER-/- mice. We performed immunohistochemical

analyses using markers of mature glia and supporting cells as well as neurons and hair cells to determine if adult DNER-/- mice have any defects in protein expression or morphology, with particular emphasis on evaluating the maturation status of supporting cells and glia. While we found that DNER immunoreactivity was abolished in mutant cochleae, we found no other defects in expression of markers of supporting cells and glia or myelin, and no abnormalities in hair cells or neurons. Due to animal housing restrictions we were unable to perform functional hearing or vestibular studies on DNER-/- mice, but our histological study suggests that DNER is dispensable for normal development and structure of the cochlea.

INTRODUCTION

The mammalian inner ear contains the five vestibular sensory epithelia and the auditory sensory epithelium. These sensory organs are composed of mechanosensory hair cells and nonsensory supporting cells. The auditory sensory epithelium, called the organ of Corti, is a highly ordered mosaic of mechanosensory hair cells and nonsensory supporting cells arranged in coiled rows that run the length of the cochlear duct. The vestibular organs include the three cristae of the semicircular canals, and the two macular organs, the utricle and saccule. Vestibular hair cells are innervated by afferent bipolar neurons in the vestibular ganglion, Scarpa's ganglion, situated in the outer part of the internal auditory meatus. Auditory hair cells in the organ of Corti are innervated by the peripheral processes of bipolar afferent neurons called spiral ganglion neurons, which have their somata in the central cochlear modiolus and project central axons through the bundled cochlear nerve to the auditory nucleus of the brainstem. There are two types of ganglion cells in the cochlea. Type I are myelinated and innervate one

inner hair cell each and make up approximately 90% of neurons in the spiral ganglion (Berglund and Ryugo, 1991; Koo et al., 2002; Ota and Kimura, 1980). Type II ganglion cells are unmyelinated, and each innervates up to 30-60 outer hair cells (Ginzberg and Morest, 1983; Kiang et al., 1982; Liberman et al., 1990; Perkins and Morest, 1975). The organ of Corti is also innervated by fibers of lateral and medial olivocochlear efferents. The lateral olivocochlear efferents (LOC) spiral through the lateral portion of the modiolus in the intraganglionic spiral bundle and enter the organ of Corti through the habenula perforata where they then run below the inner hair cells in the inner spiral bundle and in the tunnel spiral bundle, in the medial border of the tunnel of Corti. Fibers leave these bundles to terminate on the peripheral processes of Type I spiral ganglion neurons at the base of inner hair cells (Warr, 1980; Warr et al., 1997; Warr and Boche, 2003).

DNER was identified as a novel Notch ligand expressed in developing and adult CNS neurons (Eiraku et al., 2002) and, in the cerebellum, has been shown to actively promote morphological and functional maturation of glia through intercellular activation of Notch signaling (Eiraku et al., 2005; Saito and Takeshima, 2006; Tohgo et al., 2006). DNER was shown to bind to Notch1 at cell-cell contacts and activate Notch signaling in vitro (Eiraku et al., 2005). Co-culture with DNER-expressing cells and the application of the DNER extracellular domain stimulated NICD cleavage and CSL-dependent transcription in C2C12 myoblasts, demonstrating that DNER can activate CLS-dependent Notch signaling in vitro (Eiraku et al., 2005). On the other hand, DNER is expressed in Purkinje neurons, which are associated with radial fibers of Bergmann glia expressing Notch and in vitro studies showed that DNER specifically binds to Bergmann glia and induces radial process extension through gamma-secretase- and

Deltex-dependent CSL-independent (non-canonical) Notch signaling (Eiraku et al., 2005). Although the molecular basis of CSL-independent Notch signaling is largely unknown, this pathway is thought to require the cytoplasmic protein Deltex, which binds to NICD and acts as a positive regulator of Notch (Brennan and Gardner, 2002; Kishi et al., 2001).

DNER knockout mice were produced and are viable as homozygotes but exhibit mild motor discoordination in fixed bar and rota-rod tests and show morphological impairments of Bergmann glia and abnormal innervation between climbing fibers and Purkinje cells (Tohgo et al., 2006). Furthermore, DNER-/- mice exhibit impaired glutamate clearance at the Purkinje cell – climbing fiber synapses and reduced protein level of GLAST in Bergmann glia (Tohgo et al., 2006). In another study, DNER was shown to be involved in regulation of neurite outgrowth of Purkinje cells in a manner dependent on DNER endocytosis (Fukazawa et al., 2008). Most recently, DNER misexpression in glioblastoma-derived neurospheres was shown to inhibit tumor formation and promote differentiation into Tuj1-positive neurons and GFAP-positive glia (Sun et al., 2009).

In this study, we use immunolabeling and in situ hybridization to determine the expression pattern of DNER in the mouse cochlea during development and in adults. We describe the expression profile of DNER in auditory and vestibular hair cells as well as neurons and nerve fibers in the inner ear. We also examined cochleae of DNER-/- mice (Tohgo et al., 2006), performing immunohistochemical analyses using markers of mature glia and supporting cells as well as neurons and hair cells. While we found that DNER immunoreactivity was abolished in mutant cochleae, we found no other defects

in expression of markers of supporting cells and glia or myelin, and no abnormalities in hair cells or neurons.

RESULTS

DNER is expressed in spiral ganglion neurons and auditory and vestibular hair cells during embryonic and postnatal development.

We used immunolabeling as well as in situ hybridization to detect expression of DNER in the developing and neonatal mouse inner ear (Fig. 4.1). We found that during embryonic development, DNER is expressed strongly in the cell bodies of spiral ganglia neurons and at lower levels in their peripheral processes, which extend laterally to the developing organ of Corti. At E15.5 DNER expression was largely overlapping with that of Tuj1 (β-III tubulin) in the spiral ganglia (Fig. 4.1 A-A`). DNER is not expressed in auditory hair cells labeled with Atoh1-GFP during embryonic development, as shown at E17.5 (Fig. 4.1 B-B`). Similarly, DNER expression at postnatal day 2 (P2) was strong in spiral ganglia somata and less intense in the peripheral processes, and was not expressed in auditory hair cells at significant levels to detect above background (Fig. 4.2 C-C`). By P4, expression of DNER began to appear at low levels in auditory hair cells (Fig. 4.2 D-D`), but was comparatively stronger in spiral ganglia somata and peripheral terminals. Expression of DNER was progressively up-regulated in auditory hair cells during the first postnatal week so that by P7 immunolabeling with anti-DNER provided a similarly strong signal in spiral ganglia somata and auditory hair cells and peripheral nerve terminals in the organ of Corti. The anti-DNER staining in the spiral ganglion processes was weak along the length of the peripheral dendrites and became stronger at the peripheral terminals within the organ of Corti.

In contrast to the postnatal onset of DNER in auditory hair cells, we found that DNER is expressed in vestibular hair cells during embryonic development, as early as E15.5 (Fig. 4.1F). DNER was also colocalized with TuJ1 in peripheral afferent nerve processes underlying the vestibular organs, such as the saccule (Fig. 4.1F), at this age. Similarly, in the neonatal crista, DNER was expressed in hair cells and weakly expressed in peripheral neurites (Fig. 4.1G).

To detect the transcriptional profile of DNER expression and compare that to the protein expression, we performed in situ hybridization with antisense DNER riboprobe on sections from P5 inner ears (Fig. 4.1 H-I). We found that the patterns of DNER mRNA expression in the cochlea as well as the vestibular epithelia were highly similar to those observed with the antibody labeling. A transverse section through a crista probed for DNER showed expression in the hair cells (Fig. 4.1 H) similar to the antibody labeling pattern (compare to Fig. 4.1 G). A P5 cochlea section probed for DNER showed strong labeling in the spiral ganglion neurons (Fig. 4.1I) also similar to the immunolabeling pattern (compare to Fig. 4.1D).

To further validate the DNER antibody and in situ hybridization studies in the inner ear, we also performed expression studies in central nervous system tissues. In the P7 mouse retina, we found that both DNER protein and message are strongly expressed in the retinal ganglion cell (RGC) layer and at lower levels in the innermost part of the inner nuclear layer. DNER mRNA was localized to the perinuclear regions of cell bodies while DNER protein was enriched in cell bodies as well as the neurites within the inner plexiform layer (containing the dendrites of the RGCs and amacrine cells). Based on these patterns in the retina, DNER appears to be expressed in RGCs and amacrine cells. We include DNER expression in the retina here as an additional

example of overlapping localization of DNER mRNA and protein. A further description of DNER in the mammalian retina would be of interest, but is beyond the scope of this report. As a final positive control, we also stained sections of adult cerebellum with DNER antibody and obtained a highly similar pattern of expression in Purkinje neurons to that previously described by Eiraku and colleagues using a different antibody (Eiraku et al., 2002).

DNER is expressed in adult type I and type II spiral ganglion neurons.

Auditory hair cells are innervated by the spiral ganglion cells, which are bipolar neurons with their cell bodies in the cochlear modiolus. Spiral ganglion cells extend a peripheral dendrite to hair cells in the organ of Corti and a central axon along the bundled cochlear nerve to the cochlear nucleus in the brainstem. Following our observation that DNER is expressed in spiral ganglia neurons during embryonic and neonatal development we sought to investigate whether or not DNER expression was maintained in spiral ganglion cells in the hearing adult. We performed double immunolabeling experiments with anti-DNER and three other distinct markers of spiral ganglion cell populations (Fig. 4.2), to evaluate which, if any, expressed DNER in the adult. We found that all spiral ganglion cell bodies were labeled with DNER in the adult mouse cochlea (Fig. 4.2 A-C and A``-C``) and confirmed that DNER colocalized with calretinin (Fig. 4.2A`, A``), peripherin (Fig. 4.2B`, B``), and NF-M (Fig. 4.2C`, C``). calretinin is expressed in most type I spiral ganglion cells in rodents, but not in type II spiral ganglion cells (Dechesne et al., 1994; Dechesne et al., 1991; Koo et al., 2002). Consistently, we found that DNER was expressed in all calretinin-positive cell bodies and most of the cells labeled with DNER were also labeled with calretinin. About one-third of the DNER labeled cells

were negative for calretinin (arrowheads point to several examples in Fig. 4.2A-A``). The DNER-positive but calretinin-negative spiral ganglion neurons were typically small and most were located in the lateral portions of the ganglion. Based on these data and consistent with earlier studies, this population of neurons likely include includes both type II cells and a subset of type I cells (Koo et al., 2002). To confirm that DNER is expressed in type II spiral ganglion cells we double-labeled sections with antibodies to DNER and Peripherin (Fig. 4.2 B-B``), which has been shown to be expressed specifically in type II spiral ganglion neurons in adult rodents (Hafidi, 1998; Hafidi et al., 1993). Consistent with these studies and our earlier observation that DNER appeared to be expressed in all spiral ganglion neurons, we found that DNER was expressed in all of the peripherin-labeled type II spiral ganglion cells, which made up a small subset of total spiral ganglion neurons. To confirm that DNER is expressed in all types of spiral ganglion cells we double-labeled tissues with anti-DNER and rabbit anti-Neurofilament-M (145kD C-terminus, Millipore AB1987). We have previously used this antibody to label spiral ganglion cells and dendrites in the developing mouse cochlea (Hartman et al., 2007), and it has also been used to label both type I and type II spiral ganglion cells in the adult guinea pig (Corrales et al., 2006). A wide variety of other Neurofilament antibodies have been shown to label all or subsets of spiral ganglion neurons, depending on Neurofilament subtype specificity and phosphorylation status (Berglund and Ryugo, 1991). We found that this 145kD NF-M antibody labels all spiral ganglion neuron cell bodies and many of their processes (Fig. 4.2 C-C``), as well as olivocochlear efferent nerve fibers in the intraganglionic spiral bundle and the organ of Corti (see also Figs. 3, 5 and 6).

In the adult organ of Corti DNER is expressed in hair cells and afferent and efferent peripheral neural processes and terminals.

We found that DNER expression is maintained in auditory hair cells and peripheral neurites in the adult cochlea and performed immunolabeling experiments to determine the precise localization of DNER within the organ of Corti. In a 3D-rendered confocal z-series micrograph prepared from a whole mount surface preparation of adult organ of Corti, DNER immunoreactivity was strong in both inner and outer hair cells as well in neurites associated with the inner hair cells, specifically the radial fibers and inner spiral bundle fibers (ISB, Fig. 4.3A). DNER expression was also apparent in presumptive efferent terminal varicosities (Fig. 4.3A, arrowhead marks one example), which were abundant in the inner spiral bundle and radial fibers.

We performed double-immunolabeling with anti-DNER and other markers of hair cells and neurite populations in sections of adult organ of Corti. We found that DNER colocalized with myosinVI in inner and outer auditory hair cells (Fig. 4.3B-B``). The pattern of DNER immunolabeling in hair cells was punctate in the cytoplasm and mostly excluded from the nucleus. DNER was enriched in apical compartments of hair cells but was not present in hair cell bundles, labeled with anti-myosinVI. In sections, DNER immunolabeling in neurites was stronger than in whole-mount preparations, perhaps due to greater antibody penetrance in sections. We found DNER was expressed in a patchy and punctate pattern and varied in intensity in different fibers but could be detected in all afferent and efferent fiber populations. DNER expression was strong in radial fibers projecting to the inner hair cells in bundles through openings of the habenula perforata. DNER was also strongly expressed in the efferent inner spiral bundle fibers, which lie below the inner hair cells and run longitudinally. The inner spiral

bundle was labeled with NF-M and Tuj1, and lateral efferent terminals within the inner spiral bundle were also labeled with anti-synaptophysin. Sparse DNER expression was detected in the tunnel-crossing portion of medial efferent fibers, which were also labeled with NF-M and Tuj1 antibodies. Strong DNER expression was detected in neurites surrounding and below the outer hair cells, which include both type II afferent and medial efferent fibers. DNER colocalized in medial efferent fibers labeled with anti-NF-M and was abundant in medial efferent terminals labeled with synaptophysin. Outer spiral fibers from type II spiral ganglion cells cross the tunnel floor (where they are also called basilar fibers) and form three outer spiral bundles beneath the outer hair cells. These afferent fibers were colabeled with anti-Tuj1 and anti-DNER, which provided strong labeling particularly in the outer spiral bundles (Fig. 4.3E-E``).

DNER is expressed in adult vestibular hair cells and vestibular ganglion neurons. We performed immunolabeling experiments in the adult mouse vestibule and found that DNER is expressed in hair cells in all five vestibular organs and in vestibular ganglion neurons (Fig. 4.4). In sections at low magnification DNER immunolabeling was visible in all hair cells in the utricle and saccule and colocalized with Tuj1 in all of the vestibular ganglion neuron cell bodies (Fig. 4.4A-A``). At higher magnification, anti-DNER sparsely labeled afferent neurite fibers and was abundant in nerve terminals below utricular hair cells (Fig. 4.4B-B``). DNER labeling in vestibular hair cells was similar to that observed in auditory hair cells; it was strong but somewhat punctate, excluded from the nucleus, enriched in the apical portion of hair cells but very weak or not present in hair cell bundles. To confirm that DNER expression in nerve terminals below hair cells was not present in supporting cells, we double-labeled vestibular organs with anti-

DNER and anti-Sox9 (Fig. 4.4C-C`). Sox9 has been shown to be expressed in auditory and vestibular supporting cells during development (Mak et al., 2009), and we find that Sox9 labels nuclei of supporting cells and mesenchymal cells, but not hair cells, in the adult. DNER expression did not overlap with Sox9, as seen in a longitudinal optical section through a posterior crista whole-mount immunolabeled for DNER and Sox9 (Fig. 4.4C-C`). To determine the localization of DNER in nerve terminals, we colabeled sections with anti-calretinin, which specifically labels all pure calyceal afferent terminals (Dechesne et al., 1994; Desmadryl and Dechesne, 1992; Li et al., 2008a), or anti-Tuj1, which labels all afferent neurites and terminals (Li et al., 2008a). Transverse sections through cristae double-labeled with anti-DNER and anti-calretinin displayed partially overlapping expression patterns (Fig. 4.4 D-D``). DNER was found within the lower portions of calretinin-labeled calyceal endings but did not label the whole calyx (Fig. 4.4D``). A similar pattern was observed in cristae sections double-labeled with anti-DNER and anti-Tuj1 (Fig. 4.4E-E``). DNER expression was found in hair cells and underlying nerve terminals (arrowheads) and some fibers (arrows), but was not localized to the flask-shaped calyceal endings.

Organs of Corti from adult DNER-/- mice exhibit normal patterns of supporting cell maturation. Earlier studies have shown that DNER is involved in regulating maturation of glia in the CNS. DNER is expressed in cerebellar Purkinje neurons, which contact radial Bergmann glia. DNER-/- mice were shown to have defective maturation of Bergman glia; specifically, reductions in GLAST expression and impaired morphological maturation. In order to test whether DNER plays a similar role in glial and supporting cell maturation in the cochlea we examined inner ears from adult

DNER-/- mice and wild-type littermate controls. In short, we found that organs of Corti of DNER-/- mice lack DNER immunoreactivity (Fig. 4.5 B`-B``) but exhibit normal morphology and expression patterns of markers of hair cells, neurons, and mature supporting cells (Fig. 4.5). The intermediate filament, glial fibrillary acidic protein (GFAP), is expressed in cochlear supporting cells during postnatal maturation and in adult mice (Rio et al., 2002). GFAP is a classic marker for several types of glial cells, including astrocytes and nonmyelinating Schwann cells. Consistent with Rio et al., we found that GFAP is expressed in inner phalangeal cells, pillar cells, and Dieters' cells in the normal adult cochlea (Fig. 4.5 A-A``). Although the pattern of GFAP expression in supporting cells was complimentary to that of DNER in hair cells and neurites, expression of GFAP appeared normal in DNER-/- mice, which completely lacked DNER immunoreactivity (Fig. 4.5B-B). To evaluate the structure and morphology of the organ of Corti in mutant animals we immunolabeled hair cells with myosinVIIa and labeled filamentous actin with conjugated phalloidin (Fig. 4.5 C-D``). Phalloidin labeling is a useful method to evaluate the maturation and morphology of pillar cells and Dieters' cells, as both cell types contain abundant F-actin fibers, which are established during cellular maturation (Arima et al., 1986; Schick et al., 2006; Slepecky and Chamberlain, 1983). We did not detect any abnormalities in the levels or pattern of phalloidin labeling in pillars or Dieters' cells in mutant animals, and cellular morphology of these cells appeared normal (Fig. 4.5 D-D``). Previous studies have reported GLAST expression in inner phalangeal supporting cells, which surround inner hair cells in the organ of Corti (Furness and Lehre, 1997; Jin et al., 2003; Li et al., 1994). During development, GLAST immunoreactivity in inner phalangeal cells increases progressively during the second postnatal week, and reaches adult levels after two postnatal weeks in the

mouse (Jin et al., 2003). This time course correlates with DNER expression in hair cells and neurites the organ of Corti. We double-labeled cochlear sections for GLAST and NF-M and found that patterns of GLAST immunolabeling in the membranes of inner phalangeal cells and Neurofilament-M in peripheral neurites were similar in wild type and DNER-/- cochleae.

In addition to the above markers analyzed, we also labeled DNER-/- and control cochlear sections with antibodies against hair cell and neuronal markers myosinVI, synaptophysin, and Tuj1, which resulted in the same patterns as those shown in Fig. 4.3 and indicated no abnormalities in DNER-/- cochleae (data not shown). To further confirm that supporting cells were unaffected in mutant mice we labeled with antibodies to Sox2, S100A1, Jagged1, and P27kip1 and found that these supporting cell markers also stained with normal patterns in DNER-/- cochleae (data not shown).

Spiral ganglia from adult DNER-/- mice exhibit normal neuronal morphology and patterns of glia and myelin staining. We double-labeled spiral ganglia of adult DNER-/- and control mice with anti-NF-M, to label spiral ganglion neurons, and anti-GLAST or anti-CNPase, to evaluate glial maturation and myelination (Fig. 4.6). Spiral ganglion neuron morphology and NF-M immunoreactivity appeared normal in DNER-/- mice. Since DNER-/- mice exhibit impaired glial maturation and GLAST expression in the cerebellum, we looked at GLAST immunoreactivity in glia of the spiral ganglia. Previous studies have reported GLAST expression in spiral ganglion satellite cells surrounding type I spiral ganglion neurons (Furness and Lehre, 1997; Jin et al., 2003; Li et al., 1994). We double-labeled spiral ganglion sections for GLAST and NF-M and found that patterns of GLAST immunolabeling in satellite cells and NF-M in spiral

ganglion cell somata and neurites were similar in wild type and DNER-/- cochleae (Fig. 4.6 A-A`` and B-B``). To label myelin and glial cells in the spiral ganglia we used a monoclonal antibody to CNPase (RIP antigen), which has been commonly used to label myelin, oligodendrocytes, and peripheral ensheathing glia (Toma et al., 2007; Watanabe et al., 2006). We found that anti-CNPase provided strong labeling of myelin surrounding the somata and ensheathing the processes of type I spiral ganglion cells as well as myelin ensheathing efferent fibers in the intraganglionic spiral bundle (Fig. 4.6 C-C``). We double labeled DNER-/- and wild type spiral ganglia with CNPase and NF-M and found that mutants did not display any abnormalities in myelin patterns or morphology.

DISCUSSION

Earlier studies have described DNER expression in developing and adult CNS neurons (Eiraku et al., 2002; Eiraku et al., 2005). Here we described the expression pattern of DNER in developing and adult neurons and hair cells in the inner ear. In the CNS, DNER expression was shown to actively promote morphological and functional maturation of glia through intercellular activation of Notch signaling (Eiraku et al., 2005; Saito and Takeshima, 2006; Tohgo et al., 2006). In the auditory sensory epithelia, supporting cells of the organ of Corti have features similar to glia. Inner phalangeal cells ensheath the inner hair cell synapse and express the glutamate transporter GLAST (Furness and Lawton, 2003; Furness and Lehre, 1997; Jin et al., 2003; Li et al., 1994; Ottersen et al., 1998), which has been shown to mediate glutamate uptake at inner hair cell afferent synapses (Glowatzki et al., 2006) and play a role in preventing degeneration of hair cells caused by noise damage or aminoglycoside toxicity (Hakuba

et al., 2000; Shimizu et al., 2005). Cochlear supporting cells have been shown to exhibit GFAP expression and promoter activity (Rio et al., 2002; Stone et al., 2005), which is also characteristic of CNS glia. Based on these observations, we reasoned that DNER could function to promote maturation of glia and supporting cells in the inner ear and that DNER-/- mice may exhibit defects in glial and supporting cell morphology and/or protein expression. Our finding that adult DNER-/- mice display apparently normal supporting cells and glia in the cochlea suggests that DNER does not mediate maturation of these cell types through Notch signaling as it is thought to in the CNS.

While Notch signaling during inner ear development is well studied, little is known of the potential activity of this pathway in the adult inner ear. Indeed, there is evidence suggesting that Notch is not active in the adult cochlea. The Notch ligand Jagged1 is expressed specifically in supporting cells during development and immunolabeling indicates that this pattern of expression is maintained in adults (Morrison et al., 1999; Oesterle et al., 2008). On the other hand, expression of the activated Notch intracellular domain in cochlear supporting cells is reportedly ended by P7 (Murata et al., 2006). Correspondingly, expression of the hair cell-specific DSL Notch ligands Dll1, Dll3, and Jag2 in auditory hair cells is downregulated rapidly during early postnatal development and is not maintained in adults (Hartman et al., 2007). Consistently, in a recent study, we found that expression of the canonical Notch effector Hes5 is downregulated in cochlear supporting cells during postnatal development and is not expressed in the adult mouse cochlea (Hartman et al., 2009). Taken together these studies suggest that Notch signaling is absent in the adult cochlea, which would indicate that DNER expression is not sufficient to activate the pathway in this context.

Here we report the expression of DNER in developing and adult hair cells and neurons in the inner ear. The robust immunolabeling obtained with the anti-DNER antibody will be a useful tool for studies of auditory and vestibular hair cells and neurons. Functional hearing and vestibular studies of DNER-/- mice should be performed when possible to further evaluate the potential function of DNER in the inner ear. However, DNER does not appear to be required for normal development or maintenance of neuronal or glial cell types in the inner ear sensory epithelia or ganglia.

METHODS

Animals

DNER knockout mice were bred and housed at Kagoshima University Graduate School of Medical and Dental Sciences, 8-35-1 Sakuragaoka, Kagoshima-shi, Kagoshima 890-8544, Japan, under the care of professor Hirohito Miura. DNER knockout mice were shipped live to the Department of Comparative Medicine at the University of Washington (UWDCM) and were euthanized for tissue collection upon arrival. Wild type and transgenic mice were housed in the UWDCM. The Institutional Animal Care and Use Committee approved experimental methods and animal care procedures. DNER knockout mice were previously generated as described (Tohgo et al. 2005). DNER-/- and wild type mice obtained by crossing heterozygous mutants were used for the analyses in this study. To determine the mouse genotypes, PCR analysis was carried out using the synthetic primers from the mouse genomic sequence. The primers used were EGFL1 (25 mer, CTAGGTAGCCAAGACACACCTCGAG), EGFL8 (25 mer, GAGACCTCACAGGCTGGGTCCCAGG) and Neo2 (25 mer, CATCGCCATGGGTCACGACGAGATC). Adult (21-30 day old) mice were used for this

study. A total of five DNER-/- mice, one DNER+/-, and three wild-type mice were collected for analysis. Mice were euthanized according to approved procedures: mice were killed by anesthesia with CO_2 followed by cardiac perfusion with 4% PFA.

Fluorescent Immunohistochemistry

Embryos were collected from timed pregnant C57/BL6 mice and staged according to Kauffman (Kauffman, 1992). For postnatal mice, P0 was defined as the day of birth. Embryonic whole heads or P0-P5 half-heads, were fixed overnight in 4% PFA in PBS at 4^{o}C. Adult cochlea were isolated from temporal bones, the stapes was removed from the oval window, a small opening was made in the apex, and cold 4% PFA in PBS was perfused through the cochlea with a syringe. Perfused cochlea were then fixed overnight in 4% PFA in PBS at 4^{o}C, washed 3 X 30 minutes in PBS, and decalcified in 0.27M EDTA in PBS for 48hr at 4^{o}C. After fixation and decalcification (for adult cochlea) whole cochlea or heads were cryoprotected through graded sucrose in PBS (10% sucrose, 15% sucrose, 15% sucrose with 50% OCT) then embedded in OCT (Tissue Tek), frozen in a bath of ethanol and dry ice, sectioned at 10 μm, and mounted on Superfrost+ slides (Fisher Scientific). For whole-mount immunolabeling, adult cochlea were fixed and decalcified as above, then dissected to isolate the cochlear duct and expose the surface of the organ of Corti. Whole mount tissues and slides with cryosections were blocked for 1 hr in 10% FBS in PBS with 0.1% TritonX-100 at room temperature. Primary antibodies were diluted in block and incubated overnight at 4^{o}C. Slides or whole mount tissues were then washed in PBS 3 X 10 min, and incubated in species-specific fluorescent-labeled secondary antibodies AlexaFluor 488, 568, or 594 nm (1:500, Invitrogen). After immunostaining, tissues were coverslipped in on slides in

Fluoromount G (Southern Biotechnology, Birmingham, AL). Images of most stained sections were acquired on a Zeiss Axioplan 2 microscope equipped with DIC optics and a Spot camera. Images of adult cochlea sections and whole mount tissues were captured on a Zeiss LSM Pascal confocal microscope and processed using Improvision Volocity (3.0.2). Images were compiled with Adobe Photoshop 7.0.

Antibodies

Primary antibodies used were goat anti-DNER (R&D Systems Cat# AF2254) 1:100, Guinea pig anti-myosinVIIa (S. Heller) 1:500, Rabbit anti-myosinVI (Proteus Biosciences) 1:1000, mouse anti-Tuj1 (Covance) 1:500, rabbit anti-Neurofilament-M (145kD, Chemicon), rabbit anti-synaptophysin (Chemicon) 1:1500, guinea pig anti-GLAST (Chemicon) 1:1000, rabbit anti-GFAP (DAKO) 1:1000, and mouse anti-CNPase (Sigma) 1:200. Secondary antibodies used were goat anti-mouse Alexa 594, chicken anti-mouse 594, goat anti-rabbit Alexa 594, donkey anti-goat 488, and goat anti-rabbit Alexa 488, all from Molecular Probes, and goat anti-guinea pig Cy3 from Chemicon.

Paraffin *In Situ* Hybridization

DIG-labeled antisense riboprobe was prepared for in situ hybridization for mouse DNER from cDNA clone MGC: 39059 (IMAGE: 5365190). For postnatal mice, postnatal day 0 (P0) was defined as the day of birth. In situ hybridization was performed as previously described (Hayashi et al., 2007; Nelson et al., 2004). Briefly, P5 and P7 half-heads (with brains removed), were fixed overnight at 4°C in modified Carnoy's solution (60% ethanol, 11.1% formaldehyde (30% of 37% stock), 10% glacial acetic acid), dehydrated though an EtOH series, prepared for paraffin embedding, and sectioned at 6-8 µm.

Slides were baked overnight at 68^{o}C, dewaxed in Xylene, rinsed in 100% EtOH, and air-dried at room temperature. Overnight hybridization and subsequent washes were carried out at 68^{o}C. Hybridized probe was detected using anti-Digoxygenin alkaline phosphatase conjugated antibody (1:2000 dilution, Roche Biochemical, Indianapolis, IN) and visualized with NBT/BCIP for a blue precipitate. After *in situ* hybridization, sections were post-fixed in 4% PFA, rinsed in PBS, and mounted with Fluoromount G.

Figure 4.1 DNER is expressed in developing spiral ganglion neurons and auditory and vestibular hair cells. A developmental series of cryosections of cochlear turns from E15.5 to P7 immunolabeled for DNER (red, A – E`) and colabeled with anti-Tuj1 (spiral ganglia, green A`) or transgenic Atoh1GFP (hair cells, green, A`-E`). During embryonic development (E15.5 A-A` and E17.5 B-B`) DNER expression is strong in the spiral ganglion (sg) cell bodies and less intense in their peripheral processes, which extend laterally to the developing organ of Corti (oc). Spiral ganglion neurons are double-labeled with DNER and Tuj1 at E15.5 (green, A`) but DNER is not expressed in auditory hair cells labeled with Atoh1-GFP during embryonic development (B`). C-E' During postnatal development of the cochlea DNER expression becomes intense in the peripheral neurites of the organ of Corti, is initially expressed in neonatal hair cells at low levels (C – D) and is strongly expressed in hair cells by P7 (E). F-G Expression of DNER in embryonic (F) and neonatal (G) vestibular epithelia is strong in hair cells and less intense in peripheral nerve processes. DNER is expressed in vestibular hair cells as early as E15.5 (saccule, F). H-J In situ hybridization with antisense DNER probe showed comparable expression in hair cells of the crista (H) and spiral ganglion neurons (I) at P5. Similarly, DNER in situ hybridization (J, left) and immunolabeling (J, right) showed comparable expression patterns in P7 mouse retina, both methods labeling neuron cell bodies strongly in the retinal ganglion cell layer and less intense in the inner nuclear layer. K A sagital section through adult (P37) cerebellum stained with DNER antibody as a positive control showed strong expression in Purkinje neurons, similar to results previously published.

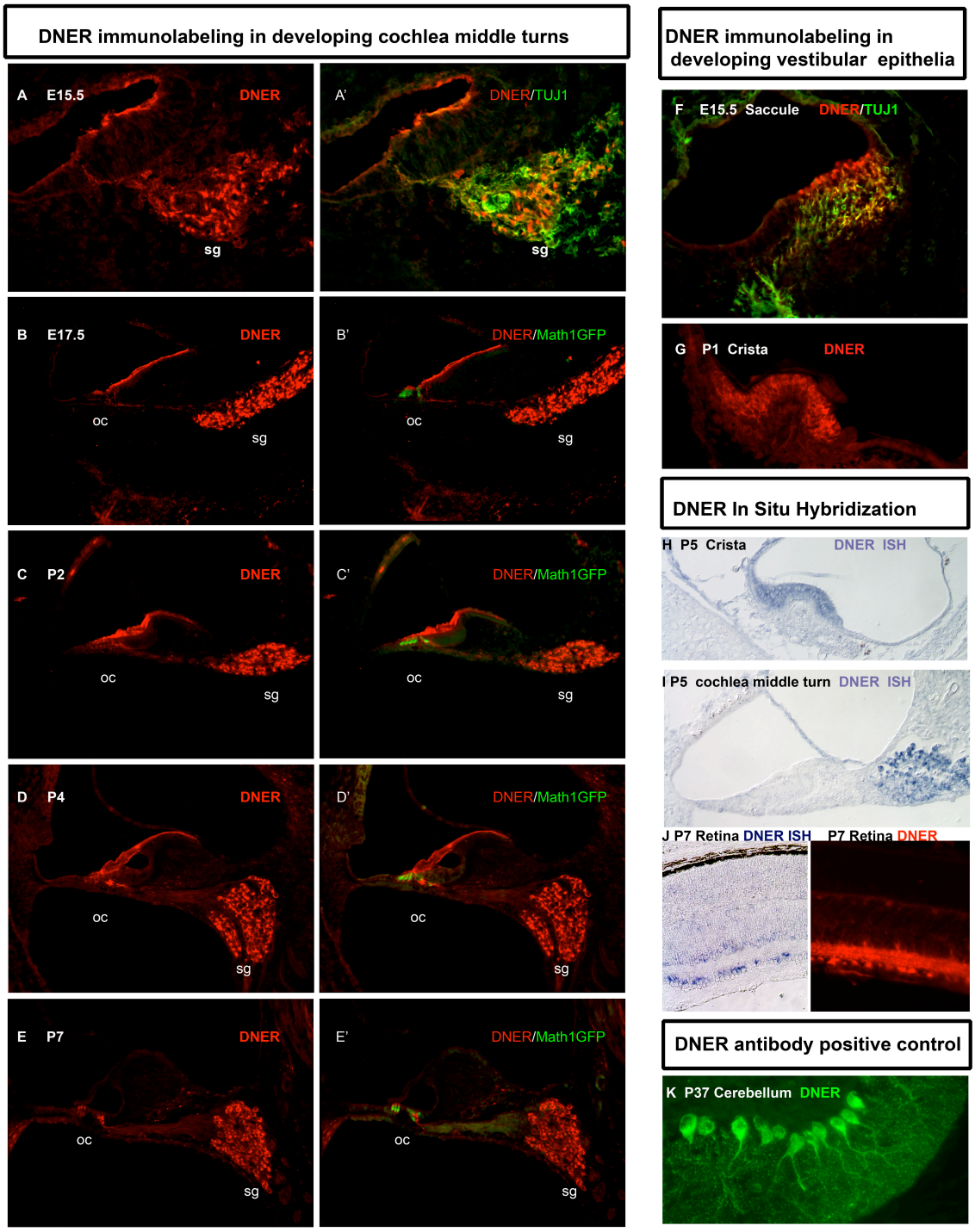
DNER immunolabeling in developing cochlea middle turns
A E15.5 DNER
sg
A' DNER/TUJ1
sg
B E17.5 DNER
oc
sg
B' DNER/Math1GFP
oc
sg
C P2 DNER
oc
sg
C' DNER/Math1GFP
oc
sg
D P4 DNER
oc
sg
D' DNER/Math1GFP
oc
sg
E P7 DNER
oc
sg
E' DNER/Math1GFP
oc
sg
DNER immunolabeling in developing vestibular epithelia
F E15.5 Saccule DNER/TUJ1
G P1 Crista DNER
DNER In Situ Hybridization
H P5 Crista DNER ISH
I P5 cochlea middle turn DNER ISH
J P7 Retina DNER ISH
P7 Retina DNER
DNER antibody positive control
K P37 Cerebellum DNER

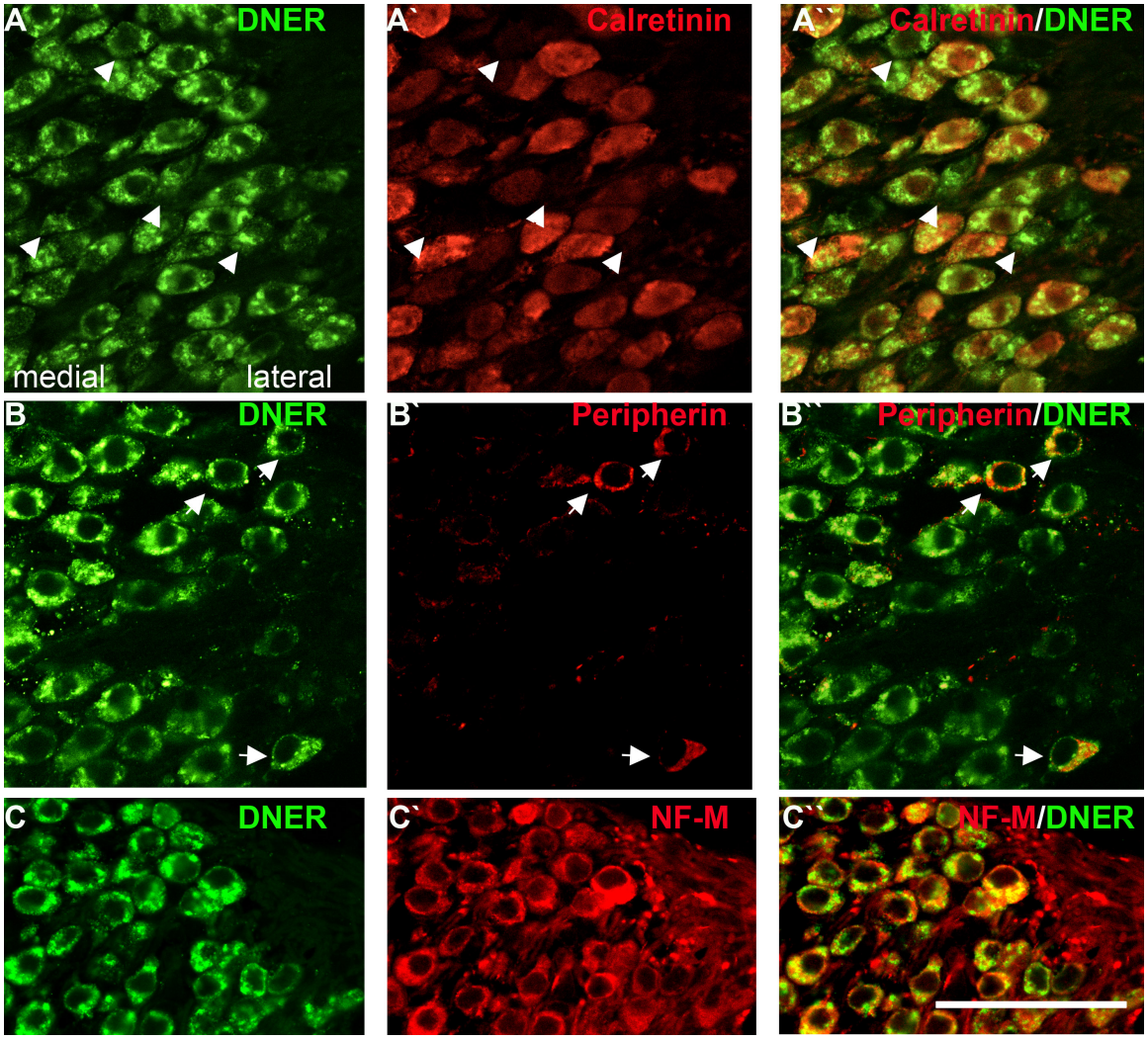

Figure 4.2 DNER is expressed in type I and type II spiral ganglion neuron somata in the adult cochlea. A-A`` DNER (green) is expressed in the cell bodies of all calretinin-positive type I spiral ganglion cells (red). A small subset of DNER-positive spiral ganglion cells are negative for calretinin (arrowheads). B-B`` DNER is expressed in the somata of all Peripherin-positive type II spiral ganglion cells (red), (arrows). C-C`` DNER expression in all spiral ganglion neuron cell bodies overlaps with that of NF-M (red), which labeled all spiral ganglion neuron cell bodies and projections.

Figure 4.3 DNER is expressed in hair cells and afferent and efferent peripheral neurites in the adult mouse cochlea. A A surface view of a 3D-rendered confocal z-series micrograph taken from an adult organ of Corti wholemount preparation immunolabeled with anti-DNER (green). In this view, expression of DNER can be seen in the three rows of outer hair cells (OHC), the row of inner hair cells (IHC) in the region of the inner spiral bundle (ISB), below and medial to the inner hair cells. Within the ISB, DNER expression is strong in many presumptive efferent varicosities (arrowhead points to one example). B-E`` Cryosections were double-labeled for DNER and myosinVI, Neurofilament-M (NF-M), synaptophysin, or Tuj1. DNER was coexpressed in hair cells with myosinVI (B-B`). C-C`` NF-M labeled the neurites of the inner spiral plexus, which are also strongly labeled with DNER, as well as the tunnel-crossing medial efferent fibers (MEF), which contained low levels of DNER. D-D`` The olivocochlear lateral efferent terminals (LET) and medial efferent terminals (MET) were labeled specifically with anti-synaptophysin and were found to express DNER with a large degree of overlap. E-E` Anti-Tuj1 was used to label all of the afferent and efferent neurites in the organ of Corti to confirm the identity of the DNER-positive fibers and the brightness of the image was increased to ensure visualization of the fibers. In addition to the ISP and tunnel-crossing MEFs, the afferent type II outer spiral fibers (OSF, also referred to as basilar fibers) can be seen running laterally crossing the floor of the tunnel to the region below the outer hair cells where they join with other type II fibers to form the three outer spiral bundles (OSB). Thus, DNER expression is enriched in all of the organ of Corti fiber populations particularly at the terminals.

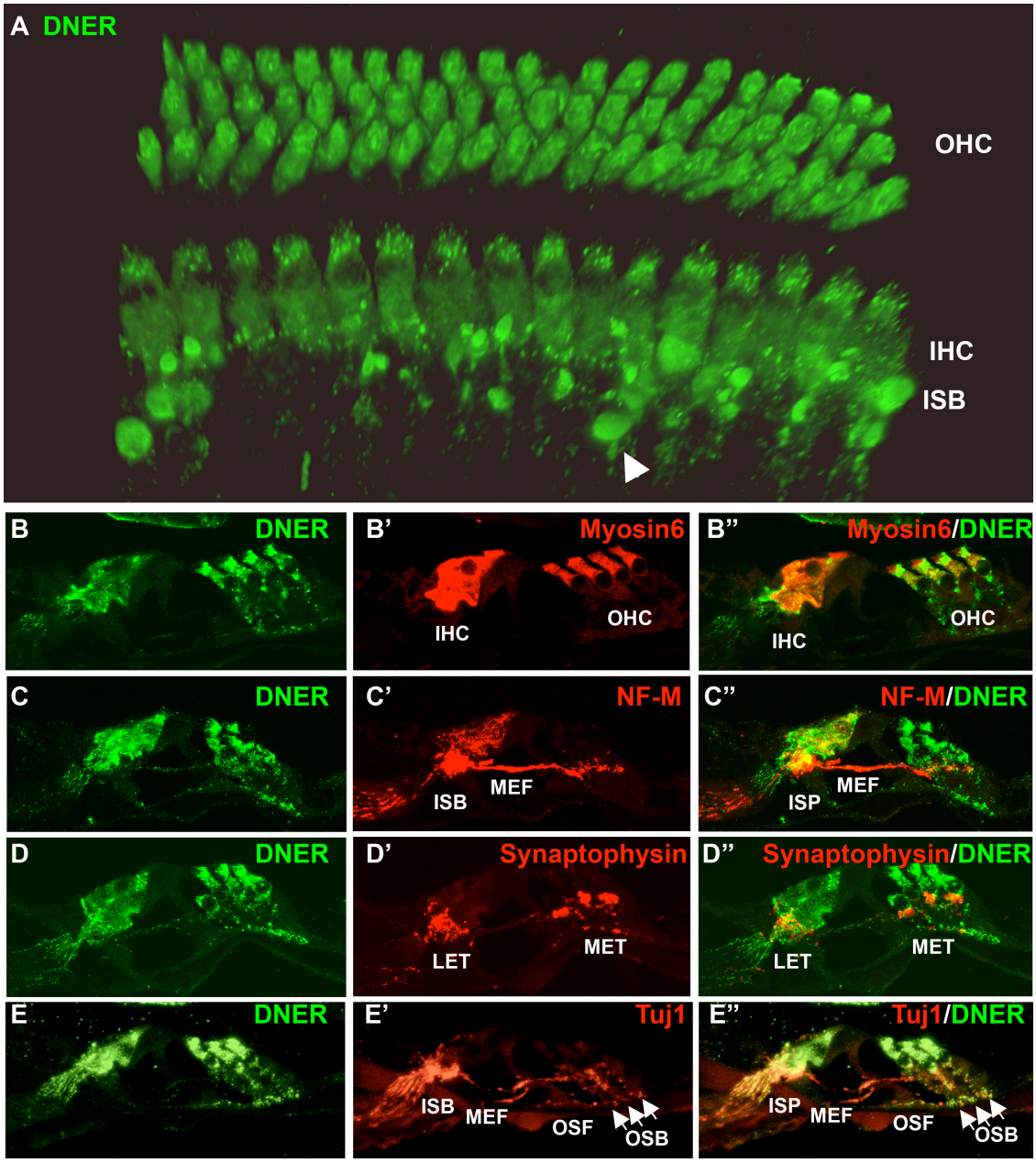
A DNER
OHC
IHC
ISB
B DNER
B' Myosin6
IHC
OHC
B'' Myosin6/DNER
IHC
OHC
C DNER
C' NF-M
ISB
MEF
C'' NF-M/DNER
ISP
MEF
D DNER
D' Synaptophysin
LET
MET
D'' Synaptophysin/DNER
LET
MET
E DNER
E' Tuj1
ISB
MEF
OSF
OSB
E'' Tuj1/DNER
ISP
MEF
OSF
OSB

Figure 4.4 DNER is expressed in adult vestibular hair cells, peripheral nerve endings and vestibular ganglion cell bodies. A-A`` A low magnification view of a section through the vestibular part of the inner ear containing utricle, saccule, and vestibular ganglion (VG) was immunolabeled with DNER (green A, A``) and Tuj1 (red A`, A``). In this view strong DNER expression can be seen in the hair cells of the utricle and crista as well as the cell bodies of the vestibular ganglia, while Tuj1 labels the vestibular ganglion cells and all of their afferent fibers in the vestibular organs. B-B`` A high magnification view of the utricle section in the boxed region of panel A, showing DNER (B), Tuj1 (B`) and the two channels merged (B``). DNER expression is strong in hair cells and can also be seen at lower levels in the Tuj1-positive afferent fibers (arrows point to two examples) and their endings beneath the hair cells. C-C` An optical section showing a longitudinal view of a posterior crista labeled with DNER (C-C`) and the supporting cell nuclear marker Sox9 (C`). Similar to the expression in the macular organs, anti-DNER labeling is strong in the hair cells and less intense in the underlying neurites. DNER is not expressed in supporting cells. D-D`` A transverse section of a crista double labeled with DNER (D, D``) and the pure calyceal afferent marker calretinin shows that DNER is expressed in the type I hair cells at the apices and is present in the calyceal nerve ending but does not completely overlap with calretinin. E-E`` A similar section to D-D`` double labeled with DNER and Tuj1 shows that DNER is expressed in some of the afferent neurites (arrow points to two examples) and terminals below the hair cells (arrowheads) but is not colocalized with Tuj1 throughout the flask-shaped calyceal endings that envelope many of the hair cells.

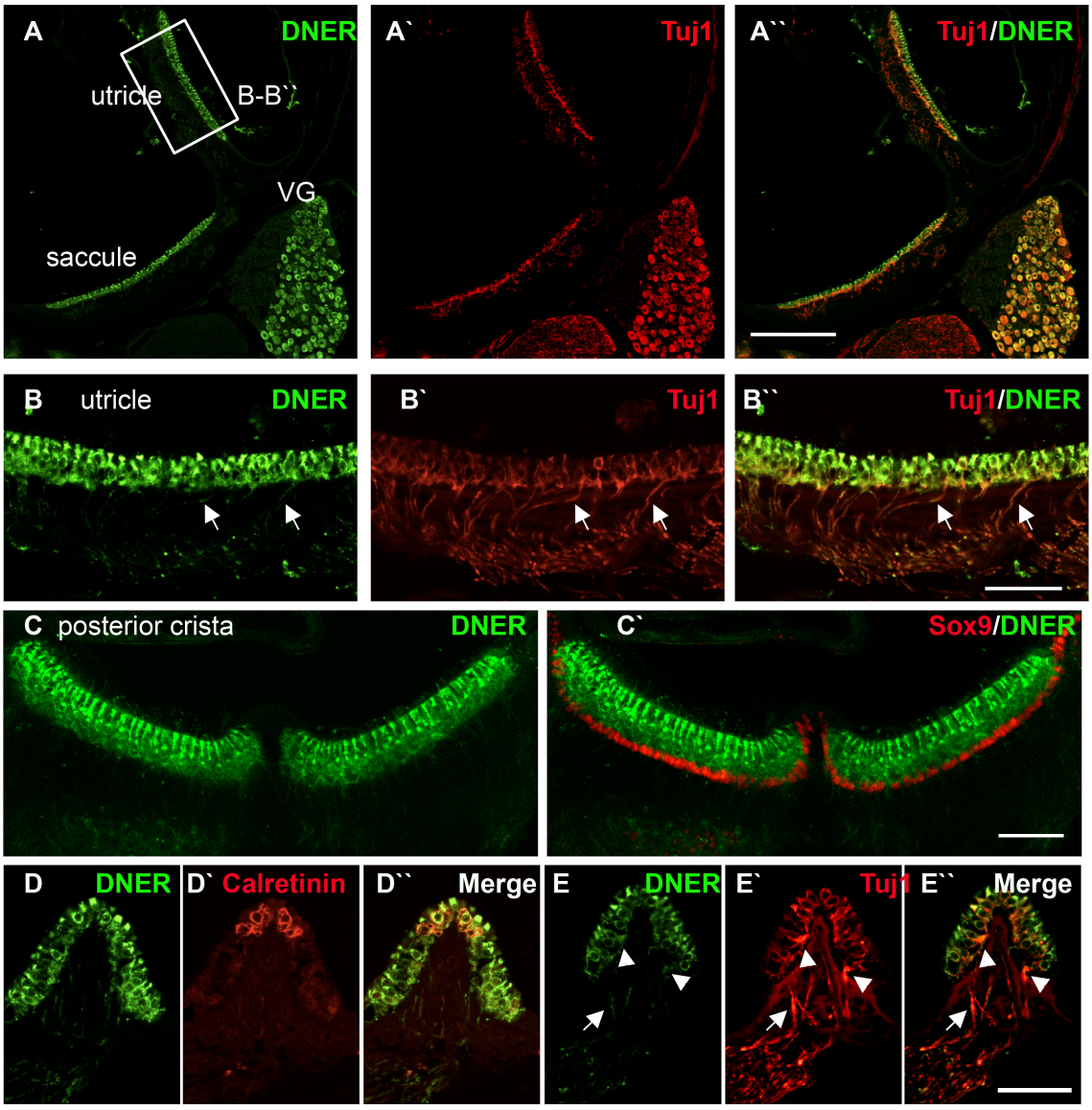
A
DNER
utricle
B-B``
VG
saccule
A`
Tuj1
A``
Tuj1/DNER
B
utricle
DNER
B`
Tuj1
B``
Tuj1/DNER
C
posterior crista
DNER
C`
Sox9/DNER
D
DNER
D`
Calretinin
D``
Merge
E
DNER
E`
Tuj1
E``
Merge

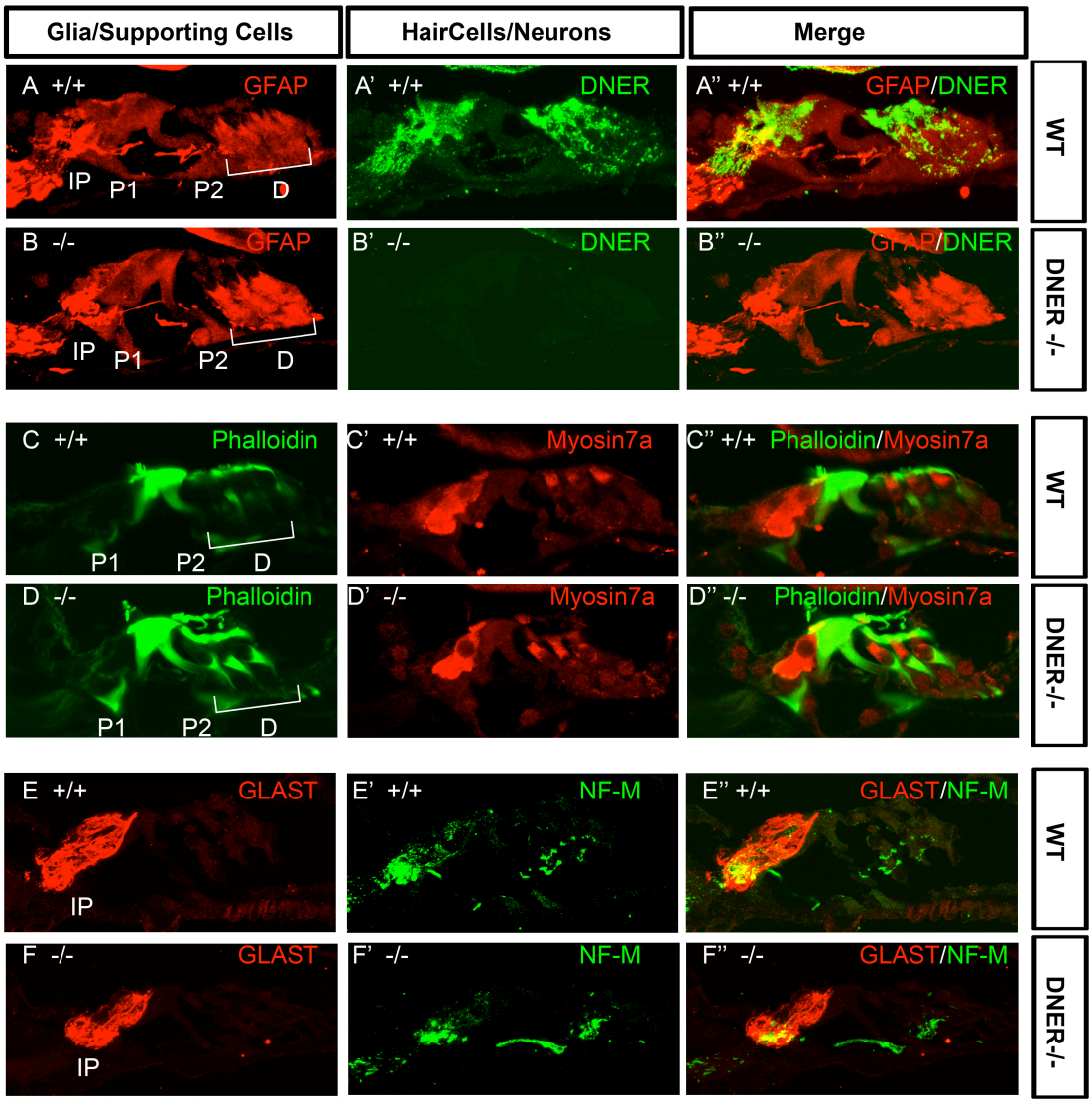

Figure 4.5 Organs of Corti of DNER-/- mice lack DNER immunoreactivity but exhibit normal morphology and expression patterns of hair cell and supporting cell markers. A-B`` Wild type (A-A``) and DNER-/- (B-B``) cochlea sections were double labeled for DNER (green) and GFAP (red), a marker of glia and mature supporting cells. DNER immunolabeling is absent in DNER-/- animals (B`-B``), but normal expression of GFAP was observed in inner phalangeal cells (IP), pillar cells (P1 and P2), and Dieters' cells (D, bracket). C-D`` In a similar set of sections from wild type (C-C``) and DNER null (D-D``) mice, F-actin (in pillar cells, Dieters' cells, and hair cell bundles) was labeled with conjugated phalloidin (green) and hair cells were labeled with anti-myosinVIIa (red). E-F`` Similarly, patterns of GLAST immunolabeling (red) in the membranes of inner phalangeal cells and Neurofilament-M (green) in peripheral neurites were similar in wild type (E-E``) and DNER-/- (F-F``) cochleae.

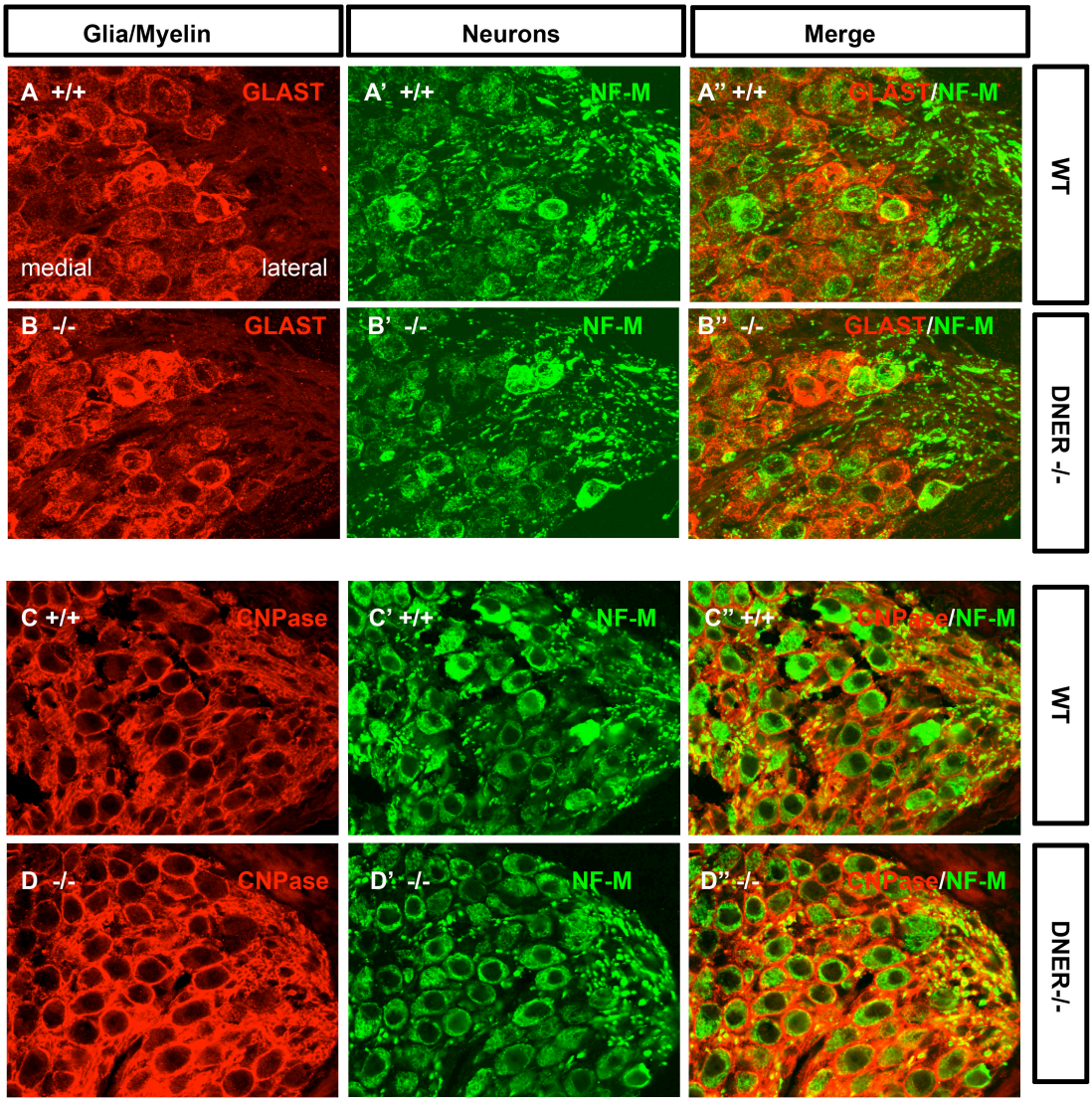

Figure 4.6 Spiral ganglia of DNER-/- mice exhibit normal neuronal and glial morphology and myelination patterns. A-B`` Sections through spiral ganglia of wild type (A-A``) and DNER-/- (B-B``) mice were double labeled with the glial marker GLAST (red) and NF-M (green) which labels all spiral ganglion cell bodies and processes. C-D`` Similar wild type (C-C``) and DNER-/- (D-D``) sections were immunostained with CNPase (red) to label myelin as well as NF-M (green).

Chapter V:
Notch signaling in the inner ear promotes sensory induction during embryonic development and later directs supporting cell vs. hair cell fate.

INTRODUCTION

During embryogenesis, the inner ear develops from the otic placode region of the head ectoderm, which invaginates and pinches off from the ectoderm to form the otic vesicle. The six sensory organs of the mammalian inner ear are derived from the otic vesicle. Through a complex series of morphogenetic events, the otic vesicle differentiates into the membranous labyrinth of the inner ear containing the cochlea and five vestibular sensory epithelia, consisting of the two macular organs (the utricle and saccule) and the three cristae of the semicircular canals. While the membranous labyrinth of the inner ear forms a continuous epithelial structure derived from the otic vesicle, the six sensory organs within the labyrinth are individually distinct neuroepithelial sensory structures. These inner ear sensory epithelia are composed of highly ordered mosaics of mechanosensory hair cells, glia-like supporting cells, and specifically targeted afferent and efferent nerve endings. During development, tightly controlled morphogenetic events regulate the specification of the prosensory regions within the labyrinthine epithelium that will give rise to sensory organs. This “prosensory specification” parses out and maintains specific cells that will later become hair cells and supporting cells, distinguishing these sensory progenitors from nascent nonsensory epithelia cells which will form the rest of the labyrinth.

The mechanism of prosensory specification is not yet well understood. However, the prosensory domains can be identified by expression of the Notch ligand Jagged1

(Jag1) and the HMG transcription factor Sox2 (Adam et al., 1998; Kiernan et al., 2005b; Morrison et al., 1999; Uchikawa et al., 2003; Uchikawa et al., 1999). Moreover, both Jag1 and Sox2 are required for prosensory specification; as mice deficient in either gene have severe defects in sensory epithelia formation (Brooker et al., 2006; Kiernan et al., 2005b; Kiernan et al., 2006; Vrijens et al., 2006). Furthermore, the partial loss of Sox2 expression in the Jag1 conditional mutant mouse suggests that Jag1 acts upstream of Sox2 (Kiernan et al., 2006). Jag1 is thought to act through the Notch1 receptor, which is expressed throughout the early otic vesicle and the activated Notch intracellular domain (NotchIC) has been detected in the early prosensory portions of the cochlea (Murata et al., 2006). Additionally, the downstream Notch effectors HesR1 and HesR2, have been detected in the early prosensory domain of the cochlea and pharmacological inhibition of Notch in mouse cochlear explants with γ-secretase inhibitors during the prosensory phase results in a severe reduction in hair cell and supporting cell numbers (Hayashi et al., 2008). Similarly, inactivation of Notch in chick embryos with the γ-secretase inhibitor DAPT resulted in disruption of sensory patch development in the otocyst (Daudet et al., 2007).

The above studies strongly suggest that Jag1-Notch signaling is required for at least some part of prosensory specification in the inner ear. As well, an earlier report showed that transient overexpression of NotchIC in the chick otocyst resulted in induction of ectopic sensory structures, containing hair cells and supporting cells (Daudet and Lewis, 2005). In the present study, we test whether constitutive activation of Notch either broadly or in mosaics in inner ear epithelia of mice is sufficient to expand the prosensory domain. We find that broad expression of NotchIC in the inner ear epithelia of FoxG1Cre/Rosa^{Notch} mice causes induction of prosensory markers

throughout the entire otic epithelium as well as enlargement of the epithelium resulting in externalization apparently from failure of otic vesicle closure. In hGFAPCre/Rosa^{Notch} mice we find that Cre recombination and Rosa^{Notch} transgene expression occurs in mosaic regions of nonsensory vestibular epithelia resulting the induction of ectopic sensory structures complete with hair cells, supporting cells, and afferent innervations. To test whether constitutive activation of Notch in mature cochlear supporting cells is sufficient to confer progenitor character or regeneration capacity we again used hGFAPCre/Rosa^{Notch} transgenic mice, which we found express the Rosa^{Notch} transgene in a subset of mature cochlear supporting cells. We found that cochlear supporting cells constitutively expressing the Rosa^{Notch} transgene do not dedifferentiate or otherwise respond either spontaneously or in response to in vitro hair cell damage.

RESULTS

Ectopic Notch activation in otocysts of FoxG1Cre/Rosa^{Notch} embryos is sufficient to expand the prosensory domain.

We used a transgenic approach to broadly and constitutively activate Notch in the otic vesicles of mouse embryos. The Rosa^{Notch} transgenic mouse was previously generated by targeting of a cDNA that encoded an intracellular fragment of mouse Notch1 (NotchIC), an internal ribosome entry sequence, and nuclear-localized enhanced GFP (EGFP) to the Rosa26 locus, preceded by a floxed STOP cassette (Murtaugh et al., 2003). In the absence of Cre recombinase, transcription of the Rosa^{Notch} transgene is blocked by the STOP sequence; in the presence of Cre, STOP is deleted, yielding heritable, constitutive coexpression of NotchIC and nuclear EGFP. The FoxG1Cre transgenic line has previously been shown to exhibit Cre recombinase activity in the telencephalon, anterior optic vesicle, otic vesicle, facial and head

ectoderm, olfactory epithelium, mid-hindbrain junction, and pharyngeal pouches (Hebert and McConnell, 2000). FoxG1Cre has been used extensively for generation of conditional mutants for studies of inner ear development (Barrionuevo et al., 2008; Kiernan et al., 2005a; Kiernan et al., 2006; Pirvola et al., 2002; Yamamoto et al., 2006).

We generated FoxG1Cre/Rosa^{Notch} double transgenic embryos and found that this combination of results in embryonic lethality after about E14. FoxG1Cre/Rosa^{Notch} embryos collected at E13.5 displayed abnormal gross morphology, including neural tube closure defects resulting in externalization of anterior neural tissues (Fig. 5.1 B). To confirm that the Notch pathway is activated in these bigenic embryos we performed in situ hybridization for the downstream Notch effector Hes5. As expected Hes5 mRNA was expressed in control embryos in the ventricular zone of the brain and spinal cord (Fig. 5.1 C). On the other hand, Hes5 was strikingly upregulated in the neuroepithelium of FoxG1Cre/Rosa^{Notch} double transgenic embryos, which displayed externalized neuroepithelia, an expanded ventricular zone and collapse of the fourth ventricle, apparently due to overproduction of the neuroepithelium (Fig. 5.1 D and G). Additionally, ectopic Hes5 expression was detected in the foregut (fg) of FoxG1Cre/Rosa^{Notch} embryos, which is consistent with previously described Cre recombination in FoxG1Cre foregut (Fig. 5.1D and (Hebert and McConnell, 2000)).

We found that the otic epithelia of FoxG1Cre/Rosa^{Notch} embryos is enlarged and externalized, and exhibits ectopic expression of Notch effectors and expansion of prosensory markers Jag1 and Sox2 throughout the epithelium. Cochlear epithelia sections from control FoxG1Cre (Fig. 5.2. A, C, E, G) embryos and similar sections through otic epithelium of double transgenic FoxG1Cre/Rosa^{Notch} (Fig. 5.2 B, D, F, H) embryos at E13.5 show the thickened and externalized morphology of the otic

epithelium in bigenic embryos. Hes5 in situ hybridization signal is not normally detected in the cochlea at this age and is not present in control (Fig2. A) but Hes5 expression is present at varying levels throughout in the bigenic otic epithelia (Fig. 5.2 B). Antibody labeling for Jag1 showed the normal pattern in the medial floor of the duct in the control (Fig. 5.2 C) and ectopic Jag1 labeling throughout the entire epithelia in the bigenic cochlea (Fig. 5.2 D). Similarly, Sox2 immunolabeling is restricted to the floor of the cochlear duct in control embryos (Fig. 5.2 E), and expanded throughout the entire externalized otic epithelium in bigenic embryos (Fig. 5.2 F). As well, the Notch effector HesR1 is normally restricted to the floor of the cochlear duct (Fig. 5.2 G) and is expressed throughout the entire otic epithelium in bigenic embryos (Fig. 5.2 H).

Notch activation in nonsensory vestibular epithelia of hGFAPCre/Rosa^{Notch} mice induces formation of ectopic vestibular sensory patches.

We analyzed the Cre recombination activity in the inner ears of hGFAPCre mice and found Cre activity in mosaic in regions within and around vestibular sensory epithelia (Fig. 5.3). To visualize Cre activity we in hGFAPCre mice we used the mT/mG double fluorescent Cre reporter mouse line (Muzumdar et al., 2007), which expresses membrane-targeted tandem dimer Tomato (mT) prior to Cre-mediated excision and membrane-targeted green fluorescent protein (mG) after excision. Wholemount views of P16 hGFAPCre/mTmG vestibular organs show cells which have undergone Cre mediated recombination labeled by expression of membrane bound GFP, while all other cells are labeled with membrane bound Tomato red fluorescent protein. In and around the utricle Cre activity was present in mosaic clusters, which included: hair cells, supporting cells, and transitional epithelial cells outside the margins

of the sensory epithelia (Fig. 5.3 A-B). Similarly, we found Cre activity in a clusters of hair cells, supporting cells, and nonsensory epithelial cells in and around the cristae, although less frequently than in the region of the utricle (Fig. 5.3C). Although we nearly always found at least some Cre activity in the regions of the vestibular organs of hGFAPCre/mTmG mice the degree and spatial patterns of recombination were highly variable.

To ectopically activate Notch in mosaic subsets of sensory and nonsensory vestibular progenitor cells, we generated hGFAPCre/Rosa^{Notch} bigenic mice. We found that ectopic sensory patches, with hair cells and afferent projections, form in vestibular epithelia of hGFAPCre/Rosa^{Notch} mice in regions where the Rosa^{Notch} transgene is activated (Fig. 5.4). Flatmount confocal projection views of vestibular epithelia from hGFAPCre/Rosa^{Notch} or hGFAPCre control (Fig. 5.4. A and B, respectively) including the utricle and adjacent horizontal crista immunolabeled with anti-GFP (green, from the RosaNotch) and antibodies against both myosinVI and calretinin (red), to label hair cells and afferent fibers. In the hGFAPCre/Rosa^{Notch} epithelium several regions of ectopic sensory patch formation are present between the utricle and horizontal crista. In the control vestibule the same region (marked by an asterisk) is nonsensory and devoid of hair cells. GFP expression is present in patches of cells within the ectopic sensory regions of the hGFAPCre/Rosa^{Notch} vestibule (Fig. 5.4, lower panels).

We found that ectopic sensory patches in nonsensory vestibular epithelia of hGFAPCre/Rosa^{Notch} mice are induced by Rosa^{Notch} expression and contain supporting cells as well as hair cells. In small clusters of ectopic sensory cells in the nonsensory regions of juvenile hGFAPCre/Rosa^{Notch} vestibular epithelia we found a high degree of

overlap between cells immunolabeled for GFP and the specific supporting cell marker GLAST (Fig. 5.5, upper panels). GLAST is normally highly expressed in plasma membranes of vestibular supporting cells but little or no immunolabeling for GLAST is normally found in the nonsensory regions. The induction of GLAST expression in ectopic sensory clusters and high degree of overlap between GFP and GLAST suggests that constitutive activation of Notch cell-autonomously directs cells toward supporting cell fate.

Constitutive Notch activation in vestibular progenitor cells promotes supporting cell fate and represses hair cell fate.

Because of the mosaic nature of recombination in hGFAPCre/Rosa^{Notch} we were also able to look at regions of GFP-positive groups of cells within sensory organs and evaluate the effect of constitutive Notch activation on sensory progenitors. We found that NotchIC expression within a sensory organ inhibits hair cell differentiation and promotes supporting cell fate. The panels in Fig. 5.6 show examples of utricular sensory epithelia from juvenile hGFAPCre/Rosa^{Notch} mice which display reduced hair cell density or increased supporting cell density in overlapping regions of GFP-positive cells. In regions where GFP is expressed within the sensory epithelium of the utricle expression of myosinVI and calretinin was reduced, indicating a reduction in hair cell differentiation in these regions (Fig. 5.6 A-C``). On the other hand, we saw an increase in the levels and density of cells labeled with supporting cell markers GLAST (Fig. 5.6 D-D``), or Sox9 (Fig. 5.6 E-E``) in regions where GFP was expressed.

Ectopic Notch activation in cochlear supporting cells of hGFAPCre/Rosa^{Notch} mice does not affect maintenance of cell fate in normal or in vitro damaged conditions. We found that Cre recombination occurs in a subset of cochlear supporting cells in hGFAPCre mice. hGFAPCre mice were crossed to mT/mG Cre-reporter mice to visualize Cre-recombinase activity (mG). Cre-mediated recombination was present in supporting cells on the medial side of the organ of Corti in a base to apex gradient (Fig. 5.7 A-C`). Cre activity was also present in most of the Schwann cells ensheathing spiral ganglion neurons. Close examination of a z-series micrograph from a middle cochlear turn indicated that Cre reporter expression was primarily restricted to inner phalangeal cells and occasionally was found in pillars or Dieters' cell in the basal regions of the cochlea (Fig. 5.7 D-D).

In contrast to the phenotype in the vestibular system of hGFAPCre/Rosa^{Notch} mice, we found that constitutive Notch expression in cochlear supporting cells does not affect supporting cell fate or cochlear morphology (Fig. 5.8). Nuclear GFP expression was detected in inner phalangeal cells and occasionally pillar and Dieters' cells, all colabeled with Sox2 (Fig. 5.8). Expression of the Rosa^{Notch} transgene did not affect expression of Sox2 or GLAST in supporting cells, which appear to remain fully differentiated (Fig. 5.8 and Fig. 5.9A-A``). Hair cell morphology and expression of myosinVI was also not affected by constitutive Notch activation in supporting cells.

To test whether or not constitutive Notch activation in supporting cells may confer regeneration potential to these cells, we induced hair cell damage in hGFAPCre/Rosa^{Notch} cochlear explant cultures (Fig. 5.9). Cultures were established at P5 and maintained for 6 days in vitro. Some of the explants were treated for 24hrs with kanamycin to kill hair cells. Cultured cochlear explants were then fixed and

immunolabeled with antibodies to GFP, calretinin, and GLAST (Fig. 5.9). The morphology and arrangement of hair cells and supporting cells was maintained fairly well in the explant cultures, and expression of calretinin in hair cells, and GLAST in supporting cell membranes appeared normal (Fig. 5.9). Kanamycin treated samples were nearly devoid of inner and outer hair cells, with only a few poor-looking calretinin-positive cells remaining. Expression of GFP in the inner phalangeal cells was not affected by hair cell damage, and GFP was not upregulated in any other supporting cell types as a result of the damage. Remarkably, GFP-positive supporting cells continued to express GLAST in their plasma membranes, indicating these cells remain differentiated despite hair cell damage and constitutive Notch activation. If anything, GLAST expression appeared to be upregulated in the kanamycin treated cochlear explants.

DISCUSSION

Activation of Notch in FoxG1Cre/Rosa^{Notch} embryos resulted in externalization of anterior neural structures including the brain and otic epithelium (Fig. 5.1). This phenotype is consistent with earlier reports of Notch gain-of-function in developing neural progenitors. In a study by Lardelli et al., embryos were generated containing a transgene encoding the intracellular domain of mouse Notch3 transcribed from the nestin promoter, driving Notch signaling in CNS progenitor cells (Lardelli et al., 1996). The transgenic activation of Notch resulted in a phenotypic series of neural tube defects in E10.5-12.5 embryos and was lethal beyond that age (Lardelli et al., 1996). Severely affected pnestin-Notch3IC embryos showed a lack of closure of the anterior neural pore, resulting externalization of neural tissue and collapse of the third and fourth

ventricles, as well as an expanded ventricular zones and an increase in the number of proliferating cells in the neural tube (Lardelli et al., 1996). We observed a strikingly similar externalization of neural tissues, collapse of the fourth ventricle and expansion of the Hes5-positive ventricular zone in the developing brain of FoxG1Cre/Rosa^{Notch} embryos (Fig. 5.1). More recently Cre-conditional activation of constitutively active Notch1 in broadly expressing Cre lines resulted in embryonic lethality before E10.5 and a variety of developmental defects, including lack of neural tube closure (Liu and Lobe, 2007). Furthermore, evidence from a study of constitutive Notch activation in ascidian embryos also resulting in defects in neural tube closure and brain vesicle formation suggests that conserved regulation of Notch activity is needed for neural progenitor regulation and unregulated Notch signaling can lead to expansion of neuroepithelia (Akanuma et al., 2002).

We observed a thickening and expansion of the otic epithelia in FoxG1Cre/Rosa^{Notch} embryos that resulted in otic vesicle closure defects similar to the phenotype of constitutive Notch activation in the developing brain (Fig. 5.1 and 2, (Lardelli et al., 1996; Liu and Lobe, 2007). The expansion and externalization of the otic epithelium that we observed in E13.5 embryos is also consistent with the findings of a recent study by Jayasena and colleagues (Jayasena et al., 2008). The authors of this study describe the effect of Notch activation in the Pax2-positive head ectoderm that gives rise to the otic placode and the surrounding epidermis. Activation of Notch in cranial ectoderm of Pax2Cre/Rosa^{Notch} embryos caused expansion of the otic placode at the expense of epidermis, while loss of Notch1 lead to a reduction in the size of the otic placode (Jayasena et al., 2008). The Pax2Cre line used by Jayasena et al. to activate Notch exhibits Cre reporter expression in the otic placode region of the head

ectoderm from the 6-7 somite stages (Ohyama and Groves, 2004), when the otic placode is developing from the pre-otic field as a thickening of head ectoderm. To activate Notch at a slightly later stage and more restricted otic region, we used the FoxG1Cre line, which exhibits Cre reporter expression in the presumptive otic vesicle several hours prior to E9 (Hebert and McConnell, 2000), when embryos typically have around 15 somites and the otic pit is rounded and indented but not yet closed. In our study, despite the later activation of Notch within the otic pit and our examination of embryos at E13.5, we observe a similar thickening and expansion of the otic epithelium at E13.5 to that of the otic placode of Pax2Cre/Rosa^{Notch} embryos analyzed between E8.75 and E9.5 (Jayasena et al., 2008).

In our study, we focus on the effect of Notch on cell-fate specification within the otic epithelium. Our finding that specific markers of the prosensory domain (Jag1, Sox2, and HesR1) are expressed throughout the otic epithelium of FoxG1Cre/Rosa^{Notch} embryos at E13.5 (Fig.5.2), when prosensory specification in the cochlea is normally underway, indicate that Notch activation is sufficient to induce prosensory character throughout the otic epithelium. This hypothesis is further supported by our finding that ectopic sensory organs are induced in nonsensory regions of vestibular epithelia in hGFAPCre/Rosa^{Notch} mice.

We also found that constitutive Notch activation biased sensory progenitor cells toward a supporting cell fate in hGFAPCre/Rosa^{Notch} mice (Fig.5.6.) Numerous recent studies in vertebrates have suggested that rather than simply inhibiting neuronal differentiation and maintaining a neural progenitor fate, Notch may, in some contexts promote the acquisition of glial identity (Chen et al., 2005; Furukawa et al., 2000; Gaiano and Fishell, 2002; Gaiano et al., 2000; Ge et al., 2002; Hojo et al., 2000;

Morrison et al., 2000; Tanigaki et al., 2001; Vetter and Moore, 2001). For example, Gaiano et al. used retroviral vectors to introduce the activated form of Notch1, Notch intracellular domain (NICD), in developing mouse brain at E9.5, they showed that NICD expressing cells later developed into radial glial cells (Gaiano et al., 2000). In the retina, Furukawa et al. and Hojo et al. showed that expression of NICD, Hes1, or Hes5 promoted differentiation of Muller glia, and that Hes5 knockout mice have decreased numbers of Muller glia (Furukawa et al., 2000; Hojo et al., 2000). Morrison et al. activated Notch in neural crest stem cells with NICD and soluble Notch ligands and found that even a transient 24hr activation of Notch was sufficient to cause a rapid and irreversible loss of neurogenic capacity and accelerated glial differentiation(Morrison et al., 2000). More recently, forced activation of Notch signal has been found to promote expression of GFAP (Ge et al., 2002; Tanigaki et al., 2001). Ge et al. identified a CSL binding site within the GFAP promoter and showed that Notch signaling promoted astroglial differentiation in part by direct binding of NICD and CSL to the GFAP promoter, to activate GFAP transcription (Ge et al., 2002).

CONCLUSIONS AND FUTURE DIRECTIONS

Based on our studies and those from other labs, Notch signaling has two key roles during mammalian inner ear development. Initially Notch is *necessary* for specification of prosensory progenitors (Brooker et al., 2006; Hayashi et al., 2008; Kiernan et al., 2006) and here we have shown that Notch activation is also *sufficient* for this process in mouse (Chapter 5) as was shown to be the case in chick (Daudet and Lewis, 2005). Specifically, both FoxG1Cre and hGFAPCre transgenic Notch gain-of-function studies show that Notch signal activation during development is capable of

conferring prosensory character to nonsensory epithelium. Later in inner ear sensory development, Notch mediates cellular development via lateral inhibition, inhibiting hair cell differentiation and maintaining nascent supporting cells (Brooker et al., 2006; Daudet and Lewis, 2005; Hartman et al., 2007; Kiernan et al., 2005a; Kiernan et al., 2006; Zine and de Ribaupierre, 2002). Consistent with the role for Notch in lateral inhibition, in the vestibular epithelia of hGFAPCre/Rosa^{Notch} mice, sustained Notch activation directs cells toward supporting cell fates and inhibits hair cell fate. This suggests that a pulse of Notch activity early in development specifies the prosensory domain, endowing cells with potential to become hair cells or supporting cells, then Notch activity needs to be downregulated, or overcome, in order for cells to differentiate as hair cells rather than supporting cells.

Despite the potent activity of Notch during embryonic development, in our earlier study we found that Notch signaling is abruptly downregulated in the mammalian cochlea during postnatal development, but Notch-Hes5 signaling remains active in a subset of adult vestibular supporting cells (Hartman et al., 2009). This finding suggests a correlation between Notch activity and regeneration capacity: Notch is active in regeneration-competent tissues (the fish lateral line, the chick BP, and the mammalian vestibule) but is absent from the mouse cochlea, which does not regenerate. Thus, we sought to determine if Notch activation in mature mouse cochlea supporting cells would confer regeneration or proliferation capacity. Constitutive Notch activation in hGFAPCre/Rosa^{Notch} cochlear supporting cells does not affect supporting cell fate or cochlear morphology and was not sufficient to confer regeneration potential. This suggests that Notch signaling alone is not sufficient to reverse the process of supporting cell differentiation. This is consistent given our data that suggests Notch

itself directs supporting cell fate establishment. Thus, future strategies to confer progenitor character or regeneration capacity to supporting cells may require other factors, perhaps in addition to pulsed, rather than constitutive, Notch signaling.

Future directions for this project include defining the time-course of hGFAPCre activity in the vestibular epithelia. This is important to determine the timing of prosensory specification in the vestibular regions. We will also perform additional immunolabeling of ectopic sensory patches in hGFAPCre/Rosa^{Notch} mice to characterize the expression of supporting cell markers such as Jag1 and Sox2. We also plan to generate hGFAPCre/ Rosa^{Notch} mice that also carry the cre-reporter mT/mG transgene. This will provide a second lineage marker for the cre-recombined cells and allow identification of hair cells and supporting cells based on visualization of cell membranes and surface stereocilia by confocal microscopy.

Additionally we plan to perform in situ hybridization on vestibular and cochlear tissues from hGFAPCre/ Rosa^{Notch} mice to see if downstream Notch effectors are ectopically expressed, which would indicate that transgenic NICD expression leads to activation of the Notch pathway. We will probe for Hes5 expression in the cochlea of late postnatal (P5-P8) bigenic mice to see if Hes5 is expressed in inner phalangeal cells as a result of transgenic NICD expression. It is possible that expression of NICD is not sufficient to activate the Notch pathway in the mature cochlea because other essential factors, such as CSL (RBPJ) or Mastermind proteins, are not present. Therefore, if we find that Hes5 is not upregulated in late postnatal hGFAPCre/ Rosa^{Notch} cochlea we will perform in situ hybridization for RBPJ and Mastermind family members (MAML1,2, and 3) to determine if either of these Notch cofactors is missing.

The overall goal of this project has been to further understand the mechanisms of specification and maintenance of sensory cell fates in the developing and adult mammalian inner ear. By understanding the way in which cell fates are developed and maintained we may be better able to determine ways to overcome the barriers to regeneration in the mammalian inner ear. We have contributed to the field of studies in cochlear development and regeneration by furthering our understanding of the status and function of Notch signaling in the developing and adult mouse and the affects of hair cell damage. This essential developmental pathway may yet prove to be a tool which can be manipulated to stimulate regeneration, however our studies indicate that simply expressing activated Notch in supporting cells is not sufficient. Given the complexity of inner ear development, it seems likely that successfully stimulating regeneration in the mammalian ear will require multiple coordinated genetic events.

METHODS

Animals

Mice were housed in the University of Washington Department of Comparative Medicine and the Institutional Animal Care and Use Committee approved experimental methods and animal care procedures. $Rosa^{Notch}$ mice and corresponding PCR genotyping were previously described (Murtaugh et al., 2003). Mice were euthanized according to approved procedures.

Fluorescent Immunohistochemistry of Frozen Sections

Embryos were collected from timed pregnant C57/BL6 mice and staged according to Kauffman (Kauffman, 1992). For postnatal mice, P0 was defined as the day of birth.

Embryonic whole heads or P0-P5 half-heads, were fixed overnight in 4% PFA in PBS at 4°C. Adult cochlea were isolated from temporal bones, the stapes was removed from the oval window, a small opening was made in the apex, and cold 4% PFA in PBS was perfused through the cochlea with a syringe. Perfused cochlea were then fixed overnight in 4% PFA in PBS at 4°C, washed 3 X 30 minutes in PBS, and decalcified in 0.27M EDTA in PBS for 48hr at 4°C. After fixation and decalcification (for adult cochlea) whole cochlea or heads were cryoprotected through graded sucrose in PBS (10% sucrose, 15% sucrose, 15% sucrose with 50% OCT) then embedded in OCT (Tissue Tek), frozen in a bath of ethanol and dry ice, sectioned at 10 µm, and mounted on Superfrost+ slides (Fisher Scientific). Slides with cryosections were then washed briefly in PBS and blocked for 1 hr in 10% FBS in PBS with 0.1% TritonX-100 at room temperature. Primary antibodies were diluted in block and incubated overnight at 4°C. Slides were then washed in PBS 3 X 10 min, and incubated in species-specific fluorescent-labeled secondary antibodies AlexaFluor 488, 568, or 594 nm (1:500, Invitrogen). After immunostaining, slides were coverslipped in Fluoromount G (Southern Biotechnology, Birmingham, AL). Images of most stained sections were acquired on a Zeiss Axioplan 2 microscope equipped with DIC optics and a Spot camera. Images of adult cochlear sections were also captured on a Zeiss LSM Pascal confocal microscope and processed using Improvision Volocity (3.0.2). Images were compiled with Adobe Photoshop 7.0.

Antibodies

Primary antibodies used were Rabbit anti-myosinVI (Proteus Biosciences) 1:1000, guinea pig anti-GLAST (Chemicon) 1:1000, chicken anti-GFP (U. Alberta). Secondary

antibodies used were goat anti-mouse Alexa 594, chicken anti-mouse 594, goat anti-rabbit Alexa 594, donkey anti-goat 488, and goat anti-rabbit Alexa 488, all from Molecular Probes, and goat anti-guinea pig Cy3 from Chemicon.

Paraffin *In Situ* Hybridization

DIG-labeled antisense riboprobe was prepared for in situ hybridization for mouse Hes5 and HesR1 from cDNA clones. Embryos were collected from timed pregnant mice and staged according to (Kauffman, 1992). In situ hybridization was performed as previously described (Hayashi et al., 2007; Nelson et al., 2004). Briefly whole embryos were fixed overnight at 4°C in modified Carnoy's solution (60% ethanol, 11.1% formaldehyde (30% of 37% stock), 10% glacial acetic acid), dehydrated though an EtOH series, prepared for paraffin embedding, and sectioned at 6-8 μm. Slides were baked overnight at 68^{o}C, dewaxed in Xylene, rinsed in 100% EtOH, and air-dried at room temperature. Overnight hybridization and subsequent washes were carried out at 68^{o}C. Hybridized probe was detected using anti-Digoxygenin alkaline phosphatase conjugated antibody (1:2000 dilution, Roche Biochemical, Indianapolis, IN) and visualized with NBT/BCIP for a blue precipitate. After *in situ* hybridization, sections were post-fixed in 4% PFA, rinsed in PBS, and processed for fluorescent immunohistochemistry as described below.

Figure 5.1 Ectopic NotchIC expression activates the Notch pathway in FoxG1Cre/Rosa^{Notch} embryos. A An E13.5 FoxG1Cre/+ control embryo exhibits normal developmental morphology. B An E13.5 FoxG1Cre/Rosa^{Notch} embryo displays neural tube closure defects resulting in externalization of anterior neural tissues. The tails of the embryos shown in A and B have been removed for genotyping. C A montage of photomicrographs shows a section through a control embryo processed for in situ hybridization with antisense Hes5 probe. The orientation of the section in panel C is transverse through the posterior part of the head as indicated by the line in panel A. Hes5 expression, blue, is visible in the control embryo in the ventricular zone of the brain surrounding the aqueduct (aq) and fourth ventricle (IV) and also the ventricular zone of the spinal cord (sc). D A similar section through a FoxG1Cre/Rosa^{Notch} double transgenic embryo probed for Hes5 expression. Hes5 is upregulated in the abnormally formed brain of the bigenic embryo, which exhibits externalized neuroepithelia, an expanded ventricular zone and collapse of the fourth ventricle. Ectopic Hes5 expression is present in the foregut (fg), while the developing spinal cord (sc) has a normal pattern of Hes5 expression. E A higher magnification view of the control embryo section in panel C shows Hes5 expression in the ventricular zone of the fourth ventricle (IV) and the normal absence of Hes5 in the cochleae (c). F A view of a comparable region in the bigenic embryo shows upregulation of Hes5 in an expanded ventricular zone around the fourth ventricle, which is abnormally collapsed and folded apparently due to overproduction of the neuroepithelium. The left and right cochlear epithelia (c) exhibit enlargement and partial externalization due to otic vesicle closure defects.

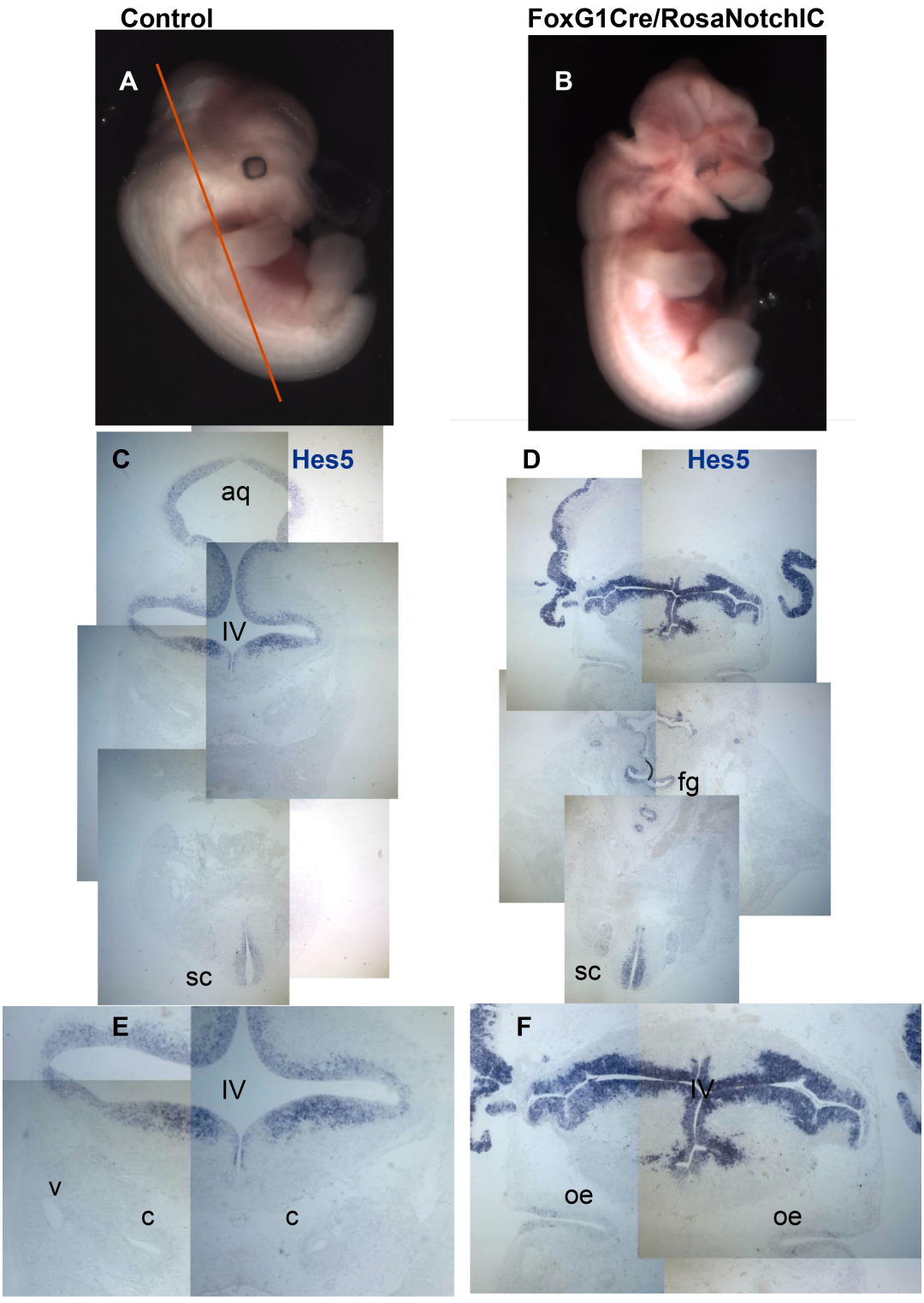
Control
FoxG1Cre/RosaNotchIC
A
B
C
Hes5
aq
IV
sc
D
Hes5
fg
sc
E
IV
v
c
c
F
IV
oe
oe

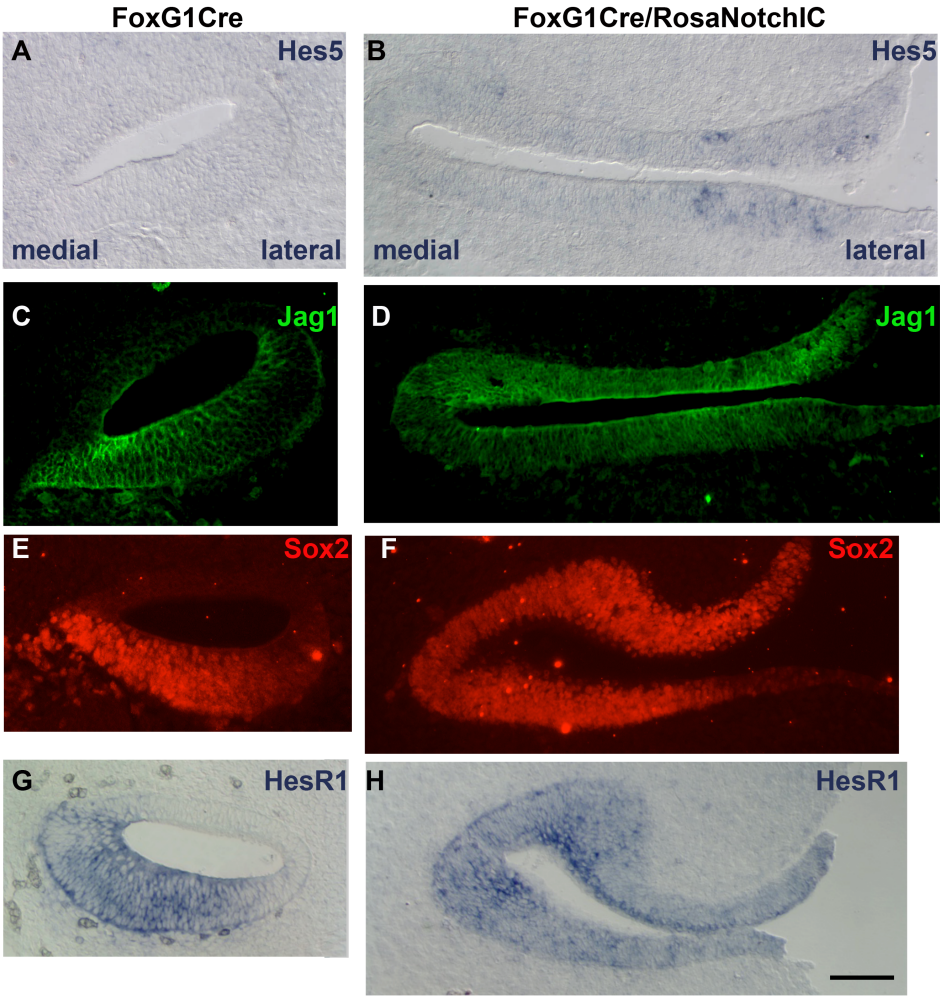

Figure 5.2 The otic epithelia of FoxG1Cre/Rosa^{Notch} embryos is enlarged and externalized, and exhibits ectopic expression of Notch effectors and expansion of prosensory markers Jag1 and Sox2 throughout the epithelium. Cochlear epithelia sections from control FoxG1Cre (A, C, E, G) embryos and similar sections through otic epithelium of double transgenic FoxG1Cre/Rosa^{Notch} (B, D, F, H) embryos at E13.5. A-B Hes5 in situ hybridization signal is not normally detected in the cochlea at this age and is not present in control (A) but Hes5 expression is present at varying levels throughout in the bigenic otic epithelia (B). C-D Similar sections to those in panels A and B immunolabeled for Jag1 show the normal pattern in the medial floor of the duct in the control (C) and ectopic labeling throughout the entire epithelia in the bigenic cochlea (D). E-F Sox2 immunolabeling is restricted to the floor of the cochlear duct in control embryos (E), and expanded throughout the externalized otic epithelium in bigenic embryos (F). G-H The Notch effector HesR1 is normally restricted to the floor of the cochlear duct (G) and is expressed throughout the entire otic epithelium in bigenic embryos (H). Scale bar in H is 50μm and applies to all panels.

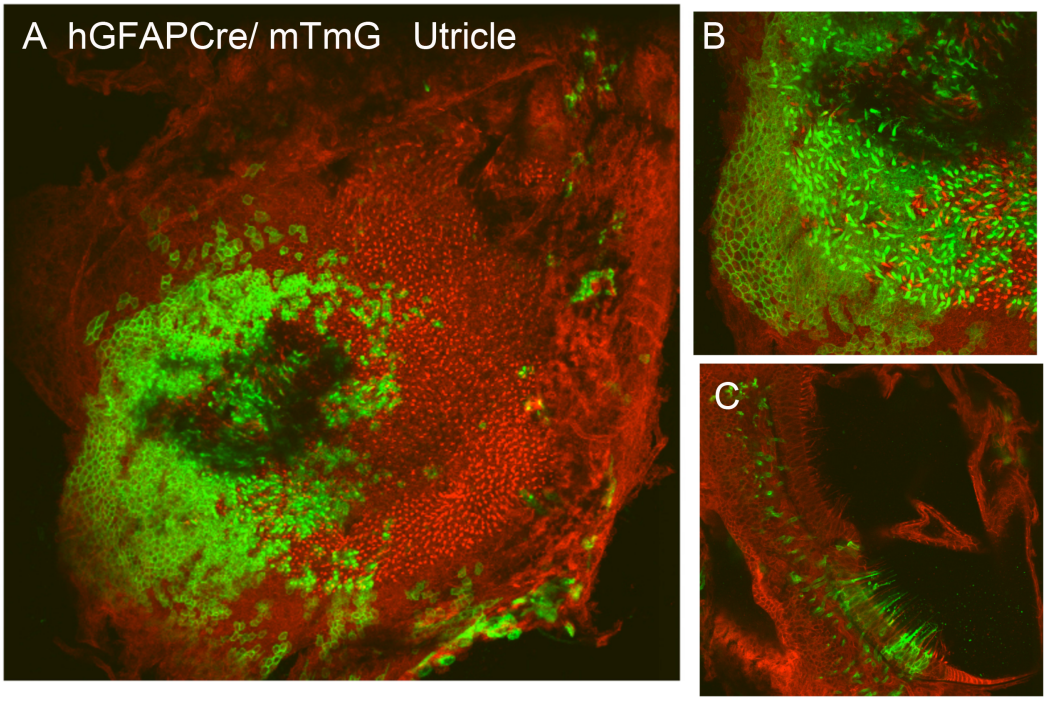

Figure 5.3 Cre recombinase activity in hGFAPCre mice is mosaic in regions within and around vestibular sensory epithelia. A-C Wholemount views of P16 hGFAPCre/mTmG vestibular organs show cells which have undergone Cre mediated recombination labeled by expression of membrane bound GFP, while all other cells are labeled with membrane bound Tomato red fluorescent protein. An example of a Utricle (A) shows Cre activity in mosaic clusters, which at higher magnification (B) are seen to include hair cells, supporting cells, and transitional epithelial cells outside the margins of the sensory epithelia. An optical section through a crista (C) shows Cre activity in a cluster of hair cells and supporting cells.

Figure 5.4 Ectopic sensory patches, with hair cells and afferent projections, form in vestibular epithelia of hGFAPCre/Rosa^{Notch} mice in regions where the Rosa^{Notch} transgene is activated. Flatmount confocal projection views of vestibular epithelia from hGFAPCre/Rosa^{Notch} (A) or hGFAPCre control (B) including the utricle and adjacent horizontal crista immunolabeled with anti-GFP and antibodies against both myosinVI and calretinin (red), to label hair cells and afferent fibers. In the hGFAPCre/Rosa^{Notch} epithelium several regions of ectopic sensory patch formation are present between the utricle and horizontal crista. In the control vestibule the same region (marked by an asterisk) is nonsensory and devoid of hair cells. High magnification views of 10-15um optical z-sections through the boxed regions in A are shown in lower panels, with merged channels in C-G and the green (GFP) channel alone in C`-G`. In all of the lower panels, GFP expression is present in patches of cells within the ectopic sensory regions. The region in panels C-C` contains an isolated patch of hair cells while the other ectopic regions appear to be expanded from and continuous with the utricle and/or horizontal crista. The region in E-E` is spheroid and contains a large cluster of calretinin-positive calyceal nerve endings typical of type I vestibular hair cells.

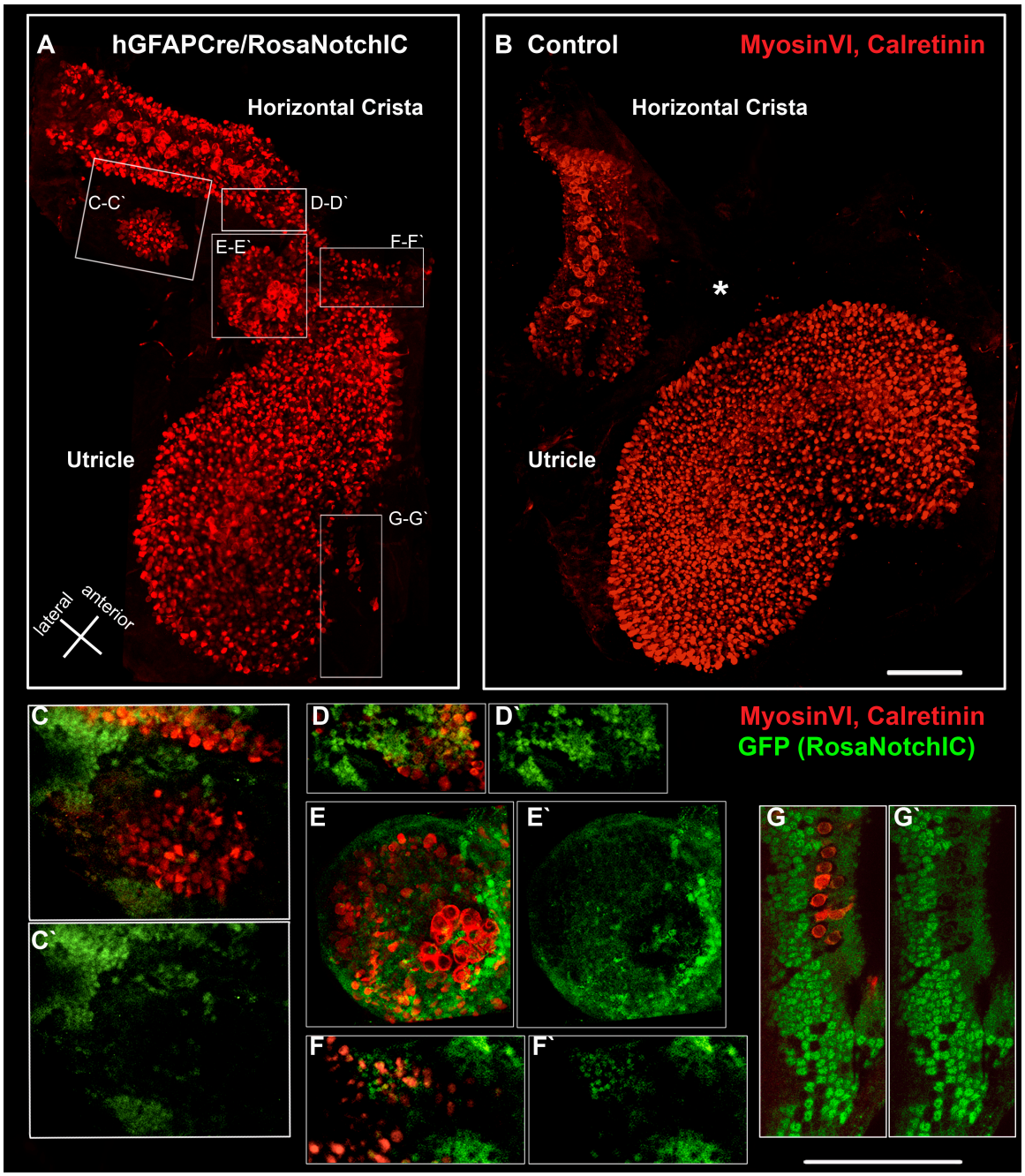
A
hGFAPCre/RosaNotchIC
Horizontal Crista
C-C`
D-D`
E-E`
F-F`
G-G`
Utricle
lateral
anterior
B Control
MyosinVI, Calretinin
Horizontal Crista
*
Utricle
C
C`
D
D`
E
E`
F
F`
G
G`
MyosinVI, Calretinin
GFP (RosaNotchIC)

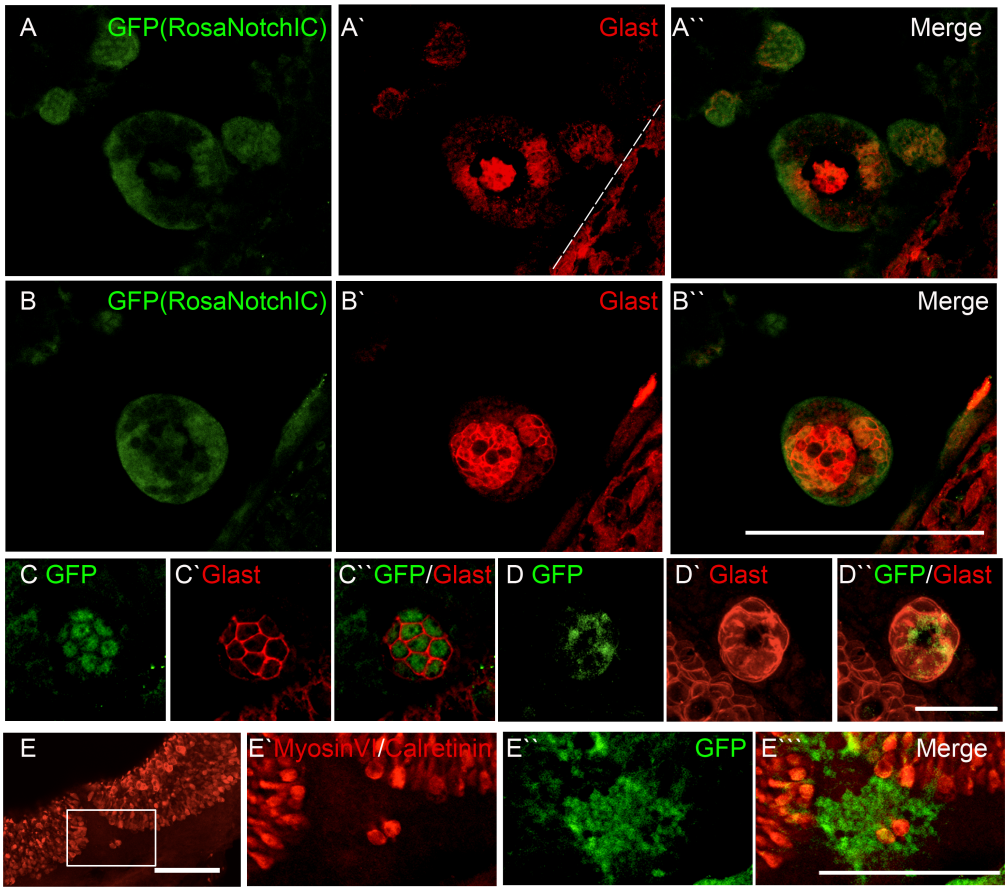

Figure 5.5 Ectopic sensory patches in nonsensory vestibular epithelia of hGFAPCre/Rosa^{Notch} mice are induced by transgene expression and contain supporting cells as well as hair cells. Examples of small ectopic clusters of sensory cells from vestibule of several different juvenile hGFAPCre/Rosa^{Notch} mice are shown. A-A`` and B-B`` Two different optical z-sections of the same region of nonsensory epithelia lateral to the utricle labeled with anti-GFP(green) and an antibody to the glutamate transporter GLAST (red), which specifically labels supporting cell plasma membranes. A-A`` A single optical z-section with GFP expression in four round clusters of cells. All four GFP-positive clusters have elevated levels of GLAST. The dashed line in A` marks the transitional epithelium on the sloping lateral margin of the utricle. B-B`` A second single optical z-section, 10μm superficial to the section shown in A, provides a view near the surface of the largest of the four clusters, which is rounded up and elevated above the surface of the surrounding epithelium. Most, but not all, of the cells in the cluster are GFP-positive and nearly all of these are also labeled with anti-GLAST. C-C`` A cluster of GFP-positive cells posterior to the utricle, all of which exhibit elevated levels of GLAST in membranes. D-D`` An optical section through a small spheroid cluster of GLAST-positive cells containing several GFP-positive cells, which was located just anterior to the edge of the utricle. E A projection of vertical crista with a pair of ectopic hair cells, shown in higher magnification in E`-E```. A patch of GFP+ cells is surrounding and underlying the pair of ectopic hair cells.

Figure 5.6 Ectopic NotchIC expression within a sensory organ inhibits hair cell differentiation and promotes supporting cell fate. Panels show examples of utricular sensory epithelia from juvenile (P16) hGFAPCre/Rosa^{Notch} mice immunolabeled for GFP and either myosinVI and calretinin (A-C``), GLAST (D-D``), or Sox9 (E-E``). A-A` Surface view of a confocal z-series projection of a utricle from a mouse labeled with antibodies to myosinVI and calretinin (both in red) and GFP (green). B-B`` and C-C`` two regions of the utricle in A-A` with high levels of GFP expression in the sensory epithelium and corresponding reductions in hair cell density are shown at higher magnification with channels presented separately and merged. Nearly all of the GFP-positive cells in these fields are negative for myosinVI/calretinin but there are a few that appear to be double labeled (arrows in B-B`` and C-C`` point to two examples). In D-D``, a large cluster of GFP-positive cells make up a region of dense labeling for GLAST with few or no hair cells. E-E`` A region of utricle with several large clusters of GFP-positive cells, all of which are double labeled with Sox9. The cluster of GFP labeled cells on the left is associated with a protruding region of expanded sensory epithelia. All scale bars are 100μm.

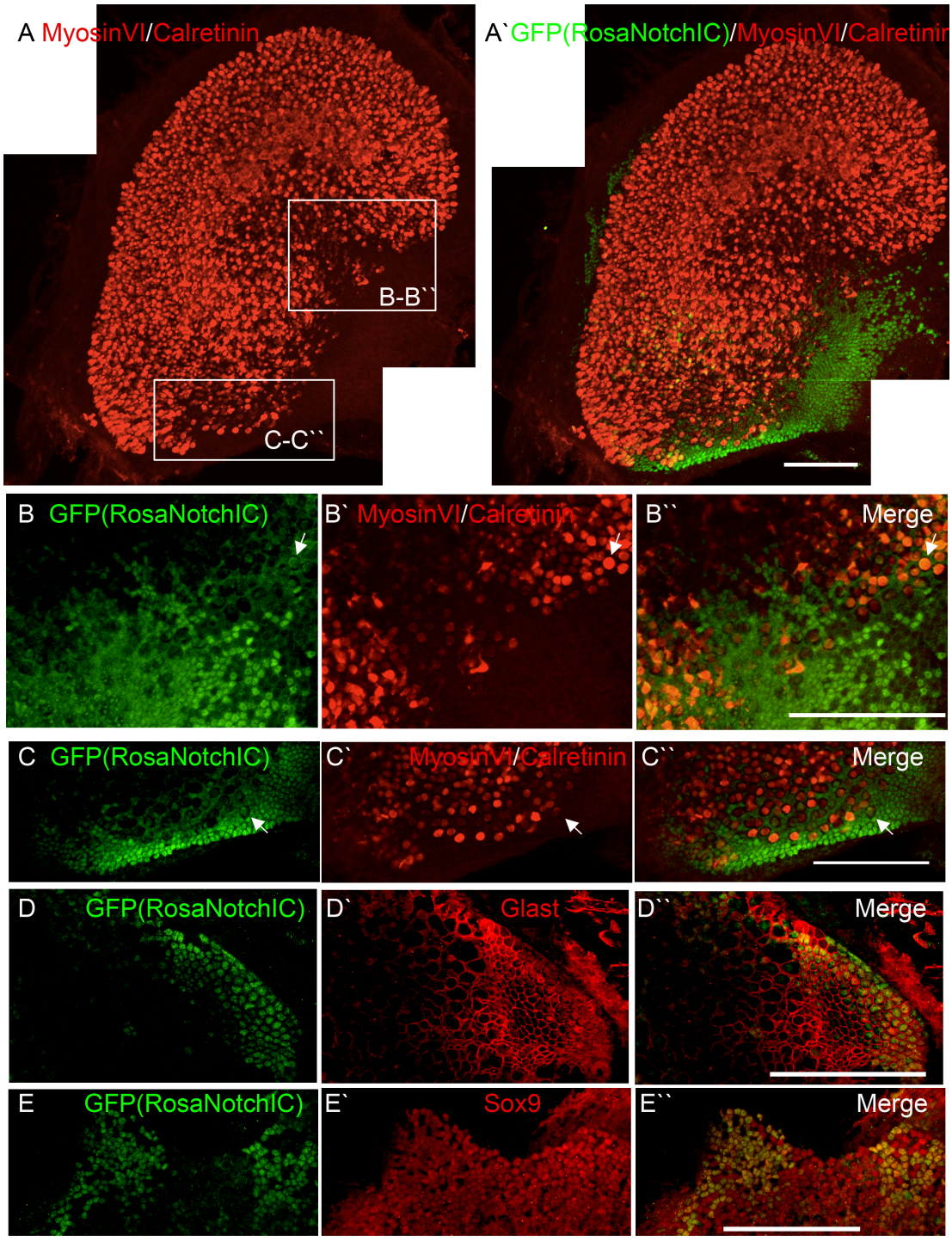
A MyosinVI/Calretinin
A`GFP(RosaNotchIC)/MyosinVI/Calretinin
B-B``
C-C``
B GFP(RosaNotchIC)
B` MyosinVI/Calretinin
B`` Merge
C GFP(RosaNotchIC)
C` MyosinVI/Calretinin
C`` Merge
D GFP(RosaNotchIC)
D` Glast
D`` Merge
E GFP(RosaNotchIC)
E` Sox9
E`` Merge

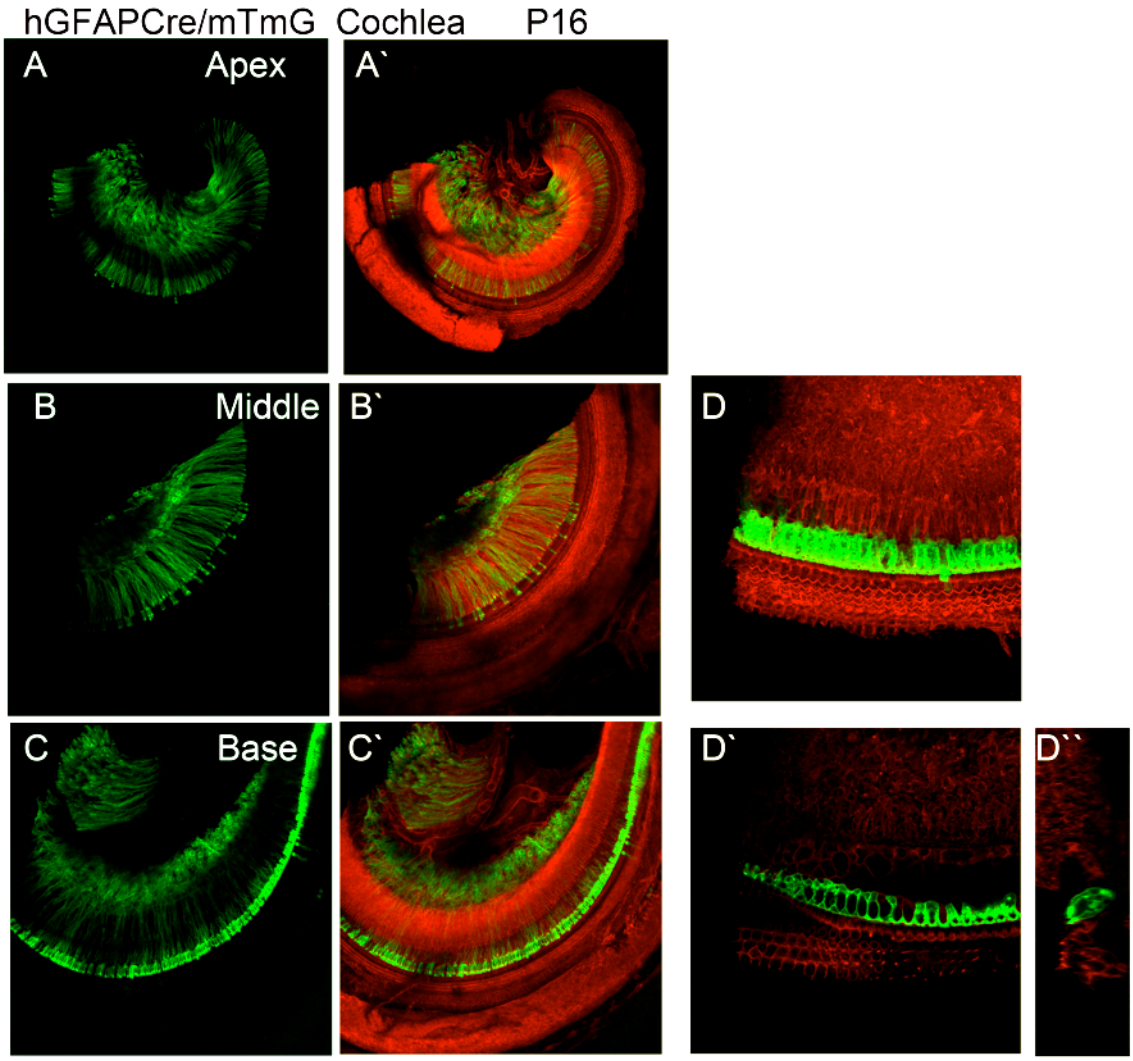

Figure 5.7 Cre recombination occurs in a subset of cochlear supporting cells in hGFAPCre mice. hGFAPCre mice were crossed to mT/mG Cre-reporter mice to visualize Cre-recombinase activity (mGFP). Cre-mediated recombination is present in supporting cells on the medial side of the organ of Corti in a base to apex gradient (A-C`). Cre activity is also present in most of the Schwann cells ensheathing spiral ganglion neurons. D A higher magnification view of a z-series projection from a middle cochlear turn shows Cre reporter expression mostly in the region of inner phalangeal cells. D` A single optical section from the same z-series in D shows that Cre reporter expression is localized to membranes of inner phalangeal cells. D`` An optical transverse section view confirms reporter expression in inner phalangeal cells.

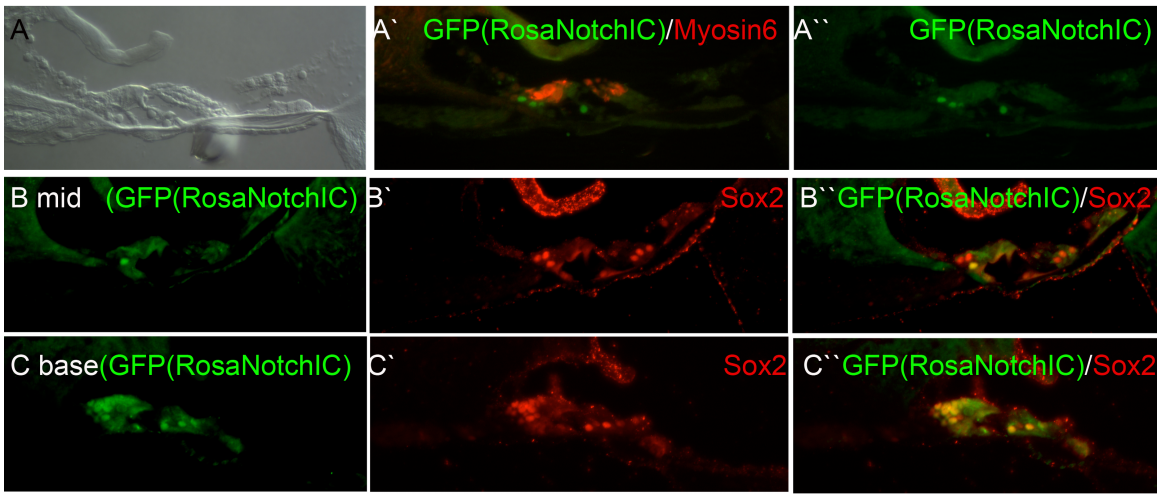

Figure 5.8 hGFAPCre/Rosa^{Notch} transgene expression in a subset of cochlear supporting cells does not affect supporting cell fate or cochlear morphology. Sections of cochlea from juvenile hGFAPCre/Rosa^{Notch} mice stained with antibodies to GFP and myosinVI or Sox2 as indicated, to label hair cells and supporting cells, respectively. Nuclear GFP expression was detected in inner phalangeal cells and occasionally pillar and Dieters' cells. Expression of the transgene, indicated by the expression of nuclear GFP, did not affect hair cell morphology or myosinVI expression. Sox2 expression in supporting cell nuclei overlaps with all of the GFP-positive cells and is not affected.

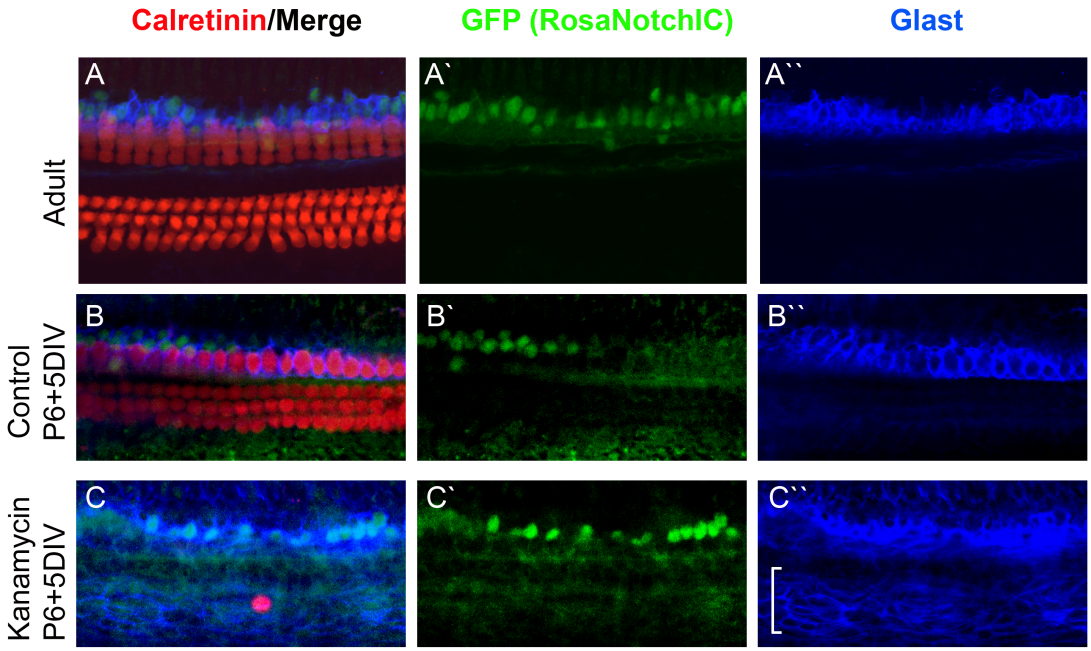

Figure 5.9 Ectopic Notch activation in cochlear supporting cells does not cause dedifferentiation or down-regulation of GLAST in vivo, in vitro, or after in vitro hair cell damage. A-A`` hGFAPCre/Rosa$^{Notch}$ D mice adult cochlea shows normal expression of GLAST in GFP+ inner phalangeal cells. B-B`` A P6+5DIV hGFAPCre/Rosa^{Notch} cochlea retains normal cell morphology and expression of GLAST in inner phalangeal cells, some of which express the Rosa^{Notch} transgene (nGFP). C-C`` A P6+5DIV hGFAPCre/Rosa^{Notch} cochlea treated with kanamycin for 24hours has extensive hair cell loss, but expression of the Rosa^{Notch} transgene is still restricted to inner phalangeal cells. GLAST expression is not diminished by Rosa^{Notch} expression in inner phalangeal cells but kanamycin treatment caused upregulation of GLAST expression in supporting cells.

REFERENCES

Adam, J., Myat, A., Le Roux, I., Eddison, M., Henrique, D., Ish-Horowicz, D., Lewis, J., 1998. Cell fate choices and the expression of Notch, Delta and Serrate homologues in the chick inner ear: parallels with Drosophila sense- organ development. Development. 125**,** 4645-54.

Akanuma, T., Hori, S., Darras, S., Nishida, H., 2002. Notch signaling is involved in nervous system formation in ascidian embryos. Dev Genes Evol. 212**,** 459-72.

Alexson, T. O., Hitoshi, S., Coles, B. L., Bernstein, A., van der Kooy, D., 2006. Notch signaling is required to maintain all neural stem cell populations--irrespective of spatial or temporal niche. Dev Neurosci. 28**,** 34-48.

Arima, T., Uemura, T., Yamamoto, T., 1986. Cytoskeletal organization in the supporting cell of the guinea pig organ of Corti. Hear Res. 24**,** 169-75.

Arumugam, T. V., Chan, S. L., Jo, D. G., Yilmaz, G., Tang, S. C., Cheng, A., Gleichmann, M., Okun, E., Dixit, V. D., Chigurupati, S., Mughal, M. R., Ouyang, X., Miele, L., Magnus, T., Poosala, S., Granger, D. N., Mattson, M. P., 2006. Gamma secretase-mediated Notch signaling worsens brain damage and functional outcome in ischemic stroke. Nat Med. 12**,** 621-3.

Barrionuevo, F., Naumann, A., Bagheri-Fam, S., Speth, V., Taketo, M. M., Scherer, G., Neubuser, A., 2008. Sox9 is required for invagination of the otic placode in mice. Dev Biol. 317**,** 213-24.

Basak, O., Taylor, V., 2007. Identification of self-replicating multipotent progenitors in the embryonic nervous system by high Notch activity and Hes5 expression. Eur J Neurosci. 25**,** 1006-22.

Berglund, A. M., Ryugo, D. K., 1991. Neurofilament antibodies and spiral ganglion neurons of the mammalian cochlea. J Comp Neurol. 306**,** 393-408.

Bermingham, N. A., Hassan, B. A., Price, S. D., Vollrath, M. A., Ben-Arie, N., Eatock, R. A., Bellen, H. J., Lysakowski, A., Zoghbi, H. Y., 1999. Math1: an essential gene for the generation of inner ear hair cells. Science. 284**,** 1837-41.

Bermingham-McDonogh, O., Oesterle, E. C., Stone, J. S., Hume, C. R., Huynh, H. M., Hayashi, T., 2006. Expression of Prox1 during mouse cochlear development. J Comp Neurol. 496**,** 172-86.

Bermingham-McDonogh, O., Rubel, E. W., 2003. Hair cell regeneration: winging our way towards a sound future. Curr Opin Neurobiol. 13**,** 119-26.

Brennan, K., Gardner, P., 2002. Notching up another pathway. Bioessays. 24**,** 405-10.

Brooker, R., Hozumi, K., Lewis, J., 2006. Notch ligands with contrasting functions: Jagged1 and Delta1 in the mouse inner ear. Development. 133**,** 1277-86.

Bryant, J., Goodyear, R. J., Richardson, G. P., 2002. Sensory organ development in the inner ear: molecular and cellular mechanisms. Br Med Bull. 63**,** 39-57.

Burgess, B. J., Adams, J. C., Nadol, J. B., Jr., 1997. Morphologic evidence for innervation of Deiters' and Hensen's cells in the guinea pig. Hear Res. 108**,** 74-82.

Cabrera, C. V., 1990. Lateral inhibition and cell fate during neurogenesis in Drosophila: the interactions between scute, Notch and Delta. Development. 110**,** 733-42.

Chardin, S., Romand, R., 1997. Factors modulating supernumerary hair cell production in the postnatal rat cochlea in vitro. International Journal of Developmental Neuroscience. 15**,** 497-507.

Chen, J., Leong, S. Y., Schachner, M., 2005. Differential expression of cell fate determinants in neurons and glial cells of adult mouse spinal cord after compression injury. Eur J Neurosci. 22**,** 1895-906.

Chen, P., Johnson, J. E., Zoghbi, H. Y., Segil, N., 2002. The role of Math1 in inner ear development: Uncoupling the establishment of the sensory primordium from hair cell fate determination. Development. 129**,** 2495-505.

Chen, P., Segil, N., 1999. p27(Kip1) links cell proliferation to morphogenesis in the developing organ of Corti. Development. 126**,** 1581-90.

Chitnis, A. B., 1995. The role of Notch in lateral inhibition and cell fate specification. Mol Cell Neurosci. 6**,** 311-21.

Chitnis, A. B., 1999. Control of neurogenesis--lessons from frogs, fish and flies. Curr Opin Neurobiol. 9**,** 18-25.

Cornbrooks, C., Bland, C., Williams, D. W., Truman, J. W., Rand, M. D., 2007. Delta expression in post-mitotic neurons identifies distinct subsets of adult-specific lineages in Drosophila. Dev Neurobiol. 67**,** 23-38.

Corrales, C. E., Pan, L., Li, H., Liberman, M. C., Heller, S., Edge, A. S., 2006. Engraftment and differentiation of embryonic stem cell-derived neural progenitor cells in the cochlear nerve trunk: growth of processes into the organ of Corti. J Neurobiol. 66**,** 1489-500.

Dabdoub, A., Puligilla, C., Jones, J. M., Fritzsch, B., Cheah, K. S., Pevny, L. H., Kelley, M. W., 2008. Sox2 signaling in prosensory domain specification and subsequent hair cell differentiation in the developing cochlea. Proc Natl Acad Sci U S A. 105**,** 18396-401.

Daudet, N., Ariza-McNaughton, L., Lewis, J., 2007. Notch signalling is needed to maintain, but not to initiate, the formation of prosensory patches in the chick inner ear. Development. 134**,** 2369-78.

Daudet, N., Lewis, J., 2005. Two contrasting roles for Notch activity in chick inner ear development: specification of prosensory patches and lateral inhibition of hair-cell differentiation. Development. 132**,** 541-51.

Dechesne, C. J., Rabejac, D., Desmadryl, G., 1994. Development of calretinin immunoreactivity in the mouse inner ear. J Comp Neurol. 346**,** 517-29.

Dechesne, C. J., Winsky, L., Kim, H. N., Goping, G., Vu, T. D., Wenthold, R. J., Jacobowitz, D. M., 1991. Identification and ultrastructural localization of a calretinin-like calcium-binding protein (protein 10) in the guinea pig and rat inner ear. Brain Res. 560**,** 139-48.

Desmadryl, G., Dechesne, C. J., 1992. Calretinin immunoreactivity in chinchilla and guinea pig vestibular end organs characterizes the calyx unit subpopulation. Exp Brain Res. 89**,** 105-8.

Doetzlhofer, A., Basch, M. L., Ohyama, T., Gessler, M., Groves, A. K., Segil, N., 2009. Hey2 regulation by FGF provides a Notch-independent mechanism for maintaining pillar cell fate in the organ of Corti. Dev Cell. 16**,** 58-69.

Duncan, L. J., Mangiardi, D. A., Matsui, J. I., Anderson, J. K., McLaughlin-Williamson, K., Cotanche, D. A., 2006. Differential expression of unconventional myosins in apoptotic and regenerating chick hair cells confirms two regeneration mechanisms. J Comp Neurol. 499**,** 691-701.

Dunwoodie, S. L., Henrique, D., Harrison, S. M., Beddington, R. S., 1997. Mouse Dll3: a novel divergent Delta gene which may complement the function of other Delta homologues during early pattern formation in the mouse embryo. Development. 124, 3065-76.

Echteler, S. M., 1992. Developmental segregation in the afferent projections to mammalian auditory hair cells. Proc Natl Acad Sci U S A. 89, 6324-7.

Eiraku, M., Hirata, Y., Takeshima, H., Hirano, T., Kengaku, M., 2002. Delta/notch-like epidermal growth factor (EGF)-related receptor, a novel EGF-like repeat-containing protein targeted to dendrites of developing and adult central nervous system neurons. J Biol Chem. 277, 25400-7.

Eiraku, M., Tohgo, A., Ono, K., Kaneko, M., Fujishima, K., Hirano, T., Kengaku, M., 2005. DNER acts as a neuron-specific Notch ligand during Bergmann glial development. Nat Neurosci. 8, 873-80.

Erkman, L., McEvilly, R. J., Luo, L., Ryan, A. K., Hooshmand, F., O'Connell, S. M., Keithley, E. M., Rapaport, D. H., Ryan, A. F., Rosenfeld, M. G., 1996. Role of transcription factors Brn-3.1 and Brn-3.2 in auditory and visual system development. Nature. 381, 603-6.

Fekete, D. M., Muthukumar, S., Karagogeos, D., 1998. Hair cells and supporting cells share a common progenitor in the avian inner ear. J Neurosci. 18, 7811-21.

Forge, A., 1985. Outer hair cell loss and supporting cell expansion following chronic gentamicin treatment. Hear Res. 19, 171-82.

Forge, A., Li, L., Corwin, J. T., Nevill, G., 1993. Ultrastructural evidence for hair cell regeneration in the mammalian inner ear. Science. 259, 1616-9.

Franklin, J. L., Berechid, B. E., Cutting, F. B., Presente, A., Chambers, C. B., Foltz, D. R., Ferreira, A., Nye, J. S., 1999. Autonomous and non-autonomous regulation of mammalian neurite development by Notch1 and Delta1. Curr Biol. 9, 1448-57.

Fredelius, L., 1988. Time sequence of degeneration pattern of the organ of Corti after acoustic overstimulation. A transmission electron microscopy study. Acta Otolaryngol. 106, 373-85.

Fukazawa, N., Yokoyama, S., Eiraku, M., Kengaku, M., Maeda, N., 2008. Receptor type protein tyrosine phosphatase zeta-pleiotrophin signaling controls endocytic trafficking of DNER that regulates neuritogenesis. Mol Cell Biol. 28, 4494-506.

Furness, D. N., Hulme, J. A., Lawton, D. M., Hackney, C. M., 2002. Distribution of the glutamate/aspartate transporter GLAST in relation to the afferent synapses of outer hair cells in the guinea pig cochlea. J Assoc Res Otolaryngol. 3, 234-47.

Furness, D. N., Lawton, D. M., 2003. Comparative distribution of glutamate transporters and receptors in relation to afferent innervation density in the mammalian cochlea. J Neurosci. 23, 11296-304.

Furness, D. N., Lehre, K. P., 1997. Immunocytochemical localization of a high-affinity glutamate-aspartate transporter, GLAST, in the rat and guinea-pig cochlea. Eur J Neurosci. 9, 1961-9.

Furukawa, T., Mukherjee, S., Bao, Z. Z., Morrow, E. M., Cepko, C. L., 2000. rax, Hes1, and notch1 promote the formation of Muller glia by postnatal retinal progenitor cells. Neuron. 26, 383-94.

Gaiano, N., Fishell, G., 2002. The role of notch in promoting glial and neural stem cell fates. Annu Rev Neurosci. 25, 471-90.

Gaiano, N., Nye, J. S., Fishell, G., 2000. Radial glial identity is promoted by Notch1 signaling in the murine forebrain. Neuron. 26, 395-404.

Ge, W., Martinowich, K., Wu, X., He, F., Miyamoto, A., Fan, G., Weinmaster, G., Sun, Y. E., 2002. Notch signaling promotes astrogliogenesis via direct CSL-mediated glial gene activation. J Neurosci Res. 69**,** 848-60.

Ginzberg, R. D., Morest, D. K., 1983. A study of cochlear innervation in the young cat with the Golgi method. Hear Res. 10**,** 227-46.

Givogri, M. I., de Planell, M., Galbiati, F., Superchi, D., Gritti, A., Vescovi, A., de Vellis, J., Bongarzone, E. R., 2006. Notch signaling in astrocytes and neuroblasts of the adult subventricular zone in health and after cortical injury. Dev Neurosci. 28**,** 81-91.

Glowatzki, E., Cheng, N., Hiel, H., Yi, E., Tanaka, K., Ellis-Davies, G. C., Rothstein, J. D., Bergles, D. E., 2006. The glutamate-aspartate transporter GLAST mediates glutamate uptake at inner hair cell afferent synapses in the mammalian cochlea. J Neurosci. 26**,** 7659-64.

Gruneburg, H., Genetical studies on the skeleton of the mouse: XXIX., Genet. Res., Vol. 2, 1961, pp. 384-393.

Hafidi, A., 1998. Peripherin-like immunoreactivity in type II spiral ganglion cell body and projections. Brain Res. 805**,** 181-90.

Hafidi, A., Despres, G., Romand, R., 1993. Ontogenesis of type II spiral ganglion neurons during development: peripherin immunohistochemistry. Int J Dev Neurosci. 11**,** 507-12.

Hakuba, N., Koga, K., Gyo, K., Usami, S. I., Tanaka, K., 2000. Exacerbation of noise-induced hearing loss in mice lacking the glutamate transporter GLAST. J Neurosci. 20**,** 8750-3.

Hartman, B. H., Basak, O., Nelson, B. R., Taylor, V., Bermingham-McDonogh, O., Reh, T. A., 2009. Hes5 Expression in the Postnatal and Adult Mouse Inner Ear and the Drug-Damaged Cochlea. J Assoc Res Otolaryngol.

Hartman, B. H., Hayashi, T., Nelson, B. R., Bermingham-McDonogh, O., Reh, T. A., 2007. Dll3 is expressed in developing hair cells in the mammalian cochlea. Dev Dyn. 236**,** 2875-83.

Hayashi, T., Cunningham, D., Bermingham-McDonogh, O., 2007. Loss of Fgfr3 leads to excess hair cell development in the mouse organ of Corti. Dev Dyn. 236**,** 525-33.

Hayashi, T., Kokubo, H., Hartman, B. H., Ray, C. A., Reh, T. A., Bermingham-McDonogh, O., 2008. Hesr1 and Hesr2 may act as early effectors of Notch signaling in the developing cochlea. Dev Biol. 316**,** 87-99.

Hayes, S., Nelson, B. R., Buckingham, B., Reh, T. A., 2007. Notch signaling regulates regeneration in the avian retina. Dev Biol. 312**,** 300-11.

Hebert, J. M., McConnell, S. K., 2000. Targeting of cre to the Foxg1 (BF-1) locus mediates loxP recombination in the telencephalon and other developing head structures. Dev Biol. 222**,** 296-306.

Heitzler, P., Simpson, P., 1991. The choice of cell fate in the epidermis of Drosophila. Cell. 64**,** 1083-92.

Henrique, D., Hirsinger, E., Adam, J., Le Roux, I., Pourquie, O., Ish-Horowicz, D., Lewis, J., 1997. Maintenance of neuroepithelial progenitor cells by Delta-Notch signalling in the embryonic chick retina. Curr Biol. 7**,** 661-70.

Hojo, M., Ohtsuka, T., Hashimoto, N., Gradwohl, G., Guillemot, F., Kageyama, R., 2000. Glial cell fate specification modulated by the bHLH gene Hes5 in mouse retina. Development. 127**,** 2515-22.

Huang, L. C., Thorne, P. R., Housley, G. D., Montgomery, J. M., 2007. Spatiotemporal definition of neurite outgrowth, refinement and retraction in the developing mouse cochlea. Development. 134**,** 2925-33.

Hume, C. R., Bratt, D. L., Oesterle, E. C., 2007. Expression of LHX3 and SOX2 during mouse inner ear development. Gene Expr Patterns. 7**,** 798-807.

Jacobsen, T. L., Brennan, K., Arias, A. M., Muskavitch, M. A., 1998. Cis-interactions between Delta and Notch modulate neurogenic signalling in Drosophila. Development. 125**,** 4531-40.

Jagger, D. J., Housley, G. D., 2003. Membrane properties of type II spiral ganglion neurones identified in a neonatal rat cochlear slice. J Physiol. 552**,** 525-33.

Jayasena, C. S., Ohyama, T., Segil, N., Groves, A. K., 2008. Notch signaling augments the canonical Wnt pathway to specify the size of the otic placode. Development. 135**,** 2251-61.

Jin, Z. H., Kikuchi, T., Tanaka, K., Kobayashi, T., 2003. Expression of glutamate transporter GLAST in the developing mouse cochlea. Tohoku J Exp Med. 200**,** 137-44.

Jurynczyk, M., Jurewicz, A., Bielecki, B., Raine, C. S., Selmaj, K., 2005. Inhibition of Notch signaling enhances tissue repair in an animal model of multiple sclerosis. J Neuroimmunol. 170**,** 3-10.

Kageyama, R., Ohtsuka, T., 1999a. The Notch-Hes pathway in mammalian neural development. Cell Res. 9**,** 179-88.

Kageyama, R., Ohtsuka, T., 1999b. The Notch-Hes pathway in mammalian neural development. Cell Res. 9**,** 179-88.

Karolyi, I. J., Probst, F. J., Beyer, L., Odeh, H., Dootz, G., Cha, K. B., Martin, D. M., Avraham, K. B., Kohrman, D., Dolan, D. F., Raphael, Y., Camper, S. A., 2003. Myo15 function is distinct from Myo6, Myo7a and pirouette genes in development of cochlear stereocilia. Hum Mol Genet. 12**,** 2797-805.

Kauffman, M. H., 1992. The Atlas of Mouse Development. Elsevier Academic Press, London.

Kawamoto, K., Izumikawa, M., Beyer, L. A., Atkin, G. M., Raphael, Y., 2008. Spontaneous hair cell regeneration in the mouse utricle following gentamicin ototoxicity. Hear Res.

Kiang, N. Y., Rho, J. M., Northrop, C. C., Liberman, M. C., Ryugo, D. K., 1982. Hair-cell innervation by spiral ganglion cells in adult cats. Science. 217**,** 175-7.

Kiernan, A. E., Ahituv, N., Fuchs, H., Balling, R., Avraham, K. B., Steel, K. P., Hrabe de Angelis, M., 2001. The Notch ligand Jagged1 is required for inner ear sensory development. Proc Natl Acad Sci U S A. 98**,** 3873-8.

Kiernan, A. E., Cordes, R., Kopan, R., Gossler, A., Gridley, T., 2005a. The Notch ligands DLL1 and JAG2 act synergistically to regulate hair cell development in the mammalian inner ear. Development. 132**,** 4353-62.

Kiernan, A. E., Pelling, A. L., Leung, K. K., Tang, A. S., Bell, D. M., Tease, C., Lovell-Badge, R., Steel, K. P., Cheah, K. S., 2005b. Sox2 is required for sensory organ development in the mammalian inner ear. Nature. 434**,** 1031-5.

Kiernan, A. E., Xu, J., Gridley, T., 2006. The Notch ligand JAG1 is required for sensory progenitor development in the mammalian inner ear. PLoS Genet. 2**,** e4.

Kirjavainen, A., Sulg, M., Heyd, F., Alitalo, K., Yla-Herttuala, S., Moroy, T., Petrova, T. V., Pirvola, U., 2008. Prox1 interacts with Atoh1 and Gfi1, and regulates cellular differentiation in the inner ear sensory epithelia. Dev Biol. 322**,** 33-45.

Kishi, N., Tang, Z., Maeda, Y., Hirai, A., Mo, R., Ito, M., Suzuki, S., Nakao, K., Kinoshita, T., Kadesch, T., Hui, C., Artavanis-Tsakonas, S., Okano, H., Matsuno, K., 2001. Murine homologs of deltex define a novel gene family involved in vertebrate Notch signaling and neurogenesis. Int J Dev Neurosci. 19, 21-35.

Koo, J. W., Homanics, G. E., Balaban, C. D., 2002. Hypoplasia of spiral and Scarpa's ganglion cells in GABA(A) receptor beta(3) subunit knockout mice. Hear Res. 167, 71-80.

Kusumi, K., Sun, E. S., Kerrebrock, A. W., Bronson, R. T., Chi, D. C., Bulotsky, M. S., Spencer, J. B., Birren, B. W., Frankel, W. N., Lander, E. S., 1998. The mouse pudgy mutation disrupts Delta homologue Dll3 and initiation of early somite boundaries. Nat Genet. 19, 274-8.

Ladi, E., Nichols, J. T., Ge, W., Miyamoto, A., Yao, C., Yang, L. T., Boulter, J., Sun, Y. E., Kintner, C., Weinmaster, G., 2005. The divergent DSL ligand Dll3 does not activate Notch signaling but cell autonomously attenuates signaling induced by other DSL ligands. J Cell Biol. 170, 983-92.

Lanford, P. J., Lan, Y., Jiang, R., Lindsell, C., Weinmaster, G., Gridley, T., Kelley, M. W., 1999a. Notch signalling pathway mediates hair cell development in mammalian cochlea. Nat Genet. 21, 289-92.

Lanford, P. J., Lan, Y., Jiang, R., Lindsell, C., Weinmaster, G., Gridley, T., Kelley, M. W., 1999b. Notch signalling pathway mediates hair cell development in mammalian cochlea. Nat Genet. 21, 289-92.

Lanford, P. J., Shailam, R., Norton, C. R., Gridley, T., Kelley, M. W., 2000. Expression of Math1 and HES5 in the cochleae of wildtype and Jag2 mutant mice. J Assoc Res Otolaryngol. 1, 161-71.

Lardelli, M., Williams, R., Mitsiadis, T., Lendahl, U., 1996. Expression of the Notch 3 intracellular domain in mouse central nervous system progenitor cells is lethal and leads to disturbed neural tube development. Mech Dev. 59, 177-90.

Lewis, A. K., Frantz, G. D., Carpenter, D. A., de Sauvage, F. J., Gao, W. Q., 1998. Distinct expression patterns of notch family receptors and ligands during development of the mammalian inner ear. Mech Dev. 78, 159-63.

Li, A., Xue, J., Peterson, E. H., 2008a. Architecture of the mouse utricle: macular organization and hair bundle heights. J Neurophysiol. 99, 718-33.

Li, H., Liu, H., Heller, S., 2003. Pluripotent stem cells from the adult mouse inner ear. Nat Med. 9, 1293-9.

Li, H. S., Niedzielski, A. S., Beisel, K. W., Hiel, H., Wenthold, R. J., Morley, B. J., 1994. Identification of a glutamate/aspartate transporter in the rat cochlea. Hear Res. 78, 235-42.

Li, S., Mark, S., Radde-Gallwitz, K., Schlisner, R., Chin, M. T., Chen, P., 2008b. Hey2 functions in parallel with Hes1 and Hes5 for mammalian auditory sensory organ development. BMC Dev Biol. 8, 20.

Liberman, M. C., Dodds, L. W., Pierce, S., 1990. Afferent and efferent innervation of the cat cochlea: quantitative analysis with light and electron microscopy. J Comp Neurol. 301, 443-60.

Lim, D. J., Anniko, M., 1985. Developmental morphology of the mouse inner ear. A scanning electron microscopic observation. Acta Otolaryngol Suppl. 422, 1-69.

Lindsell, C. E., Boulter, J., diSibio, G., Gossler, A., Weinmaster, G., 1996. Expression patterns of Jagged, Delta1, Notch1, Notch2, and Notch3 genes identify ligand-

receptor pairs that may function in neural development. Mol Cell Neurosci. 8, 14-27.
Liu, J., Lobe, C. G., 2007. Cre-conditional expression of constitutively active Notch1 in transgenic mice. Genesis. 45, 259-65.
Lopez, I., Honrubia, V., Lee, S. C., Schoeman, G., Beykirch, K., 1997. Quantification of the process of hair cell loss and recovery in the chinchilla crista ampullaris after gentamicin treatment. International Journal of Developmental Neuroscience. 15, 447-61.
Lopez, I. A., Zhao, P. M., Yamaguchi, M., de Vellis, J., Espinosa-Jeffrey, A., 2004. Stem/progenitor cells in the postnatal inner ear of the GFP-nestin transgenic mouse. Int J Dev Neurosci. 22, 205-13.
Lowenheim, H., Furness, D. N., Kil, J., Zinn, C., Gultig, K., Fero, M. L., Frost, D., Gummer, A. W., Roberts, J. M., Rubel, E. W., Hackney, C. M., Zenner, H. P., 1999. Gene disruption of p27(Kip1) allows cell proliferation in the postnatal and adult organ of corti. Proc Natl Acad Sci U S A. 96, 4084-8.
Lysakowski, A., Goldberg, J. M., Morphology of the Vestibular Periphery. In: R. J. Salvi, A. N. Popper, R. R. Fay, Eds.), The Vestibular System. Springer Handbook of Auditory Research. Springer, New York, 2004.
Ma, E. Y., Rubel, E. W., Raible, D. W., 2008. Notch signaling regulates the extent of hair cell regeneration in the zebrafish lateral line. J Neurosci. 28, 2261-73.
Mak, A. C., Szeto, I. Y., Fritzsch, B., Cheah, K. S., 2009. Differential and overlapping expression pattern of SOX2 and SOX9 in inner ear development. Gene Expr Patterns.
McDowell, B., Davies, S., Forge, A., 1989. The effect of gentamicin-induced hair cell loss on the tight junctions of the reticular lamina. Hear Res. 40, 221-32.
Morest, D. K., Cotanche, D. A., 2004. Regeneration of the inner ear as a model of neural plasticity. J Neurosci Res. 78, 455-60.
Morrison, A., Hodgetts, C., Gossler, A., Hrabe de Angelis, M., Lewis, J., 1999. Expression of Delta1 and Serrate1 (Jagged1) in the mouse inner ear. Mech Dev. 84, 169-72.
Morrison, S. J., Perez, S. E., Qiao, Z., Verdi, J. M., Hicks, C., Weinmaster, G., Anderson, D. J., 2000. Transient Notch activation initiates an irreversible switch from neurogenesis to gliogenesis by neural crest stem cells. Cell. 101, 499-510.
Murata, J., Tokunaga, A., Okano, H., Kubo, T., 2006. Mapping of notch activation during cochlear development in mice: implications for determination of prosensory domain and cell fate diversification. J Comp Neurol. 497, 502-18.
Murtaugh, L. C., Stanger, B. Z., Kwan, K. M., Melton, D. A., 2003. Notch signaling controls multiple steps of pancreatic differentiation. Proc Natl Acad Sci U S A. 100, 14920-5.
Muzumdar, M. D., Tasic, B., Miyamichi, K., Li, L., Luo, L., 2007. A global double-fluorescent Cre reporter mouse. Genesis. 45, 593-605.
Nelson, B. R., Hartman, B. H., Georgi, S. A., Lan, M. S., Reh, T. A., 2007. Transient inactivation of Notch signaling synchronizes differentiation of neural progenitor cells. Dev Biol. 304, 479-98.
Nelson, B. R., Sadhu, M., Kasemeier, J. C., Anderson, L. W., Lefcort, F., 2004. Identification of genes regulating sensory neuron genesis and differentiation in the avian dorsal root ganglia. Dev Dyn. 229, 618-29.

Oesterle, E. C., Campbell, S., Taylor, R. R., Forge, A., Hume, C. R., 2008. Sox2 and JAGGED1 expression in normal and drug-damaged adult mouse inner ear. J Assoc Res Otolaryngol. 9, 65-89.

Oesterle, E. C., Cunningham, D. E., Westrum, L. E., Rubel, E. W., 2003. Ultrastructural analysis of [3H]thymidine-labeled cells in the rat utricular macula. J Comp Neurol. 463, 177-95.

Oesterle, E. C., Stone, J. S., Hair Cell Regeneration: Mechanisms Guiding Cellular Proliferation and Differentiation. In: R. J. Salvi, A. N. Popper, R. R. Fay, Eds.), Hair Cell Regeneration, Repair, and Protection. Springer Handbook of Auditory Research. Springer New York, 2008.

Ohtsuka, T., Ishibashi, M., Gradwohl, G., Nakanishi, S., Guillemot, F., Kageyama, R., 1999. Hes1 and Hes5 as notch effectors in mammalian neuronal differentiation. Embo J. 18, 2196-207.

Ohyama, T., Groves, A. K., 2004. Generation of Pax2-Cre mice by modification of a Pax2 bacterial artificial chromosome. Genesis. 38, 195-9.

Okamura, H. O., Shibahara-Maruyama, I., Sugai, N., Adams, J. C., 2002. Innervation of supporting cells in the guinea pig cochlea detected in bloc-surface preparations. Neuroreport. 13, 1585-8.

Oshima, K., Grimm, C. M., Corrales, C. E., Senn, P., Martinez Monedero, R., Geleoc, G. S., Edge, A., Holt, J. R., Heller, S., 2007. Differential distribution of stem cells in the auditory and vestibular organs of the inner ear. J Assoc Res Otolaryngol. 8, 18-31.

Ota, C. Y., Kimura, R. S., 1980. Ultrastructural study of the human spiral ganglion. Acta Otolaryngol. 89, 53-62.

Ottersen, O. P., Takumi, Y., Matsubara, A., Landsend, A. S., Laake, J. H., Usami, S., 1998. Molecular organization of a type of peripheral glutamate synapse: the afferent synapses of hair cells in the inner ear. Prog Neurobiol. 54, 127-48.

Perkins, R. E., Morest, D. K., 1975. A study of cochlear innervation patterns in cats and rats with the Golgi method and Nomarkski Optics. J Comp Neurol. 163, 129-58.

Pickles, J. O., van Heumen, W. R., 2000. Lateral interactions account for the pattern of the hair cell array in the chick basilar papilla. Hear Res. 145, 65-74.

Pirvola, U., Ylikoski, J., Trokovic, R., Hebert, J., McConnell, S., Partanen, J., 2002. FGFR1 Is Required for the Development of the Auditory Sensory Epithelium. Neuron. 35, 671.

Pujol, R., 1985. Morphology, synaptology and electrophysiology of the developing cochlea. Acta Otolaryngol Suppl. 421, 5-9.

Raphael, Y., Altschuler, R. A., 1991. Reorganization of cytoskeletal and junctional proteins during cochlear hair cell degeneration. Cell Motil Cytoskeleton. 18, 215-27.

Raphael, Y., Altschuler, R. A., 2003. Structure and innervation of the cochlea. Brain Res Bull. 60, 397-422.

Rio, C., Dikkes, P., Liberman, M. C., Corfas, G., 2002. Glial fibrillary acidic protein expression and promoter activity in the inner ear of developing and adult mice. J Comp Neurol. 442, 156-62.

Roberson, D. W., Alosi, J. A., Cotanche, D. A., 2004. Direct transdifferentiation gives rise to the earliest new hair cells in regenerating avian auditory epithelium. J Neurosci Res. 78, 461-71.

Roberto, M., Zito, F., 1988. Scar formation following impulse noise-induced mechanical damage to the organ of Corti. J Laryngol Otol. 102, 2-9.

Ruben, R. J., 1967. Development of the inner ear of the mouse: a radioautographic study of terminal mitoses. Acta Otolaryngol Suppl. 220, 1-44.

Sage, C., Venteo, S., Jeromin, A., Roder, J., Dechesne, C. J., 2000. Distribution of frequenin in the mouse inner ear during development, comparison with other calcium-binding proteins and synaptophysin. Hear Res. 150, 70-82.

Saito, S. Y., Takeshima, H., 2006. DNER as key molecule for cerebellar maturation. Cerebellum. 5, 227-31.

Sakamoto, K., Ohara, O., Takagi, M., Takeda, S., Katsube, K., 2002. Intracellular cell-autonomous association of Notch and its ligands: a novel mechanism of Notch signal modification. Dev Biol. 241, 313-26.

Sano, H., Mukai, J., Monoo, K., Close, L. G., Sato, T. A., 2001. Expression of p75NTR and its associated protein NADE in the rat cochlea. Laryngoscope. 111, 535-8.

Sato, T., Doi, K., Taniguchi, M., Yamashita, T., Kubo, T., Tohyama, M., 2006. Progressive hearing loss in mice carrying a mutation in the p75 gene. Brain Res. 1091, 224-34.

Schick, B., Starlinger, V., Haberle, L., Eigenthaler, M., Walter, U., Knipper, M., 2006. Delayed formation of actin filaments in the outer pillar head plate of VASP-/- mice. Cells Tissues Organs. 184, 88-95.

Sestan, N., Artavanis-Tsakonas, S., Rakic, P., 1999. Contact-dependent inhibition of cortical neurite growth mediated by notch signaling. Science. 286, 741-6.

Shailam, R., Lanford, P. J., Dolinsky, C. M., Norton, C. R., Gridley, T., Kelley, M. W., 1999. Expression of proneural and neurogenic genes in the embryonic mammalian vestibular system. J Neurocytol. 28, 809-19.

Shimizu, Y., Hakuba, N., Hyodo, J., Taniguchi, M., Gyo, K., 2005. Kanamycin ototoxicity in glutamate transporter knockout mice. Neurosci Lett. 380, 243-6.

Simmons, D. D., 1994. A transient afferent innervation of outer hair cells in the postnatal cochlea. Neuroreport. 5, 1309-12.

Slepecky, N., Chamberlain, S. C., 1983. Distribution and polarity of actin in inner ear supporting cells. Hear Res. 10, 359-70.

Sparrow, D. B., Clements, M., Withington, S. L., Scott, A. N., Novotny, J., Sillence, D., Kusumi, K., Beddington, R. S., Dunwoodie, S. L., 2002. Diverse requirements for Notch signalling in mammals. Int J Dev Biol. 46, 365-74.

Stone, I. M., Lurie, D. I., Kelley, M. W., Poulsen, D. J., 2005. Adeno-associated virus-mediated gene transfer to hair cells and support cells of the murine cochlea. Mol Ther. 11, 843-8.

Stone, J. S., Choi, Y. S., Woolley, S. M., Yamashita, H., Rubel, E. W., 1999. Progenitor cell cycling during hair cell regeneration in the vestibular and auditory epithelia of the chick. J Neurocytol. 28, 863-76.

Stone, J. S., Cotanche, D. A., 2007. Hair cell regeneration in the avian auditory epithelium. Int J Dev Biol. 51, 633-47.

Stone, J. S., Rubel, E. W., 1999. Delta1 expression during avian hair cell regeneration. Development. 126, 961-73.

Stone, J. S., Shang, J. L., Tomarev, S., 2003. Expression of Prox1 defines regions of the avian otocyst that give rise to sensory or neural cells. J Comp Neurol. 460, 487-502.

Stone, J. S., Shang, J. L., Tomarev, S., 2004. cProx1 immunoreactivity distinguishes progenitor cells and predicts hair cell fate during avian hair cell regeneration. Dev Dyn. 230, 597-614.

Sun, P., Xia, S., Lal, B., Eberhart, C. G., Quinones-Hinojosa, A., Maciaczyk, J., Matsui, W., Dimeco, F., Piccirillo, S. M., Vescovi, A. L., Laterra, J., 2009. DNER, An Epigenetically Modulated Gene, Regulates Glioblastoma-Derived Neurosphere Cell Differentiation and Tumor Propagation. Stem Cells.

Takebayashi, S., Yamamoto, N., Yabe, D., Fukuda, H., Kojima, K., Ito, J., Honjo, T., 2007. Multiple roles of Notch signaling in cochlear development. Dev Biol.

Tang, L. S., Alger, H. M., Pereira, F. A., 2006. COUP-TFI controls Notch regulation of hair cell and support cell differentiation. Development. 133, 3683-93.

Tanigaki, K., Nogaki, F., Takahashi, J., Tashiro, K., Kurooka, H., Honjo, T., 2001. Notch1 and Notch3 instructively restrict bFGF-responsive multipotent neural progenitor cells to an astroglial fate. Neuron. 29, 45-55.

Tanyeri, H., Lopez, I., Honrubia, V., 1995. Histological evidence for hair cell regeneration after ototoxic cell destruction with local application of gentamicin in the chinchilla crista ampullaris. Hearing Research. 89, 194-202.

Taylor, M. K., Yeager, K., Morrison, S. J., 2007. Physiological Notch signaling promotes gliogenesis in the developing peripheral and central nervous systems. Development. 134, 2435-47.

Taylor, R. R., Nevill, G., Forge, A., 2008. Rapid Hair Cell Loss: A Mouse Model for Cochlear Lesions. J Assoc Res Otolaryngol. 9, 44-64.

Thorne, P. R., Gavin, J. B., Herdson, P. B., 1984. A quantitative study of the sequence of topographical changes in the organ of Corti following acoustic trauma. Acta Otolaryngol. 97, 69-81.

Tohgo, A., Eiraku, M., Miyazaki, T., Miura, E., Kawaguchi, S. Y., Nishi, M., Watanabe, M., Hirano, T., Kengaku, M., Takeshima, H., 2006. Impaired cerebellar functions in mutant mice lacking DNER. Mol Cell Neurosci. 31, 326-33.

Toma, J. S., McPhail, L. T., Ramer, M. S., 2007. Differential RIP antigen (CNPase) expression in peripheral ensheathing glia. Brain Res. 1137, 1-10.

Tsai, H., Hardisty, R. E., Rhodes, C., Kiernan, A. E., Roby, P., Tymowska-Lalanne, Z., Mburu, P., Rastan, S., Hunter, A. J., Brown, S. D., Steel, K. P., 2001. The mouse slalom mutant demonstrates a role for Jagged1 in neuroepithelial patterning in the organ of Corti. Hum Mol Genet. 10, 507-12.

Uchikawa, M., Ishida, Y., Takemoto, T., Kamachi, Y., Kondoh, H., 2003. Functional analysis of chicken Sox2 enhancers highlights an array of diverse regulatory elements that are conserved in mammals. Dev Cell. 4, 509-19.

Uchikawa, M., Kamachi, Y., Kondoh, H., 1999. Two distinct subgroups of Group B Sox genes for transcriptional activators and repressors: their expression during embryonic organogenesis of the chicken. Mech Dev. 84, 103-20.

Vetter, M. L., Moore, K. B., 2001. Becoming glial in the neural retina. Dev Dyn. 221, 146-53.

Vrijens, K., Thys, S., De Jeu, M. T., Postnov, A. A., Pfister, M., Cox, L., Zwijsen, A., Van Hoof, V., Mueller, M., De Clerck, N. M., De Zeeuw, C. I., Van Camp, G., Van Laer, L., 2006. Ozzy, a Jag1 vestibular mouse mutant, displays characteristics of Alagille syndrome. Neurobiol Dis. 24, 28-40.

Warchol, M. E., Lambert, P. R., Goldstein, B. J., Forge, A., Corwin, J. T., 1993. Regenerative proliferation in inner ear sensory epithelia from adult guinea pigs and humans. Science. 259**,** 1619-22.

Warr, W. B., 1980. Efferent components of the auditory system. Annals of Otology, Rhinology, and Laryngology. 89**,** 114-20.

Warr, W. B., Boche, J. B., Neely, S. T., 1997. Efferent innervation of the inner hair cell region: origins and terminations of two lateral olivocochlear systems. Hear Res. 108**,** 89-111.

Warr, W. B., Boche, J. E., 2003. Diversity of axonal ramifications belonging to single lateral and medial olivocochlear neurons. Exp Brain Res. 153**,** 499-513.

Watanabe, M., Sakurai, Y., Ichinose, T., Aikawa, Y., Kotani, M., Itoh, K., 2006. Monoclonal antibody Rip specifically recognizes 2',3'-cyclic nucleotide 3'-phosphodiesterase in oligodendrocytes. J Neurosci Res. 84**,** 525-33.

White, P. M., Doetzlhofer, A., Lee, Y. S., Groves, A. K., Segil, N., 2006. Mammalian cochlear supporting cells can divide and trans-differentiate into hair cells. Nature. 441**,** 984-7.

Woods, C., Montcouquiol, M., Kelley, M. W., 2004. Math1 regulates development of the sensory epithelium in the mammalian cochlea. Nat Neurosci. 7**,** 1310-8.

Wu, W. J., Sha, S. H., McLaren, J. D., Kawamoto, K., Raphael, Y., Schacht, J., 2001. Aminoglycoside ototoxicity in adult CBA, C57BL and BALB mice and the Sprague-Dawley rat. Hear Res. 158**,** 165-78.

Yamamoto, N., Tanigaki, K., Tsuji, M., Yabe, D., Ito, J., Honjo, T., 2006. Inhibition of Notch/RBP-J signaling induces hair cell formation in neonate mouse cochleas. J Mol Med. 84**,** 37-45.

Yamashita, H., Oesterle, E. C., 1995. Induction of cell proliferation in mammalian inner-ear sensory epithelia by transforming growth factor alpha and epidermal growth factor. Proc Natl Acad Sci U S A. 92**,** 3152-5.

Zhang, N., Martin, G. V., Kelley, M. W., Gridley, T., 2000. A mutation in the Lunatic fringe gene suppresses the effects of a Jagged2 mutation on inner hair cell development in the cochlea. Curr Biol. 10**,** 659-62.

Zheng, J. L., Gao, W. Q., 2000. Overexpression of Math1 induces robust production of extra hair cells in postnatal rat inner ears. Nat Neurosci. 3**,** 580-6.

Zheng, J. L., Shou, J., Guillemot, F., Kageyama, R., Gao, W. Q., 2000. Hes1 is a negative regulator of inner ear hair cell differentiation. Development. 127**,** 4551-60.

Zine, A., Aubert, A., Qiu, J., Therianos, S., Guillemot, F., Kageyama, R., de Ribaupierre, F., 2001. Hes1 and Hes5 activities are required for the normal development of the hair cells in the mammalian inner ear. J Neurosci. 21**,** 4712-20.

Zine, A., de Ribaupierre, F., 2002. Notch/Notch ligands and Math1 expression patterns in the organ of Corti of wild-type and Hes1 and Hes5 mutant mice. Hear Res. 170**,** 22-31.

Zine, A., Van De Water, T. R., de Ribaupierre, F., 2000. Notch signaling regulates the pattern of auditory hair cell differentiation in mammals. Development. 127**,** 3373-83.

VITA

Byron Haney Hartman was born 1978, in a log cabin in Brown County, Indiana. Byron is one of three sons of John S. Hartman and Libby I. Hartman. He attended the University of Michigan and received a Bachelor's degree in Communication Studies in 2000 and then attended Indiana University and earned a second Bachelor's degree in Biology in 2004. While at Indiana University, he worked in the lab of Anton Neff and Anthony Mescher, where he studied amphibian limb regeneration. For his graduate studies at the University of Washington, he worked under the mentorship of Thomas Reh as well as Olivia Bermingham-McDonogh. Byron earned the degree of Doctor of Philosophy from the University of Washington Biological Structure Graduate Program in 2009.